



HAL
open science

Information-Geometric Optimization Algorithms: A Unifying Picture via Invariance Principles

Yann Ollivier, Ludovic Arnold, Anne Auger, Nikolaus Hansen

► **To cite this version:**

Yann Ollivier, Ludovic Arnold, Anne Auger, Nikolaus Hansen. Information-Geometric Optimization Algorithms: A Unifying Picture via Invariance Principles. 2011. hal-00601503v2

HAL Id: hal-00601503

<https://hal.science/hal-00601503v2>

Preprint submitted on 29 Jun 2013

HAL is a multi-disciplinary open access archive for the deposit and dissemination of scientific research documents, whether they are published or not. The documents may come from teaching and research institutions in France or abroad, or from public or private research centers.

L'archive ouverte pluridisciplinaire **HAL**, est destinée au dépôt et à la diffusion de documents scientifiques de niveau recherche, publiés ou non, émanant des établissements d'enseignement et de recherche français ou étrangers, des laboratoires publics ou privés.

Information-Geometric Optimization Algorithms: A Unifying Picture via Invariance Principles

Yann Ollivier, Ludovic Arnold, Anne Auger, Nikolaus Hansen

Abstract

We present a canonical way to turn any smooth parametric family of probability distributions on an arbitrary search space X into a continuous-time black-box optimization method on X , the *information-geometric optimization* (IGO) method. Invariance as a major design principle keeps the number of arbitrary choices to a minimum. The resulting *IGO flow* is the flow of an ordinary differential equation conducting the natural gradient ascent of an adaptive, time-dependent transformation of the objective function. It makes no particular assumptions on the objective function to be optimized.

The IGO method produces explicit IGO algorithms through time discretization. It naturally recovers versions of known algorithms and offers a systematic way to derive new ones. In continuous search spaces, IGO algorithms take a form related to natural evolution strategies (NES). The cross-entropy method is recovered in a particular case with a large time step, and can be extended into a smoothed, parametrization-independent maximum likelihood update (IGO-ML). When applied to the family of Gaussian distributions on \mathbb{R}^d , the IGO framework recovers a version of the well-known CMA-ES algorithm and of xNES. For the family of Bernoulli distributions on $\{0, 1\}^d$, we recover the seminal PBIL algorithm. For the distributions of restricted Boltzmann machines, we naturally obtain a novel algorithm for discrete optimization on $\{0, 1\}^d$. All these algorithms are natural instances of, and unified under, the single information-geometric optimization framework.

The IGO method achieves, thanks to its intrinsic formulation, maximal invariance properties: invariance under reparametrization of the search space X , under a change of parameters of the probability distribution, and under increasing transformation of the function to be optimized. The latter is achieved through an adaptive formulation of the objective.

Theoretical considerations strongly suggest that IGO algorithms are essentially characterized by a minimal change of the distribution over time. Therefore they have minimal loss in diversity through the course of optimization, provided the initial diversity is high. First experiments using restricted Boltzmann machines confirm this insight. As a simple consequence, IGO seems to provide, from information theory, an elegant way to spontaneously explore several valleys of a fitness landscape in a single run.

Contents

Introduction	2
1 Algorithm description	5
1.1 The natural gradient on parameter space	6
1.2 IGO: Information-geometric optimization	9
2 First properties of IGO	13
2.1 Consistency of sampling	13
2.2 Monotonicity: quantile improvement	14
2.3 The IGO flow for exponential families	14
2.4 Invariance properties	15
2.5 Speed of the IGO flow	17
2.6 Noisy objective function	18
2.7 Implementation remarks	19
3 IGO, maximum likelihood, and the cross-entropy method	21
4 CMA-ES, NES, EDAs and PBIL from the IGO framework	24
4.1 PBIL as IGO algorithm for Bernoulli measures	24
4.2 Multivariate normal distributions (Gaussians)	26
4.3 Computing the IGO flow for some simple examples	30
5 Multimodal optimization using restricted Boltzmann machines	33
5.1 IGO for restricted Boltzmann machines	33
5.2 Experimental setup	39
5.3 Experimental results	40
5.4 Convergence to the continuous-time limit	46
6 Further discussion and perspectives	47
Summary and conclusion	53

Introduction

Optimization problems are at the core of many disciplines. Given an objective function $f : X \rightarrow \mathbb{R}$, to be optimized on some space X , the goal of black-box optimization is to find solutions $x \in X$ with small (in the case of minimization) value $f(x)$, using the least number of calls to the function f . In a *black-box* scenario, knowledge about the function f is restricted to the handling of a device (e.g., a simulation code) that delivers the value $f(x)$ for any input $x \in X$. The search space X may be finite, discrete infinite, or continuous. However, optimization algorithms are often designed for a specific type of search space, exploiting its specific structure.

One major design principle in general and in optimization in particular is related to *invariance*, which allows to extend performance observed on a given function to its whole associated invariance class. Thus invariance hopefully provides better robustness w.r.t. changes in the presentation of a problem. For continuous search spaces, invariance under translation of the coordinate system is standard in optimization. Invariance under general affine-linear changes of the coordinates has been—we believe—one of the keys to the success of the *covariance matrix adaptation evolution strategy* (CMA-ES, [HO01]). While these relate to transformations in the search

space, another important invariance concerns the application of monotonically increasing transformations to f , so that it is indifferent whether the function f , f^3 or $f \times |f|^{-2/3}$ is minimized. This way some non-convex or non-smooth functions can be as “easily” optimised as convex ones. Invariance under f -transformation is not uncommon, e.g., for evolution strategies [Sch95] or pattern search methods [HJ61, Tor97, NM65]; however it has not always been recognized as an attractive feature.

Many stochastic optimization methods have been proposed to tackle black-box optimization. The underlying (often hidden) principle of these stochastic methods is to iteratively update a probability distribution P_θ defined on X , parametrized by a set of parameters θ . At a given iteration, the distribution P_θ represents, loosely speaking, the current belief about where solutions with the smallest values of the function f may lie. Over time, P_θ is expected to concentrate around the minima of f . The update of the distribution involves querying the function with points sampled from the current probability distribution P_θ . Although implicit in the presentation of many stochastic optimization algorithms, this is the natural setting for the wide family of *estimation of distribution algorithms* (EDA) [LL02, BC95, PGL02]. Updates of the probability distribution often rely on heuristics (nevertheless in [Tou04] the possible interest of information geometry to exploit the structure of probability distributions for designing better grounded heuristics is pointed out). In addition, in the EDA setting we can distinguish two theoretically founded approaches to update P_θ . First, the *cross-entropy* method consists in taking θ minimizing the Kullback–Leibler divergence between P_θ and the indicator of the best points according to f [dBKMR05]. Second, one can transfer the objective function f to the space of parameters θ by taking the average of f under P_θ , seen as a function of θ . This average is a new function from a Euclidian space to \mathbb{R} and is minimal when P_θ is concentrated on minima of f . Consequently, θ can be updated by following a gradient descent of this function with respect to θ . This has been done in various situations such as $X = \{0, 1\}^d$ and the family of Bernoulli measures [Ber00b] or of Boltzmann machines [Ber02], or on $X = \mathbb{R}^d$ for the family of Gaussian distributions [Ber00a, GF05].

However, taking the ordinary gradient with respect to θ depends on the precise way a parameter θ is chosen to represent the distribution P_θ , and does not take advantage of the Riemannian metric structure of families of probability distributions. In the context of machine learning, Amari noted the shortcomings of the ordinary gradient for families of probability distributions [Ama98] and proposed instead to use the natural gradient with respect to the Fisher metric [Rao45, Jef46, AN00]. In the context of optimization, the natural gradient with respect to the Fisher metric has been used for exponential families on $X = \{0, 1\}^d$ [MMS08, MMP11] and for the family of Gaussian distributions on $X = \mathbb{R}^d$ with so-called natural evolution strategies (NES) [WSPS08, SWSS09, GSS⁺10].

However, none of the previous attempts using gradient updates captures the invariance under increasing transformations of the objective function, which is instead, in some cases, enforced *a posteriori* with heuristics arguments.

Building on these ideas, this paper overcomes the invariance problem of previous attempts and provides a consistent, unified picture of optimization on arbitrary search spaces via invariance principles. More specifically, we consider an arbitrary search space X , either discrete or continuous, and a black-box optimization problem on X . We assume that a family of probabil-

ity distributions P_θ on X depending on a continuous multicomponent parameter $\theta \in \Theta$ has been chosen. A classical example is to take $X = \mathbb{R}^d$ and to consider the family of all Gaussian distributions P_θ on \mathbb{R}^d , with $\theta = (m, C)$ the mean and covariance matrix. Another simple example is $X = \{0, 1\}^d$ equipped with the family of Bernoulli measures, i.e. $\theta = (\theta_i)_{1 \leq i \leq d}$ and $P_\theta(x) = \prod \theta_i^{x_i} (1 - \theta_i)^{1-x_i}$ for $x = (x_i) \in X$.

From this setting, *information-geometric optimization* (IGO) can be defined in a natural way. At each (continuous) time t , we maintain a value θ^t of the parameter of the distribution. The function f to be optimized is transferred to the parameter space Θ by means of a suitable time-dependent transformation based on the P_{θ^t} -quantiles of f (Definition 2). The *IGO flow*, introduced in Definition 3, follows the natural gradient of the expected value of this function of θ^t in the parameter space Θ , where the natural gradient derives from the Fisher information metric. The IGO flow is thus the flow of an ordinary differential equation in space Θ . This continuous-time gradient flow is turned into a family of explicit *IGO algorithms* by taking an Euler time discretization of the differential equation and approximating the distribution P_{θ^t} by using samples. From the start, the IGO flow is invariant under strictly increasing transformations of f (Proposition 8); we also prove that the sampling procedure is consistent (Theorem 5). IGO algorithms share their final algebraic form with the *natural evolution strategies* (NES) introduced in the Gaussian setting [WSPS08, SWSS09, GSS⁺10]; the latter are thus recovered in the IGO framework as an Euler approximation to a well-defined flow, without heuristic arguments.

The IGO method also has an equivalent description as an *infinitesimal maximum likelihood update* (Theorem 14); this reveals a new property of the natural gradient and does not require a smooth parametrization by θ anymore. This also establishes a link (Theorem 16) between IGO and the *cross-entropy method* [dBKMR05].

When we instantiate IGO using the family of Gaussian distributions on \mathbb{R}^d , we naturally obtain versions of the well-known *covariance matrix adaptation evolution strategy* (CMA-ES) [HO01, HK04, JA06] and of *natural evolution strategies*. With Bernoulli measures on the discrete cube $\{0, 1\}^d$, we recover (Proposition 18) the well-known *population-based incremental learning* (PBIL) [BC95, Bal94]; this derivation of PBIL as a natural gradient ascent appears to be new, and sheds some light on the common ground between continuous and discrete optimization.

From the IGO framework, it is immediate (theoretically) to build new optimization algorithms using more complex families of distributions than Gaussian or Bernoulli. As an illustration, distributions associated with restricted Boltzmann machines (RBMs) provide a new but natural algorithm for discrete optimization on $\{0, 1\}^d$ which is able to handle dependencies between the bits (see also [Ber02]). The probability distributions associated with RBMs are multimodal; combined with the specific information-theoretic properties of IGO that guarantee minimal change in diversity over time, this allows IGO to reach multiple optima at once very naturally, at least in a simple experimental setup (Section 5).

The IGO framework is built to achieve maximal *invariance properties*. Invariance in the search space is related to invariance under θ -reparametrization which is the main idea behind *information geometry* [AN00]. First, the IGO flow is invariant under reparametrization of the family of distributions P_θ , that is, it only depends on P_θ and not on the way we write the parameter θ (Proposition 9). For instance, for Gaussian measures it should not matter

whether we use the covariance matrix or its inverse or a Cholesky factor as the parameter. This limits the influence of encoding choices on the behavior of the algorithm. Second, the IGO flow is invariant under a change of coordinates in the search space X , provided that this change of coordinates globally preserves the family of distributions P_θ (Proposition 10). For instance, for Gaussian distributions on \mathbb{R}^d , this includes all affine changes of coordinates. This means that the algorithm, apart from initialization, does not depend on the precise way the data is presented. Last, IGO algorithms are invariant under applying a strictly increasing function to f (Proposition 8). Contrary to previous formulations using natural gradients [WSPS08, GSS⁺10, ANOK10], this invariance is achieved from the start. Such invariance properties mean that we deal with *intrinsic* properties of the objects themselves, and not with the way we encode them as collections of numbers in \mathbb{R}^d . It also means, most importantly, that we make a minimal number of arbitrary choices.

In Section 1, we define the IGO flow and the IGO algorithm. We begin with standard facts about the definition and basic properties of the natural gradient, and its connection with Kullback–Leibler divergence and diversity. We then proceed to the detailed description of the algorithm.

In Section 2, we state some first mathematical properties of IGO. These include monotone improvement of the objective function, invariance properties, the form of IGO for exponential families of probability distributions, and the case of noisy objective functions.

In Section 3 we explain the theoretical relationships between IGO, maximum likelihood estimates and the cross-entropy method. In particular, IGO is uniquely characterized by a weighted log-likelihood maximization property.

In Section 4, we derive several well-known optimization algorithms from the IGO framework. These include PBIL, versions of CMA-ES and other Gaussian evolutionary algorithms such as EMNA and xNES. This also illustrates how a large step size results in more and more differing algorithms w.r.t. the continuous-time IGO flow. We also study the IGO flow solution on linear functions for discrete and continuous search spaces.

In Section 5, we illustrate how IGO can be used to design new optimization algorithms. As a proof of concept, we derive the IGO algorithm associated with restricted Boltzmann machines for discrete optimization, allowing for multimodal optimization. We perform a preliminary experimental study of the specific influence of the Fisher information matrix on the performance of the algorithm and on diversity of the optima obtained.

In Section 6, we discuss related work, and in particular, IGO’s relationship with and differences from various other optimization algorithms such as natural evolution strategies or the cross-entropy method. We also sum up the main contributions of the paper and the design philosophy of IGO.

1 Algorithm description

We now present the outline of the algorithm. Each step is described in more detail in the sections below.

The IGO flow can be seen as an *estimation of distribution algorithm*: at each time t , we maintain a probability distribution P_{θ^t} on the search space X , where $\theta^t \in \Theta$. The value of θ^t will evolve so that, over time, P_{θ^t} gives more weight to points x with better values of the function $f(x)$ to optimize.

A straightforward way to proceed is to transfer f from x -space to θ -space: define a function $F(\theta)$ as the P_θ -average of f and then do a gradient descent for $F(\theta)$ in space Θ [Ber00b, Ber02, Ber00a, GF05]. This way, θ will converge to a point such that P_θ yields a good average value of f . We depart from this approach in two ways:

- At each time, we replace f with an adaptive transformation of f representing how good or bad observed values of f are relative to other observations. This provides invariance under all monotone transformations of f .
- Instead of the vanilla gradient for θ , we use the so-called *natural gradient* given by the Fisher information matrix. This reflects the intrinsic geometry of the space of probability distributions, as introduced by Rao and Jeffreys [Rao45, Jef46] and later elaborated upon by Amari and others [AN00]. This provides invariance under reparametrization of θ and, importantly, minimizes the change of diversity of P_θ .

The algorithm is constructed in two steps: we first give an “ideal” version, namely, a version in which time t is continuous so that the evolution of θ^t is given by an ordinary differential equation in Θ . Second, the actual algorithm is a time discretization using a finite time step and Monte Carlo sampling instead of exact P_θ -averages.

1.1 The natural gradient on parameter space

About gradients and the shortest path uphill. Let g be a smooth function from \mathbb{R}^d to \mathbb{R} , to be maximized. We first recall the interpretation of gradient ascent as “the shortest path uphill”.

Let $y \in \mathbb{R}^d$. Define the vector z by

$$z = \lim_{\varepsilon \rightarrow 0} \arg \max_{z, \|z\| \leq 1} g(y + \varepsilon z). \quad (1)$$

Then one can check that z is the normalized gradient of g at y : $z_i = \frac{\partial g / \partial y_i}{\|\partial g / \partial y_k\|}$. (This holds only at points y where the gradient of g does not vanish.)

This shows that, for small δt , the well-known gradient ascent of g given by

$$y_i^{t+\delta t} = y_i^t + \delta t \frac{\partial g}{\partial y_i}$$

realizes the largest increase of the value of g , for a given step size $\|y^{t+\delta t} - y^t\|$.

The relation (1) depends on the choice of a norm $\|\cdot\|$ (the gradient of g is given by $\partial g / \partial y_i$ only in an orthonormal basis). If we use, instead of the standard metric $\|y - y'\| = \sqrt{\sum (y_i - y'_i)^2}$ on \mathbb{R}^d , a metric $\|y - y'\|_A = \sqrt{\sum A_{ij}(y_i - y'_i)(y_j - y'_j)}$ defined by a positive definite matrix A_{ij} , then the gradient of g with respect to this metric is given by $\sum_j A_{ij}^{-1} \frac{\partial g}{\partial y_j}$. This follows from the textbook definition of gradients by $g(y + \varepsilon z) = g(y) + \varepsilon \langle \nabla g, z \rangle_A + O(\varepsilon^2)$ with $\langle \cdot, \cdot \rangle_A$ the scalar product associated with the matrix A_{ij} [Sch92].

It is possible to write the analogue of (1) using the A -norm. We then find that the gradient ascent associated with metric A is given by

$$y^{t+\delta t} = y^t + \delta t A^{-1} \frac{\partial g}{\partial y_i},$$

for small δt and maximizes the increment of g for a given A -distance $\|y^{t+\delta t} - y^t\|_A$ —it realizes the steepest A -ascent. Maybe this viewpoint clarifies the

relationship between gradient and metric: this steepest ascent property can actually be used as a definition of gradients.

In our setting we want to use a gradient ascent in the parameter space Θ of our distributions P_θ . The “vanilla” gradient $\frac{\partial}{\partial \theta_i}$ is associated with the metric $\|\theta - \theta'\| = \sqrt{\sum(\theta_i - \theta'_i)^2}$ and clearly depends on the choice of parametrization θ . Thus this metric, and the direction pointed by this gradient, are not intrinsic, in the sense that they do not depend only on the *distribution* P_θ . A metric depending on θ only through the distributions P_θ can be defined as follows.

Fisher information and the natural gradient on parameter space.

Let $\theta, \theta' \in \Theta$ be two values of the distribution parameter. A widely used way to define a “distance” between two generic distributions P_θ and $P_{\theta'}$ is the *Kullback–Leibler divergence* from information theory, defined [Kul97] as

$$\text{KL}(P_{\theta'} \parallel P_\theta) = \int_x \ln \frac{P_{\theta'}(x)}{P_\theta(x)} P_{\theta'}(dx).$$

When $\theta' = \theta + \delta\theta$ is close to θ , under mild smoothness assumptions we can expand the Kullback–Leibler divergence at second order in $\delta\theta$. This expansion defines the Fisher information matrix I at θ [Kul97]:

$$\text{KL}(P_{\theta+\delta\theta} \parallel P_\theta) = \frac{1}{2} \sum I_{ij}(\theta) \delta\theta_i \delta\theta_j + O(\delta\theta^3).$$

An equivalent definition of the Fisher information matrix is by the usual formulas [CT06]

$$I_{ij}(\theta) = \int_x \frac{\partial \ln P_\theta(x)}{\partial \theta_i} \frac{\partial \ln P_\theta(x)}{\partial \theta_j} P_\theta(dx) = - \int_x \frac{\partial^2 \ln P_\theta(x)}{\partial \theta_i \partial \theta_j} P_\theta(dx).$$

The Fisher information matrix defines a (Riemannian) metric on Θ : the distance, in this metric, between two very close values of θ is given by the square root of twice the Kullback–Leibler divergence. Since the Kullback–Leibler divergence depends only on P_θ and not on the parametrization of θ , this metric is intrinsic.

If $g : \Theta \rightarrow \mathbb{R}$ is a smooth function on the parameter space, its *natural gradient* [Ama98] at θ is defined in accordance with the Fisher metric as

$$(\tilde{\nabla}_\theta g)_i = \sum_j I_{ij}^{-1}(\theta) \frac{\partial g(\theta)}{\partial \theta_j}$$

or more synthetically

$$\tilde{\nabla}_\theta g = I^{-1} \frac{\partial g}{\partial \theta}.$$

From now on, we will use $\tilde{\nabla}_\theta$ to denote the natural gradient and $\frac{\partial}{\partial \theta}$ to denote the vanilla gradient.

By construction, the natural gradient descent is intrinsic: it does not depend on the chosen parametrization θ of P_θ , so that it makes sense to speak of the natural gradient ascent of a function $g(P_\theta)$. The Fisher metric is essentially the only way to obtain this property [AN00, Section 2.4].

Given that the Fisher metric comes from the Kullback–Leibler divergence, the “shortest path uphill” property of gradients mentioned above translates as follows (see also [Ama98, Theorem 1]):

Proposition 1. *The natural gradient ascent points in the direction $\delta\theta$ achieving the largest change of the objective function, for a given distance between P_θ and $P_{\theta+\delta\theta}$ in Kullback–Leibler divergence. More precisely, let g be a smooth function on the parameter space Θ . Let $\theta \in \Theta$ be a point where $\tilde{\nabla}g(\theta)$ does not vanish. Then, if*

$$\delta\theta = \frac{\tilde{\nabla}g(\theta)}{\|\tilde{\nabla}g(\theta)\|}$$

is the direction of the natural gradient of g , we have

$$\delta\theta = \lim_{\varepsilon \rightarrow 0} \frac{1}{\varepsilon} \arg \max_{\substack{\delta\theta \text{ such that} \\ \text{KL}(P_{\theta+\delta\theta} \| P_\theta) \leq \varepsilon^2/2}} g(\theta + \delta\theta).$$

Here we have implicitly assumed that the parameter space Θ is such that no two points $\theta \in \Theta$ define the same probability distribution, and the mapping $P_\theta \mapsto \theta$ is continuous.

Why use the Fisher metric gradient for optimization? Relationship to diversity. The first reason for using the natural gradient is its reparametrization invariance, which makes it the only gradient available in a general abstract setting [AN00]. Practically, this invariance also limits the influence of encoding choices on the behavior of the algorithm. More prosaically, the Fisher matrix can be also seen as an *adaptive learning rate* for different components of the parameter vector θ_i : components i with a high impact on P_θ will be updated more cautiously.

Another advantage comes from the relationship with Kullback–Leibler distance in view of the “shortest path uphill” (see also [Ama98]). To minimize the value of some function $g(\theta)$ defined on the parameter space Θ , the naive approach follows a gradient descent for g using the “vanilla” gradient

$$\theta_i^{t+\delta t} = \theta_i^t + \delta t \frac{\partial g}{\partial \theta_i}$$

and, as explained above, this maximizes the increment of g for a given increment $\|\theta^{t+\delta t} - \theta^t\|$. On the other hand, the Fisher gradient

$$\theta_i^{t+\delta t} = \theta_i^t + \delta t I^{-1} \frac{\partial g}{\partial \theta_i}$$

maximizes the increment of g for a given Kullback–Leibler distance $\text{KL}(P_{\theta^{t+\delta t}} \| P_{\theta^t})$.

In particular, if we choose an initial value θ^0 such that P_{θ^0} covers the whole space X uniformly (or a wide portion, in case X is unbounded), the Kullback–Leibler divergence between P_{θ^t} and P_{θ^0} is the Shannon entropy of the uniform distribution minus the Shannon entropy of P_{θ^t} , and so this divergence measures the loss of diversity of P_{θ^t} with respect to the uniform distribution. So following the natural gradient of a function g , starting at or close to the uniform distribution, amounts to optimizing the function g while staying as close as possible to uniform in Kullback–Leibler divergence, i.e., optimizing the function g with *minimal loss of diversity, provided the initial diversity is large*. (This is valid, of course, only at the beginning; once one gets too far from uniform, a better interpretation is minimal *change* of diversity.) On the other hand, the vanilla gradient descent optimizes g with minimal change in the numerical values of the parameter θ , which is of little interest.

So arguably this method realizes the best trade-off between optimization and loss of diversity. (Though, as can be seen from the detailed algorithm

description below, maximization of diversity occurs only greedily at each step, and so there is no guarantee that after a given time, IGO will provide the highest possible diversity for a given objective function value.)

An experimental confirmation of the positive influence of the Fisher matrix on diversity is given in Section 5 below. This may also provide a theoretical explanation to the good performance of CMA-ES.

1.2 IGO: Information-geometric optimization

Quantile rewriting of f . Our original problem is to minimize a function $f : X \rightarrow \mathbb{R}$. A simple way to turn f into a function on Θ is to use the expected value $-\mathbb{E}_{P_\theta} f$ [Ber00b, WSPS08], but expected values can be unduly influenced by extreme values and using them can be rather unstable [Whi89]; moreover $-\mathbb{E}_{P_\theta} f$ is not invariant under increasing transformation of f (this invariance implies we can only compare f -values, not sum them up).

Instead, we take an adaptive, quantile-based approach by first replacing the function f with a monotone rewriting $W_{\theta^t}^f$, depending on the current parameter value θ^t , and then following the gradient of $\mathbb{E}_{P_\theta} W_{\theta^t}^f$, seen as a function of θ . A due choice of $W_{\theta^t}^f$ allows to control the range of the resulting values and achieves the desired invariance. Because the rewriting $W_{\theta^t}^f$ depends on θ^t , it might be viewed as an *adaptive* f -transformation.

The goal is that if $f(x)$ is “small” then $W_\theta^f(x) \in \mathbb{R}$ is “large” and vice versa, and that W_θ^f remains invariant under increasing transformations of f . The meaning of “small” or “large” depends on $\theta \in \Theta$ and is taken with respect to typical values of f under the current distribution P_θ . This is measured by the P_θ -quantile in which the value of $f(x)$ lies.

Definition 2. *The lower and upper P_θ - f -quantiles of $x \in X$ are defined as*

$$\begin{aligned} q_\theta^<(x) &= \Pr_{x' \sim P_\theta}(f(x') < f(x)) \\ q_\theta^\leq(x) &= \Pr_{x' \sim P_\theta}(f(x') \leq f(x)) . \end{aligned} \quad (2)$$

Let $w : [0; 1] \rightarrow \mathbb{R}$ be a non-increasing function, the selection scheme.

The transform $W_\theta^f(x)$ of an objective function $f : X \rightarrow \mathbb{R}$ is defined as a function of the P_θ - f -quantile of x as

$$W_\theta^f(x) = \begin{cases} w(q_\theta^\leq(x)) & \text{if } q_\theta^\leq(x) = q_\theta^<(x), \\ \frac{1}{q_\theta^\leq(x) - q_\theta^<(x)} \int_{q=q_\theta^<(x)}^{q=q_\theta^\leq(x)} w(q) \, dq & \text{otherwise.} \end{cases} \quad (3)$$

The quantile functions q reflect the probability to sample a better value than $f(x)$. They are monotone in f (if $f(x_1) \leq f(x_2)$ then $q_\theta^<(x_1) \leq q_\theta^<(x_2)$, and likewise for q_θ^\leq) and invariant under strictly increasing transformations of f .

A typical choice for w is $w(q) = 1_{q \leq q_0}$ for some fixed value q_0 , the *selection quantile*. In what follows, we suppose that a selection scheme has been chosen once and for all.

As desired, the definition of W_θ^f is invariant under a strictly increasing transformation of f . For instance, the P_θ -median of f gets remapped to $w(\frac{1}{2})$.

Note that $\mathbb{E}_{x \sim P_\theta} W_\theta^f(x)$ is always equal to $\int_0^1 w$, independently of f and θ : indeed, by definition, the P_θ -quantile of a random point under P_θ is uniformly distributed in $[0; 1]$. In the following, our objective will be to maximize the expected value of $W_{\theta^t}^f$ over θ , that is, to maximize

$$\mathbb{E}_{P_\theta} W_{\theta^t}^f = \int W_{\theta^t}^f(x) P_\theta(dx) \quad (4)$$

over θ , where θ^t is fixed at a given step but will adapt over time.

Importantly, $W_\theta^f(x)$ can be estimated in practice: indeed, the quantiles $\Pr_{x' \sim P_\theta}(f(x') < f(x))$ can be estimated by taking samples of P_θ and ordering the samples according to the value of f (see below). The estimate remains invariant under strictly increasing f -transformations.

The IGO gradient flow. At the most abstract level, IGO is a continuous-time gradient flow in the parameter space Θ , which we define now. In practice, discrete time steps (a.k.a. iterations) are used, and P_θ -integrals are approximated through sampling, as described in the next section.

Let θ^t be the current value of the parameter at time t , and let $\delta t \ll 1$. We define $\theta^{t+\delta t}$ in such a way as to increase the P_θ -weight of points where f is small, while not going too far from P_{θ^t} in Kullback–Leibler divergence. We use the adaptive weights $W_{\theta^t}^f$ as a way to measure which points have large or small values. In accordance with (4), this suggests taking the gradient ascent

$$\theta^{t+\delta t} = \theta^t + \delta t \tilde{\nabla}_\theta \int W_{\theta^t}^f(x) P_\theta(dx) \quad (5)$$

where the natural gradient is suggested by Proposition 1.

Note again that we use $W_{\theta^t}^f$ and not W_θ^f in the integral. So the gradient $\tilde{\nabla}_\theta$ does not act on the adaptive objective $W_{\theta^t}^f$. If we used W_θ^f instead, we would face a paradox: right after a move, previously good points do not seem so good any more since the distribution has improved. More precisely, $\int W_\theta^f(x) P_\theta(dx)$ is constant and always equal to the average weight $\int_0^1 w$, and so the gradient would always vanish.

Using the log-likelihood trick $\tilde{\nabla} P_\theta = P_\theta \tilde{\nabla} \ln P_\theta$ (assuming P_θ is smooth), we get an equivalent expression of the update above as an integral under the current distribution P_{θ^t} ; this is important for practical implementation. This leads to the following definition.

Definition 3 (IGO flow). *The IGO flow is the set of continuous-time trajectories in space Θ , defined by the ordinary differential equation*

$$\frac{d\theta^t}{dt} = \tilde{\nabla}_\theta \int W_{\theta^t}^f(x) P_\theta(dx) \quad (6)$$

$$= \int W_{\theta^t}^f(x) \tilde{\nabla}_\theta \ln P_\theta(x) P_{\theta^t}(dx) \quad (7)$$

$$= I^{-1}(\theta^t) \int W_{\theta^t}^f(x) \frac{\partial \ln P_\theta(x)}{\partial \theta} P_{\theta^t}(dx). \quad (8)$$

where the gradients are taken at point $\theta = \theta^t$, and I is the Fisher information matrix.

Natural evolution strategies (NES, [WSPS08, GSS⁺10, SWSS09]) feature a related gradient *descent* with $f(x)$ instead of $W_{\theta^t}^f(x)$. The associated flow would read

$$\frac{d\theta^t}{dt} = -\tilde{\nabla}_\theta \int f(x) P_\theta(dx) , \quad (9)$$

where the gradient is taken at θ^t (in the sequel when not explicitly stated, gradients in θ are taken at $\theta = \theta^t$). However, in the end NESs always implement algorithms using sample quantiles, as if derived from the gradient ascent of $W_{\theta^t}^f(x)$.

The update (7) is a weighted average of “intrinsic moves” increasing the log-likelihood of some points. We can slightly rearrange the update as

$$\frac{d\theta^t}{dt} = \int \underbrace{W_{\theta^t}^f(x)}_{\text{preference weight}} \underbrace{\tilde{\nabla}_\theta \ln P_\theta(x)}_{\text{current sample distribution}} \underbrace{P_{\theta^t}(dx)}_{\text{intrinsic move to reinforce } x} \quad (10)$$

$$= \tilde{\nabla}_\theta \int \underbrace{W_{\theta^t}^f(x) \ln P_\theta(x)}_{\text{weighted log-likelihood}} P_{\theta^t}(dx). \quad (11)$$

which provides an interpretation for the IGO gradient flow as a gradient ascent optimization of the weighted log-likelihood of the “good points” of the current distribution. In a precise sense, IGO is in fact the “best” way to increase this log-likelihood (Theorem 14).

For exponential families of probability distributions, we will see later that the IGO flow rewrites as a nice derivative-free expression (19).

IGO algorithms: time discretization and sampling. The above is a mathematically well-defined continuous-time flow in parameter space. Its practical implementation involves three approximations depending on two parameters N and δt :

- the integral under P_{θ^t} is approximated using N samples taken from P_{θ^t} ;
- the value $W_{\theta^t}^f$ is approximated for each sample taken from P_{θ^t} ;
- the time derivative $\frac{d\theta^t}{dt}$ is approximated by a δt time increment.

We also assume that the Fisher information matrix $I(\theta)$ and $\frac{\partial \ln P_\theta(x)}{\partial \theta}$ can be computed (see discussion below if $I(\theta)$ is unknown).

At each step, we draw N samples x_1, \dots, x_N under P_{θ^t} . To approximate the quantiles, we rank the samples according to the value of f . Define $\text{rk}(x_i) = \#\{j, f(x_j) < f(x_i)\}$ and let the estimated weight of sample x_i be

$$\hat{w}_i = \frac{1}{N} w \left(\frac{\text{rk}(x_i) + 1/2}{N} \right), \quad (12)$$

using the selection scheme function w introduced above. (This is assuming there are no ties in our sample; in case several sample points have the same value of f , we define \hat{w}_i by averaging the above over all possible rankings of the ties¹.)

Then we can approximate the IGO flow as follows.

Definition 4 (IGO algorithms). *The IGO algorithm associated with parametrization θ , sample size N and step size δt is the following update rule for the parameter θ^t . At each step, N sample points x_1, \dots, x_N are drawn according to the distribution P_{θ^t} . The parameter is updated according to*

$$\theta^{t+\delta t} = \theta^t + \delta t \sum_{i=1}^N \hat{w}_i \tilde{\nabla}_\theta \ln P_\theta(x_i) \Big|_{\theta=\theta^t} \quad (14)$$

$$= \theta^t + \delta t I^{-1}(\theta^t) \sum_{i=1}^N \hat{w}_i \frac{\partial \ln P_\theta(x_i)}{\partial \theta} \Big|_{\theta=\theta^t} \quad (15)$$

¹A mathematically neater but less intuitive version would be

$$\hat{w}_i = \frac{1}{\text{rk}^{\leq}(x_i) - \text{rk}^{<}(x_i)} \int_{u=\text{rk}^{<}(x_i)/N}^{u=\text{rk}^{\leq}(x_i)/N} w(u) du \quad (13)$$

with $\text{rk}^{<}(x_i) = \#\{j, f(x_j) < f(x_i)\}$ and $\text{rk}^{\leq}(x_i) = \#\{j, f(x_j) \leq f(x_i)\}$.

where \widehat{w}_i is the weight (12) obtained from the ranked values of the objective function f .

Equivalently one can fix the weights $w_i = \frac{1}{N} w\left(\frac{i-1/2}{N}\right)$ once and for all and rewrite the update as

$$\theta^{t+\delta t} = \theta^t + \delta t I^{-1}(\theta^t) \sum_{i=1}^N w_i \left. \frac{\partial \ln P_\theta(x_{i:N})}{\partial \theta} \right|_{\theta=\theta^t} \quad (16)$$

where $x_{i:N}$ denotes the i^{th} sampled point ranked according to f , i.e. $f(x_{1:N}) < \dots < f(x_{N:N})$ (assuming again there are no ties). Note that $\{x_{i:N}\} = \{x_i\}$ and $\{w_i\} = \{\widehat{w}_i\}$.

As will be discussed in Section 4, this update applied to multivariate normal distributions or Bernoulli measures allows to neatly recover versions of some well-established algorithms, in particular CMA-ES and PBIL. Actually, in the Gaussian context updates of the form (15) have already been introduced [GSS⁺10, ANOK10], though not formally derived from a continuous-time flow with quantiles.

When $N \rightarrow \infty$, the IGO algorithm using samples approximates the continuous-time IGO gradient flow, see Theorem 5 below. Indeed, the IGO algorithm, with $N = \infty$, is simply the Euler approximation scheme for the ordinary differential equation defining the IGO flow (6). The latter result thus provides a sound mathematical basis for currently used rank-based updates.

IGO flow versus IGO algorithms. The IGO flow (6) is a well-defined continuous-time set of trajectories in the space of probability distributions P_θ , depending only on the objective function f and the chosen family of distributions. It does not depend on the chosen parametrization for θ (Proposition 9).

On the other hand, there are several IGO *algorithms* associated with this flow. Each IGO algorithm approximates the IGO flow in a slightly different way. An IGO algorithm depends on three further choices: a sample size N , a time discretization step size δt , and a choice of parametrization for θ in which to implement (15).

If δt is small enough, and N large enough, the influence of the parametrization θ disappears and all IGO algorithms are approximations of the “ideal” IGO flow trajectory. However, the larger δt , the poorer the approximation gets.

So for large δt , different IGO algorithms for the same IGO flow may exhibit different behaviors. We will see an instance of this phenomenon for Gaussian distributions: both CMA-ES and the maximum likelihood update (EMNA) can be seen as IGO algorithms, but the latter with $\delta t = 1$ is known to exhibit premature loss of diversity (Section 4.2).

Still, two IGO algorithms for the same IGO flow will differ less from each other than from a non-IGO algorithm: at each step the difference is only $O(\delta t^2)$ (Section 2.4). On the other hand, for instance, the difference between an IGO algorithm and the vanilla gradient ascent is, generally, not smaller than $O(\delta t)$ at each step, i.e. roughly as big as the steps themselves.

Unknown Fisher matrix. The algorithm presented so far assumes that the Fisher matrix $I(\theta)$ is known as a function of θ . This is the case for Gaussian distributions in CMA-ES and for Bernoulli distributions. However, for restricted Boltzmann machines as considered below, no analytical

form is known. Yet, provided the quantity $\frac{\partial}{\partial \theta} \ln P_\theta(x)$ can be computed or approximated, it is possible to approximate the integral

$$I_{ij}(\theta) = \int_x \frac{\partial \ln P_\theta(x)}{\partial \theta_i} \frac{\partial \ln P_\theta(x)}{\partial \theta_j} P_\theta(dx)$$

using P_θ -Monte Carlo samples for x . These samples may or may not be the same as those used in the IGO update (15): in particular, it is possible to use as many Monte Carlo samples as necessary to approximate I_{ij} , at no additional cost in terms of the number of calls to the black-box function f to optimize.

Note that each Monte Carlo sample x will contribute $\frac{\partial \ln P_\theta(x)}{\partial \theta_i} \frac{\partial \ln P_\theta(x)}{\partial \theta_j}$ to the Fisher matrix approximation. This is a rank-1 non-negative matrix². So, for the approximated Fisher matrix to be invertible, the number of (distinct) samples x needs to be at least equal to, and ideally much larger than, the number of components of the parameter θ : $N_{\text{Fisher}} \geq \dim \Theta$.

For exponential families of distributions, the IGO update has a particular form (19) which simplifies this matter somewhat. More details are given below (see Section 5) for the concrete situation of restricted Boltzmann machines.

2 First properties of IGO

2.1 Consistency of sampling

The first property to check is that when $N \rightarrow \infty$, the update rule using N samples converges to the IGO update rule. This is *not* a straightforward application of the law of large numbers, because the estimated weights \hat{w}_i depend (non-continuously) on the whole sample x_1, \dots, x_N , and not only on x_i .

Theorem 5 (Consistency). *When $N \rightarrow \infty$, the N -sample IGO update rule (15):*

$$\theta^{t+\delta t} = \theta^t + \delta t I^{-1}(\theta^t) \sum_{i=1}^N \hat{w}_i \left. \frac{\partial \ln P_\theta(x_i)}{\partial \theta} \right|_{\theta=\theta^t}$$

converges with probability 1 to the update rule (5):

$$\theta^{t+\delta t} = \theta^t + \delta t \tilde{\nabla}_\theta \int W_{\theta^t}^f(x) P_\theta(dx).$$

The proof is given in the Appendix, under mild regularity assumptions. In particular we do not require that w be continuous.

This theorem may clarify previous claims [WSPS08, ANOK10] where rank-based updates similar to (5), such as in NES or CMA-ES, were derived from optimizing the expected value $-\mathbb{E}_{P_\theta} f$. The rank-based weights \hat{w}_i were then introduced somewhat arbitrarily. Theorem 5 shows that, for large N , CMA-ES and NES actually follow the gradient flow of the quantity $\mathbb{E}_{P_\theta} W_{\theta^t}^f$: the update can be rigorously derived from optimizing the expected value of the quantile-rewriting $W_{\theta^t}^f$.

²The alternative, equivalent formula $I_{ij}(\theta) = -\int_x \frac{\partial^2 \ln P_\theta(x)}{\partial \theta_i \partial \theta_j} P_\theta(dx)$ for the Fisher matrix would not necessarily yield non-negative matrices through Monte Carlo sampling.

2.2 Monotonicity: quantile improvement

Gradient descents come with a guarantee that the fitness value decreases over time. Here, since we work with probability distributions on X , we need to define a “fitness” of the distribution $P_{\theta t}$. An obvious choice is the expectation $\mathbb{E}_{P_{\theta t}} f$, but it is not invariant under f -transformation and moreover may be sensitive to extreme values.

It turns out that the monotonicity properties of the IGO gradient flow depend on the choice of the selection scheme w . For instance, if $w(u) = 1_{u \leq 1/2}$, then the median of f under $P_{\theta t}$ improves over time.

Proposition 6 (Quantile improvement). *Consider the IGO flow (6), with the weight $w(u) = 1_{u \leq q}$ where $0 < q < 1$ is fixed. Then the value of the q -quantile of f improves over time: if $t_1 \leq t_2$ then $Q_{P_{\theta t_2}}^q(f) \leq Q_{P_{\theta t_1}}^q(f)$. Here the q -quantile value $Q_P^q(f)$ of f under a probability distribution P is defined as the largest number m such that $\Pr_{x \sim P}(f(x) \geq m) \geq 1 - q$.*

Assume moreover that the objective function f has no plateau, i.e. for any $v \in \mathbb{R}$ and any $\theta \in \Theta$ we have $\Pr_{x \sim P_\theta}(f(x) = v) = 0$. Then for $t_1 < t_2$ either $\theta^{t_1} = \theta^{t_2}$ or $Q_{P_{\theta^{t_2}}}^q(f) < Q_{P_{\theta^{t_1}}}^q(f)$.

The proof is given in the Appendix, together with the necessary regularity assumptions. Note that on a discrete search space, the objective function has only plateaus, and the q -quantile will evolve by successive jumps even as θ evolves continuously.

Of course this property holds only for the IGO gradient flow (6) with $N = \infty$ and $\delta t \rightarrow 0$. For an IGO algorithm with finite N , the dynamics is random and one cannot expect monotonicity. Still, Theorem 5 ensures that, with high probability, trajectories of a large enough finite population stay close to the infinite-population limit trajectory.

2.3 The IGO flow for exponential families

The expressions for the IGO update simplify somewhat if the family P_θ happens to be an exponential family of probability distributions (see also [MMS08, MMP11] for optimization using the natural gradient for exponential families). Suppose that P_θ can be written as

$$P_\theta(x) = \frac{1}{Z(\theta)} \exp\left(\sum \theta_i T_i(x)\right) H(dx)$$

where T_1, \dots, T_k is a finite family of functions on X , $H(dx)$ is an arbitrary reference measure on X , and $Z(\theta)$ is the normalization constant. It is well-known [AN00, (2.33)] that

$$\frac{\partial \ln P_\theta(x)}{\partial \theta_i} = T_i(x) - \mathbb{E}_{P_\theta} T_i \quad (17)$$

so that [AN00, (3.59)]

$$I_{ij}(\theta) = \text{Cov}_{P_\theta}(T_i, T_j). \quad (18)$$

Consequently we find:

Proposition 7. *Let P_θ be an exponential family parametrized by the natural parameters θ as above. Then the IGO flow is given by*

$$\frac{d\theta}{dt} = \text{Cov}_{P_\theta}(T, T)^{-1} \text{Cov}_{P_\theta}(T, W_\theta^f) \quad (19)$$

where $\text{Cov}_{P_\theta}(T, W_\theta^f)$ denotes the vector $(\text{Cov}_{P_\theta}(T_i, W_\theta^f))_i$, and $\text{Cov}_{P_\theta}(T, T)$ the matrix $(\text{Cov}_{P_\theta}(T_i, T_j))_{ij}$.

Note that the right-hand side does not involve derivatives w.r.t. θ any more. This result makes it easy to simulate the IGO flow using, e.g., a Gibbs sampler for P_θ : both covariances in (19) may be approximated by sampling, so that neither the Fisher matrix nor the gradient term need to be known in advance, and no derivatives are involved.

The CMA-ES uses the family of all Gaussian distributions on \mathbb{R}^d . Then, the family T_i is the family of all linear and quadratic functions of the coordinates on \mathbb{R}^d . The expression above is then a particularly concise rewriting of a CMA-ES update, see also Section 4.2.

The values of the variables $\bar{T}_i = \mathbb{E}T_i$, namely the expected value of T_i under the current distribution, can often be used as an alternative parametrization for an exponential family (e.g. for a one-dimensional Gaussian, these are the mean μ and the second moment $\mu^2 + \sigma^2$). The IGO flow (7) may be rewritten using these variables, using the relation $\tilde{\nabla}_{\theta_i} = \frac{\partial}{\partial \bar{T}_i}$ for the natural gradient of exponential families (Appendix, Proposition 27). One finds that the variables \bar{T}_i satisfy the simple evolution equation under the IGO flow

$$\frac{d\bar{T}_i}{dt} = \text{Cov}(T_i, W_\theta^f) = \mathbb{E}(T_i W_\theta^f) - \bar{T}_i \mathbb{E}W_\theta^f. \quad (20)$$

The proof is given in the Appendix, in the proof of Theorem 16. We shall further exploit this fact in Section 3.

Exponential families with latent variables. Similar formulas hold when the distribution $P_\theta(x)$ is the marginal of an exponential distribution $P_\theta(x, h)$ over a “hidden” or “latent” variable h , such as the restricted Boltzmann machines of Section 5.

Namely, with $P_\theta(x) = \frac{1}{Z(\theta)} \sum_h \exp(\sum_i \theta_i T_i(x, h)) H(dx, dh)$ we have

$$\frac{\partial \ln P_\theta(x)}{\partial \theta_i} = U_i(x) - \mathbb{E}_{P_\theta} U_i \quad (21)$$

where

$$U_i(x) = \mathbb{E}_{P_\theta}(T_i(x, h)|x) \quad (22)$$

is the expectation of $T_i(x, h)$ knowing x . Then the Fisher matrix is

$$I_{ij}(\theta) = \text{Cov}_{P_\theta}(U_i, U_j) \quad (23)$$

and consequently, the IGO flow takes the form

$$\frac{d\theta}{dt} = \text{Cov}_{P_\theta}(U, U)^{-1} \text{Cov}_{P_\theta}(U, W_\theta^f). \quad (24)$$

2.4 Invariance properties

Here we formally state the invariance properties of the IGO flow under various reparametrizations. Since these results follow from the very construction of the algorithm, the proofs are omitted.

Proposition 8 (*f*-invariance). *Let $\varphi : \mathbb{R} \rightarrow \mathbb{R}$ be a strictly increasing function. Then the trajectories of the IGO flow when optimizing the functions f and $\varphi(f)$ are the same.*

The same is true for the discretized algorithm with population size N and step size $\delta t > 0$.

Proposition 9 (θ -invariance). *Let $\theta' = \varphi(\theta)$ be a bijective function of θ and let $P'_{\theta'} = P_{\varphi^{-1}(\theta')}$. Let θ^t be the trajectory of the IGO flow when optimizing a function f using the distributions P_{θ} , initialized at θ^0 . Then the IGO flow trajectory $(\theta')^t$ obtained from the optimization of the function f using the distributions $P'_{\theta'}$, initialized at $(\theta')^0 = \varphi(\theta^0)$, is the same, namely $(\theta')^t = \varphi(\theta^t)$.*

For the algorithm with finite N and $\delta t > 0$, invariance under reparametrization of θ is only true approximately, in the limit when $\delta t \rightarrow 0$. As mentioned above, the IGO update (15), with $N = \infty$, is simply the Euler approximation scheme for the ordinary differential equation (6) defining the IGO flow. At each step, the Euler scheme is known to make an error $O(\delta t^2)$ with respect to the true flow. This error actually depends on the parametrization of θ .

So the IGO updates for different parametrizations coincide at first order in δt , and may, in general, differ by $O(\delta t^2)$. For instance the difference between the CMA-ES and xNES updates is indeed $O(\delta t^2)$, see Section 4.2.

For comparison, using the vanilla gradient results in a divergence of $O(\delta t)$ at each step between different parametrizations, so this divergence could be of the same magnitude as the steps themselves.

In that sense, one can say that IGO algorithms are “more parametrization-invariant” than other algorithms. This stems from their origin as a discretization of the IGO flow.

However, if the map φ is affine then this phenomenon disappears: parametrizations that differ by an affine map on θ yield the same IGO algorithm.

The next proposition states that, for example, if one uses a family of distributions on \mathbb{R}^d which is invariant under affine transformations, then IGO algorithms optimize equally well a function and its image under any affine transformation (up to an obvious change in the initialization). This proposition generalizes the well-known corresponding property of CMA-ES [HO01].

Here, as usual, the image of a probability distribution P by a transformation $\varphi : X \rightarrow X$ is defined as the probability distribution P' such that $P'(Y) = P(\varphi^{-1}(Y))$ for any subset $Y \subset X$. In the continuous domain, the density of the new distribution P' is obtained by the usual change of variable formula involving the Jacobian of φ .

We say that a transformation $\varphi : X \rightarrow X$ *globally preserves* a family of probability distributions (P_{θ}) , if the image of any P_{θ} by φ is equal to some distribution $P_{\theta'}$ in the same family, and if moreover the correspondence $\theta \mapsto \theta'$ is locally a diffeomorphism.

Proposition 10 (X -invariance). *Let $\varphi : X \rightarrow X$ be a one-to-one transformation of the search space which globally preserves the family of measures P_{θ} . Let θ^t be the IGO flow trajectory for the optimization of function f , initialized at P_{θ^0} . Let $(\theta')^t$ be the IGO flow trajectory for optimization of $f \circ \varphi^{-1}$, initialized at the image of P_{θ^0} by φ . Then $P_{(\theta')^t}$ is the image of P_{θ^t} by φ .*

For the discretized algorithm with population size N and step size $\delta t > 0$, the same is true up to an error of $O(\delta t^2)$ per iteration. This error disappears if the map φ acts on Θ in an affine way.

The latter case of affine transforms is well exemplified by CMA-ES: here, using the variance and mean as the parametrization of Gaussians, the new mean and variance after an affine transform of the search space are an affine

function of the old mean and variance; specifically, for the affine transformation $A : x \mapsto Ax + b$ we have $(m, C) \mapsto (Am + b, ACA^\top)$. Another example, on the discrete search space $X = \{0, 1\}^d$, is the exchange of 0 and 1: for reasonable choices of the family P_θ , the IGO flow and IGO algorithms will be invariant under such a change in the way the data is presented.

2.5 Speed of the IGO flow

Proposition 11. *The speed of the IGO flow, i.e. the norm of $\frac{d\theta^t}{dt}$ in the Fisher metric, is at most $\sqrt{\int_0^1 w^2 - (\int_0^1 w)^2}$ where w is the selection scheme.*

The proof is given in the Appendix.

A bounded speed means that the IGO flow will not explode in finite time, or go out-of-domain if the Fisher metric on the statistical manifold Θ is complete (for instance, the IGO flow on Gaussian distributions will not yield non-positive or degenerate covariance matrices). Due to the approximation terms $O(\delta t^2)$, this may not be true of IGO algorithms.

This speed can be monitored in practice in at least two ways. The first is just to compute the Fisher norm of the increment $\theta^{t+\delta t} - \theta^t$ using the Fisher matrix; for small δt this is close to $\delta t \|\frac{d\theta}{dt}\|$ with $\|\cdot\|$ the Fisher metric. The second is as follows: since the Fisher metric coincides with the Kullback–Leibler divergence up to a factor 1/2, we have $\text{KL}(P_{\theta^{t+\delta t}} \| P_{\theta^t}) \approx \frac{1}{2} \delta t^2 \|\frac{d\theta}{dt}\|^2$ at least for small δt . Since it is relatively easy to estimate $\text{KL}(P_{\theta^{t+\delta t}} \| P_{\theta^t})$ by comparing the new and old log-likelihoods of points in a Monte Carlo sample, one can obtain an estimate of $\|\frac{d\theta}{dt}\|$.

Corollary 12. *Consider an IGO algorithm with selection scheme w , step size δt and sample size N . Then, for small δt and large N we have*

$$\text{KL}(P_{\theta^{t+\delta t}} \| P_{\theta^t}) \leq \frac{1}{2} \delta t^2 \text{Var}_{[0,1]} w + O(\delta t^3) + o(1)_{N \rightarrow \infty}.$$

For instance, with $w(q) = 1_{q \leq q_0}$ and neglecting the error terms, an IGO algorithm introduces at most $\frac{1}{2} \delta t^2 q_0(1 - q_0)$ bits of information (in base e) per iteration into the probability distribution P_θ .

Thus, the time discretization parameter δt is not just an arbitrary variable: it has an intrinsic interpretation related to a number of bits introduced at each step of the algorithm. This kind of relationship suggests, more generally, to use the Kullback–Leibler divergence as an external and objective way to measure learning rates in those optimization algorithms which use probability distributions.

The result above is only an upper bound. Maximal speed can be achieved only if all “good” points point in the same direction. If the various good points in the sample suggest moves in inconsistent directions, then the IGO update will be much smaller. While non-consistent moves are generally to be expected if $N < \dim \Theta$, it may also be a sign that the signal is noisy, or that the family of distributions P_θ is not well suited to the problem at hand and should be enriched.

As an example, using a family of Gaussian distributions with unknown mean and fixed identity variance on \mathbb{R}^d , one checks that for the optimization of a linear function on \mathbb{R}^d , with the weight $w(u) = -1_{u > 1/2} + 1_{u < 1/2}$, the IGO flow moves at constant speed $1/\sqrt{2\pi} \approx 0.4$, whatever the dimension d . On a rapidly varying sinusoidal function, the moving speed will be much slower because there are “good” and “bad” points in all directions.

This may suggest ways to design the selection scheme w to achieve maximal speed in some instances. Indeed, looking at the proof of the proposition, which involves a Cauchy–Schwarz inequality, one can see that the maximal speed is achieved only if there is a linear relationship between the weights $W_\theta^f(x)$ and the gradient $\tilde{\nabla}_\theta \ln P_\theta(x)$. For instance, for the optimization of a linear function on \mathbb{R}^d using Gaussian measures of known variance, the maximal speed will be achieved when the selection scheme $w(u)$ is the inverse of the Gaussian cumulative distribution function. (In particular, $w(u)$ tends to $+\infty$ when $u \rightarrow 0$ and to $-\infty$ when $u \rightarrow 1$.) This is in accordance with previously known results: the expected value of the i -th order statistic of N standard Gaussian variates is the optimal \hat{w}_i value in evolution strategies [Bey01, Arn06]. For $N \rightarrow \infty$, this order statistic converges to the inverse Gaussian cumulative distribution function.

2.6 Noisy objective function

Suppose that the objective function f is non-deterministic: each time we ask for the value of f at a point $x \in X$, we get a random result. In this setting we may write the random value $f(x)$ as $f(x) = \tilde{f}(x, \omega)$ where ω is an unseen random parameter, and \tilde{f} is a deterministic function of x and ω . Without loss of generality, up to a change of variables we can assume that ω is uniformly distributed in $[0, 1]$.

We can still use the IGO algorithm without modification in this context. One might wonder which properties (consistency of sampling, etc.) still apply when f is not deterministic. Actually, IGO algorithms for noisy functions fit very nicely into the IGO framework: the following proposition allows to transfer any property of IGO to the case of noisy functions.

Proposition 13 (Noisy IGO). *Let f be a random function of $x \in X$, namely, $f(x) = \tilde{f}(x, \omega)$ where ω is a random variable uniformly distributed in $[0, 1]$, and \tilde{f} is a deterministic function of x and ω . Then the two following algorithms coincide:*

- *The IGO algorithm (14), using a family of distributions P_θ on space X , applied to the noisy function f , and where the samples are ranked according to the random observed value of f (here we assume that, for each sample, the noise ω is independent from everything else);*
- *The IGO algorithm on space $X \times [0, 1]$, using the family of distributions $\tilde{P}_\theta = P_\theta \otimes U_{[0,1]}$, applied to the deterministic function \tilde{f} . Here $U_{[0,1]}$ denotes the uniform law on $[0, 1]$.*

The (easy) proof is given in the Appendix.

This proposition states that noisy optimization is the same as ordinary optimization using a family of distributions which cannot operate any selection or convergence over the parameter ω . More generally, any component of the search space in which a distribution-based evolutionary strategy cannot perform selection or specialization will effectively act as a random noise on the objective function.

As a consequence of this result, all properties of IGO can be transferred to the noisy case. Consider, for instance, consistency of sampling (Theorem 5). The N -sample IGO update rule for the noisy case is identical to the non-noisy case (15):

$$\theta^{t+\delta t} = \theta^t + \delta t I^{-1}(\theta^t) \sum_{i=1}^N \hat{w}_i \left. \frac{\partial \ln P_\theta(x_i)}{\partial \theta} \right|_{\theta=\theta^t}$$

where each weight \hat{w}_i computed from (12) now incorporates noise from the objective function because the rank of x_i is computed on the random function, or equivalently on the deterministic function \tilde{f} : $\text{rk}(x_i) = \#\{j, \tilde{f}(x_j, \omega_j) < \tilde{f}(x_i, \omega_i)\}$.

Consistency of sampling (Theorem 5) thus takes the following form: When $N \rightarrow \infty$, the N -sample IGO update rule on the noisy function f converges with probability 1 to the update rule

$$\begin{aligned} \theta^{t+\delta t} &= \theta^t + \delta t \tilde{\nabla}_\theta \int_0^1 \int W_{\theta^t}^{\tilde{f}}(x, \omega) P_\theta(\mathrm{d}x) \mathrm{d}\omega. \\ &= \theta^t + \delta t \tilde{\nabla}_\theta \int \bar{W}_{\theta^t}^f(x) P_\theta(\mathrm{d}x) \end{aligned} \quad (25)$$

where $\bar{W}_\theta^f(x) = \mathbb{E}_\omega W_\theta^{\tilde{f}}(x, \omega)$. This entails, in particular, that when $N \rightarrow \infty$, the noise disappears asymptotically, as could be expected.

Note that there are a priori two ways to define the IGO flow in the noisy case, depending on whether one applies the selection function w to the observed quantile of the noisy value observed for x , or whether one applies the selection function w to the average quantile in which a point x lies. Consistency as just written suggests to define the IGO flow in the noisy case as the $\delta t \rightarrow 0$ limit of the update (25), that is, as the gradient flow of $\mathbb{E}_\theta \bar{W}_{\theta^t}^f(x)$, with \bar{W} as above; this version using \bar{W} is the $N \rightarrow \infty$ limit of the algorithm in which one directly applies the selection scheme to the observed noisy values $\tilde{f}(x, \omega)$. The other option would have been to formally apply Definition 2 unchanged: indeed the quantiles $q_\theta(x)$ defined by (2) are the probabilities that another point x' yields a smaller value of f , which still make sense in the noisy case where f is a random variable; thus the quantiles $q_\theta(x)$ from (2) are deterministic functions of x taking into account the average effect of noise; then, $W_\theta^f(x)$ can also be defined by (3) and is deterministic, and we could take its gradient flow. These two options coincide only when the selection scheme $w(q)$ is affine; in general $\bar{W}_\theta^f(x)$ is different from $W_\theta^f(x)$. This second version would be the $N \rightarrow \infty$ limit of a slightly more complex algorithm using several evaluations of f for each sample x_i in order to compute noise-free ranks and quantiles.

2.7 Implementation remarks

Influence of the selection scheme w . The selection scheme w directly affects the update rule (16).

A natural choice is $w(u) = 1_{u \leq q}$. This, as we have proved, results in an improvement of the q -quantile over the course of optimization. Taking $q = 1/2$ springs to mind; however, this is not selective enough, and both theory and experiments confirm that for the Gaussian case (CMA-ES), most efficient optimization requires $q < 1/2$ (see Section 4.2). The optimal q is about 0.27 if N is not larger than the search space dimension d [Bey01] and even smaller otherwise [JA10].

Second, replacing w with $w+c$ for some constant c clearly has no influence on the IGO continuous-time flow (5), since the gradient will cancel out the constant. However, this is not the case for the update rule (16) with a finite sample of size N .

Indeed, adding a constant c to w adds a quantity $c \frac{1}{N} \sum \tilde{\nabla}_\theta \ln P_\theta(x_i)$ to the update. In expectation, this quantity vanishes because the P_θ -expected value of $\tilde{\nabla}_\theta \ln P_\theta$ is 0 (because $\int (\tilde{\nabla}_\theta \ln P_\theta) P_\theta = \int \tilde{\nabla}_\theta P_\theta = \tilde{\nabla}_\theta 1 = 0$). So adding a constant to w does not change the expected value of the update, but it

may change, e.g., its variance. The empirical average of $\tilde{\nabla}_\theta \ln P_\theta(x_i)$ in the sample will be $O(1/\sqrt{N})$. So translating the weights results in a $O(1/\sqrt{N})$ change in the update. See also Section 4 in [SWSS09].

Thus, one may be tempted to introduce a non-zero value of c so as to reduce the variance of the update. However, determining an optimal value for c is difficult: the optimal value actually depends on possible correlations between $\tilde{\nabla}_\theta \ln P_\theta$ and the function f . The only general result is that one should shift w so that 0 lies within its range. Assuming independence, or dependence with enough symmetry, the optimal shift is when the weights average to 0.

Complexity. The complexity of the IGO algorithm depends much on the computational cost model. In optimization, it is fairly common to assume that the objective function f is very costly compared to any other calculations performed by the algorithm [MGH81, DM02]. Then the cost of IGO in terms of number of f -calls is N per iteration, and the cost of using quantiles and computing the natural gradient is negligible.

Setting the cost of f aside, the complexity of the IGO algorithm depends mainly on the computation of the (inverse) Fisher matrix. Assume an analytical expression for this matrix is known. Then, with $p = \dim \Theta$ the number of parameters, the cost of storage of the Fisher matrix is $O(p^2)$ per iteration, and its inversion typically costs $O(p^3)$ per iteration. However, depending on the situation and on possible algebraic simplifications, strategies exist to reduce this cost (e.g. [LRMB07] in a learning context). For instance, for CMA-ES the cost is $O(Np)$ [SHI09]. More generally, parametrization by expectation parameters (see above), when available, may reduce the cost to $O(p)$ as well.

If no analytical form of the Fisher matrix is known and Monte Carlo estimation is required, then complexity depends on the particular situation at hand and is related to the best sampling strategies available for a particular family of distributions. For Boltzmann machines, for instance, a host of such strategies are available [AHS85, SM08, Sal09, DCB⁺10]. Still, in such a situation, IGO may be competitive if the objective function f is costly.

Recycling old samples. To compute the ranks of samples in (12), it might be advisable to re-use samples from previous iterations, so that a smaller number of samples is necessary, see e.g. [SWSS09]. For $N = 1$ this is indispensable (see also Section 4.2, Elitist Selection). In order to preserve sampling consistency (Theorem 5) the old samples need to be reweighted using the ratio of their likelihood under the current versus old distribution, as in importance sampling.

Initialization. As with other optimization algorithms, it is probably a good idea to initialize in such a way as to cover a wide portion of the search space, i.e. θ^0 should be chosen so that P_{θ^0} has maximal diversity. For IGO algorithms this is particularly interesting, since, as explained above, the natural gradient provides minimal change of diversity (greedily at each step) for a given change in the objective function.

3 IGO, maximum likelihood, and the cross-entropy method

IGO as a smooth-time maximum likelihood estimate. The IGO flow turns out to be the only way to maximize a *weighted* log-likelihood, where points of the current distribution are slightly reweighted according to f -preferences.

This relies on the following interpretation of the natural gradient as a weighted maximum likelihood update with infinitesimal learning rate. This result singles out, in yet another way, the *natural* gradient among all possible gradients. The proof is given in the Appendix.

Theorem 14 (Natural gradient as ML with infinitesimal weights). *Let $\varepsilon > 0$ and $\theta_0 \in \Theta$. Let $W(x)$ be a function of x and let θ be the solution of*

$$\theta = \arg \max_{\theta} \left\{ (1 - \varepsilon) \underbrace{\int \ln P_{\theta}(x) P_{\theta_0}(dx)}_{\text{maximal for } \theta = \theta_0} + \varepsilon \int \ln P_{\theta}(x) W(x) P_{\theta_0}(dx) \right\}.$$

Then, when $\varepsilon \rightarrow 0$ we have

$$\theta = \theta_0 + \varepsilon \int \tilde{\nabla}_{\theta} \ln P_{\theta}(x) W(x) P_{\theta_0}(dx) + O(\varepsilon^2).$$

Likewise for discrete samples: with $x_1, \dots, x_N \in X$, let θ be the solution of

$$\theta = \arg \max_{\theta} \left\{ (1 - \varepsilon) \int \ln P_{\theta}(x) P_{\theta_0}(dx) + \varepsilon \sum_i W(x_i) \ln P_{\theta}(x_i) \right\}.$$

Then when $\varepsilon \rightarrow 0$ we have

$$\theta = \theta_0 + \varepsilon \sum_i W(x_i) \tilde{\nabla}_{\theta} \ln P_{\theta}(x_i) + O(\varepsilon^2).$$

So if $W(x) = W_{\theta_0}^f(x)$ is the weight of the points according to quantized f -preferences, the weighted maximum log-likelihood necessarily is the IGO flow (7) using the natural gradient—or the IGO update (15) when using samples.

Thus the IGO flow is the unique flow that, continuously in time, slightly changes the distribution to maximize the log-likelihood of points with good values of f . (In addition IGO continuously updates the weight $W_{\theta^t}^f(x)$ depending on f and on the current distribution, so that we keep optimizing.)

This theorem suggests a way to approximate the IGO flow by enforcing this interpretation for a given non-infinitesimal step size δt , as follows.

Definition 15 (IGO-ML algorithm). *The IGO-ML algorithm with step size δt updates the value of the parameter θ^t according to*

$$\theta^{t+\delta t} = \arg \max_{\theta} \left\{ (1 - \delta t \sum_i \hat{w}_i) \int \ln P_{\theta}(x) P_{\theta^t}(dx) + \delta t \sum_i \hat{w}_i \ln P_{\theta}(x_i) \right\} \quad (26)$$

where x_1, \dots, x_N are sample points drawn according to the distribution P_{θ^t} , and \hat{w}_i is the weight (12) obtained from the ranked values of the objective function f .

The IGO-ML algorithm is obviously independent of the parametrization θ : indeed it only depends on P_θ itself. Furthermore, the IGO-ML update (26) does not even require a smooth parametrization of the distribution anymore (though in this case, a small δt will likely result in stalling: $\theta^{t+\delta t} = \theta^t$ if the set of possible values for θ is discrete).

Like the cross-entropy method below, the IGO-ML algorithm can be applied only when the argmax can be computed.

It turns out that for exponential families, IGO-ML is just the IGO algorithm in a particular parametrization (see Theorem 16).

The cross-entropy method. Taking $\delta t = 1$ in (26) above corresponds to a full maximum likelihood update; when using the truncation selection scheme w , this is the *cross-entropy method* (CEM). The cross-entropy method can be defined as follows [dBKMR05] in an optimization setting. Like IGO, it depends on a family of probability distributions P_θ parametrized by $\theta \in \Theta$, and a number of samples N at each iteration. Let also $N_e = \lceil qN \rceil$ ($0 < q < 1$) be a number of *elite* samples.

At each step, the cross-entropy method for optimization samples N points x_1, \dots, x_N from the current distribution P_{θ^t} . Let \hat{w}_i be $1/N_e$ if x_i belongs to the N_e samples with the best value of the objective function f , and $\hat{w}_i = 0$ otherwise. Then the *cross-entropy method* or *maximum likelihood update* (CEM/ML) for optimization is ([dBKMR05], Algorithm 3.1)

$$\theta^{t+1} = \arg \max_{\theta} \sum \hat{w}_i \ln P_{\theta}(x_i) \quad (27)$$

(assuming the argmax is tractable). This corresponds to $\delta t = 1$ in (26).

A commonly used version of CEM with a smoother update depends on a step size parameter $0 < \alpha \leq 1$ and is given [dBKMR05] by

$$\theta^{t+1} = (1 - \alpha)\theta^t + \alpha \arg \max_{\theta} \sum \hat{w}_i \ln P_{\theta}(x_i). \quad (28)$$

The standard CEM/ML update is $\alpha = 1$.

For $\alpha = 1$ the standard cross-entropy method is independent of the parametrization θ , whereas for $\alpha < 1$ this is not the case.

Note the difference between the IGO-ML algorithm (26) and the smoothed CEM update (28) with step size $\alpha = \delta t$: the smoothed CEM update performs a weighted average of the parameter value *after* taking the maximum likelihood estimate, whereas IGO-ML uses a weighted average of current and previous likelihoods, *then* takes a maximum likelihood estimate. In general, these two rules can greatly differ, as they do for Gaussian distributions (Section 4.2).

This interversion of averaging makes IGO-ML parametrization-independent whereas the smoothed CEM update is not.

Yet, for exponential families of probability distributions, there exists one particular parametrization θ in which the IGO algorithm and the smoothed CEM update coincide. We now proceed to this construction.

IGO for expectation parameters and maximum likelihood. The particular form of IGO for exponential families has an interesting consequence if the parametrization chosen for the exponential family is the set of *expectation parameters*. Let $P_\theta(x) = \frac{1}{Z(\theta)} \exp(\sum \theta_j T_j(x)) H(dx)$ be an exponential family as above. The *expectation parameters* are $\bar{T}_j = \bar{T}_j(\theta) = \mathbb{E}_{P_\theta} T_j$, (denoted η_j in [AN00, (3.56)]). The notation \bar{T} will denote the collection

(\bar{T}_j). We shall use the notation $P_{\bar{T}}$ to denote the probability distribution P parametrized by the expectation parameters.

It is well-known that, in this parametrization, the maximum likelihood estimate for a sample of points x_1, \dots, x_N is just the empirical average of the expectation parameters over that sample:

$$\arg \max_{\bar{T}} \frac{1}{N} \sum_{i=1}^N \ln P_{\bar{T}}(x_i) = \frac{1}{N} \sum_{i=1}^N T(x_i). \quad (29)$$

In the discussion above, one main difference between IGO and smoothed CEM was whether we took averages before or after taking the maximum log-likelihood estimate. For the expectation parameters \bar{T}_i , we see that these operations commute. (One can say that these expectation parameters “linearize maximum likelihood estimates”.) After some work we get the following result.

Theorem 16 (IGO, CEM and maximum likelihood). *Let*

$$P_{\theta}(x) = \frac{1}{Z(\theta)} \exp\left(\sum \theta_j T_j(x)\right) H(dx)$$

be an exponential family of probability distributions, where the T_j are functions of x and H is some reference measure. Let us parametrize this family by the expected values $\bar{T}_j = \mathbb{E}T_j$.

Let us assume the chosen weights \hat{w}_i sum to 1. For a sample x_1, \dots, x_N , let

$$T_j^* = \sum_i \hat{w}_i T_j(x_i).$$

Then the IGO update (15) in this parametrization reads

$$\bar{T}_j^{t+\delta t} = (1 - \delta t) \bar{T}_j^t + \delta t T_j^*. \quad (30)$$

Moreover these three algorithms coincide:

- The IGO-ML algorithm (26).
- The IGO algorithm (15) written in the parametrization \bar{T}_j (30).
- The smoothed CEM algorithm (28) written in the parametrization \bar{T}_j , with $\alpha = \delta t$.

Corollary 17. *For exponential families, the standard CEM/ML update (27) coincides with the IGO algorithm in parametrization \bar{T}_j with $\delta t = 1$.*

Beware that the expectation parameters \bar{T}_j are not always the most obvious parameters [AN00, Section 3.5]. For example, for 1-dimensional Gaussian distributions, these expectation parameters are the mean μ and the second moment $\mu^2 + \sigma^2$. When expressed back in terms of mean and variance, with the update (30) the new mean is $(1 - \delta t)\mu + \delta t\mu^*$, but the new variance is $(1 - \delta t)\sigma^2 + \delta t(\sigma^*)^2 + \delta t(1 - \delta t)(\mu^* - \mu)^2$.

On the other hand, when using smoothed CEM with mean and variance as parameters, the new variance is $(1 - \delta t)\sigma^2 + \delta t(\sigma^*)^2$, which can be significantly smaller for $\delta t \in (0, 1)$. This proves, in passing, that the smoothed CEM update in other parametrizations is generally *not* an IGO algorithm (because it can differ at first order in δt).

The case of Gaussian distributions is further exemplified in Section 4.2 below: in particular, smoothed CEM in the (μ, σ) parametrization exhibits premature reduction of variance, preventing good convergence.

For these reasons we think that the IGO-ML algorithm is the sensible way to perform an interpolated ML estimate for $\delta t < 1$, in a parametrization-independent way. In Section 6 we further discuss IGO and CEM and sum up the differences and relative advantages.

Taking $\delta t = 1$ is a bold approximation choice: the “ideal” continuous-time IGO flow itself, after time 1, does not coincide with the maximum likelihood update of the best points in the sample. Since the maximum likelihood algorithm is known to converge prematurely in some instances (Section 4.2), using the parametrization by expectation parameters with large δt may not be desirable.

The considerable simplification of the IGO update in these coordinates reflects the duality of coordinates \bar{T}_i and θ_i . More precisely, the natural gradient ascent w.r.t. the parameters \bar{T}_i is given by the vanilla gradient w.r.t. the parameters θ_i :

$$\tilde{\nabla}_{\bar{T}_i} = \frac{\partial}{\partial \theta_i}$$

(Proposition 27 in the Appendix).

4 CMA-ES, NES, EDAs and PBIL from the IGO framework

In this section we investigate the IGO algorithms for Bernoulli measures and for multivariate normal distributions, and show the correspondence to well-known algorithms. In addition, we discuss the influence of the parametrization of the distributions.

4.1 PBIL as IGO algorithm for Bernoulli measures

Let us consider on $X = \{0, 1\}^d$ a family of Bernoulli measures $P_\theta(x) = p_{\theta_1}(x_1) \times \dots \times p_{\theta_d}(x_d)$ with $p_{\theta_i}(x_i) = \theta_i^{x_i} (1 - \theta_i)^{1 - x_i}$, with each $\theta_i \in [0; 1]$. As this family is a product of probability measures $p_{\theta_i}(x_i)$, the different components of a random vector y following P_θ are independent and all off-diagonal terms of the Fisher information matrix are zero. Diagonal terms are given by $\frac{1}{\theta_i(1-\theta_i)}$. Therefore the inverse of the Fisher matrix is a diagonal matrix with diagonal entries equal to $\theta_i(1 - \theta_i)$. In addition, the partial derivative of $\ln P_\theta(x)$ w.r.t. θ_i is computed in a straightforward manner resulting in

$$\frac{\partial \ln P_\theta(x)}{\partial \theta_i} = \frac{x_i}{\theta_i} - \frac{1 - x_i}{1 - \theta_i} .$$

Let x_1, \dots, x_N be N samples at step t with distribution P_{θ^t} and let $x_{1:N}, \dots, x_{N:N}$ be the samples ranks according to f value. The natural gradient update (16) with Bernoulli measures is then

$$\theta_i^{t+\delta t} = \theta_i^t + \delta t \theta_i^t (1 - \theta_i^t) \sum_{j=1}^N w_j \left(\frac{[x_{j:N}]_i}{\theta_i^t} - \frac{1 - [x_{j:N}]_i}{1 - \theta_i^t} \right) \quad (31)$$

where $w_j = w((j - 1/2)/N)/N$ and $[y]_i$ denotes the i^{th} coordinate of $y \in X$. The previous equation simplifies to

$$\theta_i^{t+\delta t} = \theta_i^t + \delta t \sum_{j=1}^N w_j \left([x_{j:N}]_i - \theta_i^t \right) , \quad (32)$$

or, denoting \bar{w} the sum of the weights $\sum_{j=1}^N w_j$,

$$\theta_i^{t+\delta t} = (1 - \bar{w}\delta t)\theta_i^t + \delta t \sum_{j=1}^N w_j [x_{j:N}]_i . \quad (33)$$

The algorithm so obtained coincides with the so-called *population-based incremental learning* algorithm (PBIL, [BC95]). Different variants of PBIL correspond to different choices of the selection scheme w . We have thus proved the following.

Proposition 18. *The IGO algorithm on $\{0, 1\}^d$ using Bernoulli measures parametrized by θ as above, coincides with PBIL, with the following correspondence of parameters.*

The PBIL algorithm using the μ best solutions, after [BC95, Figure 4], is recovered³ using $\delta t = \text{LR}$, $w_j = (1 - \text{LR})^{j-1}$ for $j = 1, \dots, \mu$, and $w_j = 0$ for $j = \mu + 1, \dots, N$.

If the selection scheme of IGO is chosen as $w_1 = 1$, $w_j = 0$ for $j = 2, \dots, N$, IGO recovers the PBIL/EGA algorithm with update rule towards the best solution [Bal94, Figure 4], with $\delta t = \text{LR}$ (the learning rate of PBIL) and $\text{MUT_PROBABILITY} = 0$ (no random mutation of θ).

Interestingly, the parameters θ_i are the expectation parameters described in Section 3: indeed, the expectation of x_i is θ_i . So the formulas above are particular cases of (30). Thus, by Theorem 16, PBIL is both a smoothed CEM in these parameters and an IGO-ML algorithm.

Let us now consider another, so-called “logit” representation, given by the logistic function $P(x_i = 1) = \frac{1}{1 + \exp(-\tilde{\theta}_i)}$. This $\tilde{\theta}$ is the exponential parametrization of Section 2.3. We find that

$$\frac{\partial \ln P_{\tilde{\theta}}(x)}{\partial \tilde{\theta}_i} = (x_i - 1) + \frac{\exp(-\tilde{\theta}_i)}{1 + \exp(-\tilde{\theta}_i)} = x_i - \mathbb{E}x_i \quad (34)$$

(cf. (17)) and that the diagonal elements of the Fisher information matrix are given by $\exp(-\tilde{\theta}_i)/(1 + \exp(-\tilde{\theta}_i))^2 = \text{Var } x_i$ (as per (18)). So the natural gradient update (16) with Bernoulli measures now reads

$$\tilde{\theta}_i^{t+\delta t} = \tilde{\theta}_i^t + \delta t (1 + \exp(\tilde{\theta}_i^t)) \left(-\bar{w} + (1 + \exp(-\tilde{\theta}_i^t)) \sum_{j=1}^N w_j [x_{j:N}]_i \right) . \quad (35)$$

To better compare the update with the previous representation, note that $\theta_i = \frac{1}{1 + \exp(-\tilde{\theta}_i)}$ and thus we can rewrite

$$\tilde{\theta}_i^{t+\delta t} = \tilde{\theta}_i^t + \frac{\delta t}{\theta_i^t(1 - \theta_i^t)} \sum_{j=1}^N w_j \left([x_{j:N}]_i - \theta_i^t \right) . \quad (36)$$

So the direction of the update is the same as before and is given by the proportion of bits set to 0 or 1 in the best samples, compared to its expected value under the current distribution. The magnitude of the update

³Note that the pseudocode for the algorithm in [BC95, Figure 4] is slightly erroneous since it gives smaller weights to better individuals. The error can be fixed by updating the probability in reversed order, looping from `NUMBER_OF_VECTORS_TO_UPDATE_FROM` to 1. This was confirmed by S. Baluja in personal communication. We consider here the corrected version of the algorithm.

is different since the parameter $\tilde{\theta}$ ranges from $-\infty$ to $+\infty$ instead of from 0 to 1. We did not find this algorithm in the literature.

These updates also illustrate the influence of setting the sum of weights to 0 or not (Section 2.7). If, at some time, the first bit is equal to 1 both for a majority of good points and for a majority of bad points, then the original PBIL will increase the probability of setting the first bit to 1, which is counterintuitive. If the weights w_i are chosen to sum to 0 this noise effect disappears; otherwise, it disappears only on average.

4.2 Multivariate normal distributions (Gaussians)

Evolution strategies [Rec73, Sch95, BS02] are black-box optimization algorithms for the continuous search domain, $X \subseteq \mathbb{R}^d$ (for simplicity we assume $X = \mathbb{R}^d$ in the following), which use multivariate normal distributions to sample new solutions. In the context of continuous black-box optimization, *Natural Evolution Strategies* (NES) introduced the idea of using a natural gradient update of the distribution parameters [WSPS08, SWSS09, GSS⁺10]. Surprisingly, the well-known *Covariance Matrix Adaption Evolution Strategy*, CMA-ES [HO96, HO01, HMK03, HK04, JA06], also turns out to conduct a natural gradient update of distribution parameters [ANOK10, GSS⁺10].

Let $x \in \mathbb{R}^d$. As the most prominent example, we use mean vector $m = \mathbb{E}x$ and covariance matrix $C = \mathbb{E}(x - m)(x - m)^\top = \mathbb{E}(xx^\top) - mm^\top$ to parametrize a normal distribution via $\theta = (m, C)$. The IGO update in (15) or (16) in this parametrization can now be entirely reformulated without the (inverse) Fisher matrix, similarly to (30) or (19). The complexity of the update is linear in the number of parameters (size of $\theta = (m, C)$, where $(d^2 - d)/2$ parameters are redundant).

Let us discuss known algorithms that implement updates of this kind.

CMA-ES. The rank- μ -update CMA-ES implements the equations⁴

$$m^{t+1} = m^t + \eta_m \sum_{i=1}^N \hat{w}_i (x_i - m^t) \quad (37)$$

$$C^{t+1} = C^t + \eta_c \sum_{i=1}^N \hat{w}_i ((x_i - m^t)(x_i - m^t)^\top - C^t) \quad (38)$$

where \hat{w}_i are the weights based on ranked f -values, see (12) and (15).

Proposition 19. *The IGO update (15) for Gaussian distributions in the parametrization by mean and covariance matrix (m, C) , coincides with the CMA-ES update equations (37) and (38) with $\eta_c = \eta_m$.*

This result is essentially due to [ANOK10, GSS⁺10], who showed that the CMA-ES update with $\eta_c = \eta_m$ is a natural gradient update⁵. However, in deviation from the IGO algorithm, the learning rates η_m and η_c are assigned different values if $N \ll \dim \Theta$ in CMA-ES⁶. Note that the Fisher information

⁴The CMA-ES implements these equations given the parameter setting $c_1 = 0$ and $c_\sigma = 0$ (or $d_\sigma = \infty$, see e.g. [Han09]) that disengages the effect of the rank-one update and of step size control and therefore of both so-called evolution paths.

⁵In these articles the result has been derived for $\theta \leftarrow \theta + \eta \tilde{\nabla}_\theta \mathbb{E}_{P_\theta} f$, see (9), leading to $f(x_i)$ in place of \hat{w}_i . No assumptions on f have been used besides that it does not depend on θ . Consequently, by replacing f with $W_{\theta^t}^f$, where θ^t is fixed, the derivation holds equally well for $\theta \leftarrow \theta + \eta \tilde{\nabla}_\theta \mathbb{E}_{P_\theta} W_{\theta^t}^f$.

⁶Specifically, let $\sum |\hat{w}_i| = 1$, then $\eta_m = 1$ and $\eta_c \approx 1 \wedge 1/(d^2 \sum \hat{w}_i^2)$.

matrix is block-diagonal in m and C [ANOK10], so that application of the different learning rates and of the inverse Fisher matrix commute.

Convenient reparametrizations over time. For practical purposes, at each step it is convenient to work in a representation of θ in which the diagonal Fisher matrix $I(\theta^t)$ has a simple form, e.g., diagonal with simple diagonal entries. It is generally not possible to obtain such a representation for all θ simultaneously. Still it is always possible to find a transformation achieving a diagonal Fisher matrix at a single parameter θ^t , in multiple ways (it amounts to choosing a basis of parameter space which is orthogonal in the Fisher metric). Such a representation is never unique and not intrinsic, yet it still provides a convenient way to write the algorithms.

For CMA-ES, one such representation can be found by sending the current covariant matrix C^t to the identity, e.g., by representing the mean and covariance matrix by $((C^t)^{-1/2}m, (C^t)^{-1/2}C(C^t)^{-1/2})$ instead of (m, C) . Then the Fisher matrix $I(\theta^t)$ at (m^t, C^t) becomes diagonal. The next algorithm we discuss, xNES [GSS⁺10], exploits this possibility in a logarithmic representation of the covariance matrix.

Natural evolution strategies. Natural evolution strategies (NES) [WSPS08, SWSS09] implement (37) as well, while using a Cholesky decomposition of C as parametrization for the update of the variance parameters. The resulting update that originally replaces (38) is neither particularly elegant nor numerically efficient. However, the more recent xNES [GSS⁺10] chooses an “exponential” parametrization that naturally depends on the current parameters. This leads to an elegant formulation where the additive update in exponential parametrization becomes a multiplicative update for C in (38). With $C = AA^T$, the matrix update reads

$$A \leftarrow A \times \exp\left(\frac{\eta_c}{2} \sum_{i=1}^N \hat{w}_i \times (z_i z_i^T - I_d)\right) \quad (39)$$

where $z_i = A^{-1}(x_i - m)$ and I_d is the identity matrix. From (39) the updated covariance matrix becomes $C \leftarrow A \times \exp^2(\dots) \times A^T$.

The update has the advantage over (38) that even negative weights, $\hat{w}_i < 0$, always lead to a feasible covariance matrix. By default, xNES sets $\eta_m \neq \eta_c$ in the same circumstances as in CMA-ES, but contrary to CMA-ES the past evolution path is not taken into account [GSS⁺10].

When $\eta_c = \eta_m$, xNES is consistent with the IGO flow (6), and implements an IGO algorithm (15) slightly generalized in that it uses a θ^t -dependent parametrization, which represents the current covariance matrix by 0. Namely, we have:

Proposition 20. *Let (m^t, C^t) be the current mean and covariance matrix. Let $C^t = AA^T$. Let θ be the time-dependent parametrization of the space of Gaussian distributions, which parametrizes the Gaussian distribution (m, C) by*

$$\theta = (m, R), \quad R = \ln(A^{-1}C(A^T)^{-1})$$

where \ln is the logarithm of positive matrices.

Then the IGO update (15) in the parametrization θ is as follows: the mean m is updated as in CMA-ES (37), and the parameter R is updated as

$$R \leftarrow \delta t \sum_{i=1}^N \hat{w}_i \times (A^{-1}(x_i - m)(x_i - m)^T (A^T)^{-1} - I_d) \quad (40)$$

(note that the current value of C is represented as $R = 0$), thus resulting in the same update as (39) (with $\eta_c = \delta t$) for the covariance matrix: $C \leftarrow A \exp(R) A^\top$.

Indeed, by basic differential geometry, if parametrization $\theta' = f(\theta)$ is used, the IGO update for θ' is $Df(\theta^t)$ applied to the IGO update for θ , where Df is the differential of f . Here to find the update for R we have to compute the differential of the map $C \mapsto \ln(A^{-1}C(A^\top)^{-1})$ taken at $C = AA^\top$: for any matrix M we have $\ln(A^{-1}(AA^\top + \varepsilon M)(A^\top)^{-1}) = \varepsilon A^{-1}M(A^\top)^{-1} + O(\varepsilon^2)$. So to find the update for the variable R we have to apply $A^{-1} \dots (A^\top)^{-1}$ to the update (38) for C .

Cross-entropy method and EMNA. *Estimation of distribution algorithms* (EDA) and the *cross-entropy method* (CEM) [Rub99, RK04] estimate a new distribution from a censored sample. Generally, the new parameter value can be written as

$$\begin{aligned} \theta_{\max\text{LL}} &= \arg \max_{\theta} \sum_{i=1}^N \hat{w}_i \ln P_{\theta}(x_i) \\ &\longrightarrow_{N \rightarrow \infty} \arg \max_{\theta} \mathbb{E}_{P_{\theta^t}} W_{\theta^t}^f \ln P_{\theta} \end{aligned} \quad (41)$$

Here, the weights \hat{w}_i are equal to $1/\mu$ for the μ best points (censored or elitist sample) and 0 otherwise. This $\theta_{\max\text{LL}}$ maximizes the weighted log-likelihood of $x_1 \dots x_N$; equivalently, it minimizes the cross-entropy and the Kullback–Leibler divergence to the distribution of the best μ samples⁷.

For Gaussian distributions, Equation (41) can be explicitly written in the form

$$m^{t+1} = m^* = \sum_{i=1}^N \hat{w}_i x_i \quad (42)$$

$$C^{t+1} = C^* = \sum_{i=1}^N \hat{w}_i (x_i - m^*)(x_i - m^*)^\top \quad (43)$$

the empirical mean and variance of the elite sample.

Equations (42) and (43) also define the simplest continuous domain EDA, the *estimation of multivariate normal algorithm* (EMNA_{global}, [LL02]). Interestingly, (42) and (43) only differ from (37) and (38) (with $\eta_m = \eta_c = 1$) in that the new mean m^{t+1} instead of m^t is used in the covariance matrix update [Han06b].

The smoothed CEM in this parametrization thus writes $m^{t+\delta t} = (1 - \delta t)m^t + \delta t m^*$ and $C^{t+\delta t} = (1 - \delta t)C^t + \delta t C^*$. Note that *this is not an IGO algorithm* (i.e., there is no parametrization of the set of Gaussian distributions in which the IGO algorithm coincides with this update): indeed, all IGO algorithms coincide at first order in δt when $\delta t \rightarrow 0$ (because they recover the IGO flow), while this update for $C^{t+\delta t}$ does not coincide with (38) in this limit, due to the use of m^* instead of m^t . (This does not contradict Theorem 16: smoothed CEM is an IGO algorithm only in the expectation parametrization, which (m, C) is not.)

⁷Let P_w denote the distribution of the weighted samples: $\Pr(x = x_i) = \hat{w}_i$ and $\sum_i \hat{w}_i = 1$. Then the cross-entropy between P_w and P_{θ} reads $\sum_i P_w(x_i) \ln 1/P_{\theta}(x_i)$ and the KL-divergence reads $\text{KL}(P_w \| P_{\theta}) = \sum_i P_w(x_i) \ln 1/P_{\theta}(x_i) - \sum_i P_w(x_i) \ln 1/P_w(x_i)$. Minimization of both terms in θ result in $\theta_{\max\text{LL}}$.

CMA-ES, smoothed CEM, and IGO-ML. Let us compare IGO-ML (26), CMA (37)–(38), and smoothed CEM (28) in the parametrization with mean and covariance matrix. These algorithms all update the distribution mean in the same way, while the update of the covariance matrix depends on the algorithm. With learning rate δt , these updates are computed to be

$$\begin{aligned} m^{t+1} &= (1 - \delta t) m^t + \delta t m^* \\ C^{t+1} &= (1 - \delta t) C^t + \delta t C^* + \delta t (1 - \delta t)^j (m^* - m^t)(m^* - m^t)^\top, \end{aligned} \quad (44)$$

for different values of j , where m^* and C^* are the mean and covariance matrix computed over the elite sample (with positive weights \hat{w}_i summing to one) as above. The rightmost term of (44) is reminiscent of the so-called rank-one update in CMA-ES (not included in (38)).

For $j = 0$ we recover the rank- μ CMA-ES update (38), for $j = 1$ we recover IGO-ML, and for $j = \infty$ we recover smoothed CEM (the rightmost term is absent). The case $j = 2$ corresponds to an update that uses m^{t+1} instead of m^t in (38). For $0 < \delta t < 1$, the larger j , the smaller is C^{t+1} . For $\delta t = 1$, IGO-ML and smoothed CEM/EMNA realize $\theta_{\max\text{LL}}$ from (41)–(43).

For $\delta t \rightarrow 0$, the update is independent of j at first order in δt if $j < \infty$: this reflects compatibility with the IGO flow of CMA and of IGO-ML, but not of smoothed CEM.

In full CMA-ES (as opposed to rank- μ CMA-ES), the coefficient preceding $(m^* - m^t)(m^* - m^t)^\top$ in (44) reads approximately $3\delta t$, where the additional $2\delta t$ originate from the so-called rank-one update and are moreover modulated by so-called cumulation up to a factor of about \sqrt{d} .

Critical δt . Let us assume that $\mu < N$ weights are set to $\hat{w}_i = 1/\mu$ and the remaining weights to zero, so that the selection quantile is $q = \mu/N$.

Then there is a critical value of δt depending on this quantile q , such that above this critical δt the algorithms given by IGO-ML and smoothed CEM are prone to premature convergence. Indeed, let f be a linear function on \mathbb{R}^d , and consider the variance in the direction of the gradient of f . Assuming further $N \rightarrow \infty$ and $q \leq 1/2$, then the variance C^* of the elite sample is smaller than the current variance C^t , by a constant factor. Depending on the precise update for C^{t+1} , if δt is too large, the variance C^{t+1} is going to be smaller than C^t by a constant factor as well. This implies that the algorithm is going to stall. (On the other hand, the continuous-time IGO flow corresponding to $\delta t \rightarrow 0$ does not stall, see Section 4.3.)

We now study the critical δt (in the limit $N \rightarrow \infty$) under which the algorithm does not stall. For IGO-ML, ($j = 1$ in (44)), or equivalently for the smoothed CEM in the expectation parameters $(m, C + mm^\top)$, see Section 3), the variance increases if and only if δt is smaller than the critical value $\delta t_{\text{crit}} = qb\sqrt{2\pi}e^{b^2/2}$ where b is the percentile function of q , i.e. b is such that $q = \int_b^\infty e^{-x^2/2}/\sqrt{2\pi}$. This value δt_{crit} is plotted as a solid line in Fig. 1. For $j = 2$, δt_{crit} is smaller, related to the above by $\delta t_{\text{crit}} \leftarrow \sqrt{1 + \delta t_{\text{crit}}} - 1$ and plotted as a dashed line in Fig. 1. For CEM ($j = \infty$), the critical δt is zero (reflecting the non-IGO behavior of CEM in this parametrization). For CMA-ES ($j = 0$), the critical δt is infinite for $q < 1/2$. When the selection quantile q is above $1/2$, for all algorithms the critical δt becomes zero.

We conclude that, despite the principled approach of ascending the natural gradient, the choice of the selection function w , the choice of δt , and possible choices in the update for $\delta t > 0$, need to be taken with care in relation to the choice of parametrization.

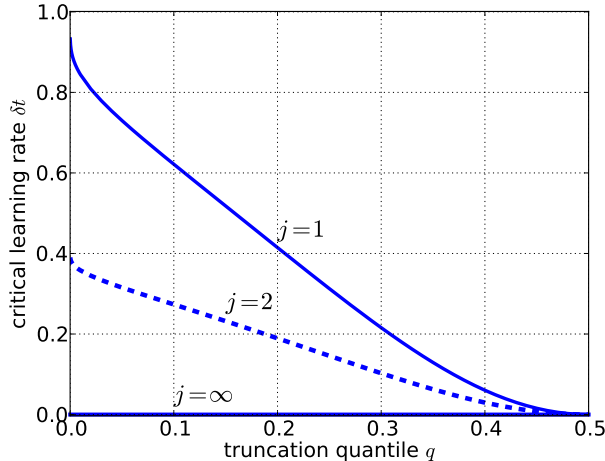


Figure 1: Critical δt versus truncation quantile q for three values of j in (44). With δt above the critical δt , the variance decreases systematically when optimizing a linear function, indicating failure of the algorithm. For CMA-ES/NES, the critical δt for $q < 0.5$ is infinite.

Gaussian distributions with restricted parametrization. When considering a restricted parametrization of multivariate normal distributions, IGO recovers other known algorithms. In particular for sep-CMA-ES [RH08] and SNES [SGS11], the update has been restricted to the diagonal of the covariance matrix.

Elitist Selection. In evolution strategies like CMA-ES, elitist selection (also called plus-selection) is another common approach. In plus-selection, all-time best points are taken into account in each iteration. We model plus-selection in the IGO framework by using the current all-time best samples in addition to samples from P_θ . Specifically, in the $(\mu + \lambda)$ -selection scheme, we set $N = \mu + \lambda$ and let x_1, \dots, x_μ be the current all-time μ best points. Then we sample λ new points, $x_{\mu+1}, \dots, x_N$, from P_θ and apply (14) with $w(q) = (N/\mu)1_{q \leq \mu/N}$. If no better points are sampled this will lead to the concentration of P_θ on the already previously found all-time best points. However, in order to prevent quick loss of diversity, one might choose to reduce the weights of these points to a smaller value.

4.3 Computing the IGO flow for some simple examples

In this section we take a closer look at the IGO differential equation solutions of (6) for some simple examples of fitness functions, for which it is possible to obtain exact information about these IGO trajectories.

We start with the discrete search space $X = \{0, 1\}^d$ and linear functions (to be minimized) defined as $f(x) = c - \sum_{i=1}^d \alpha_i x_i$ with $\alpha_i > 0$. (So maximization of the classical onemax function $f_{\text{onemax}}(x) = \sum_{i=1}^d x_i$ is covered by setting $\alpha_i = 1$.) The differential equation of the IGO flow (6) for the Bernoulli measures $P_\theta(x) = p_{\theta_1}(x_1) \dots p_{\theta_d}(x_d)$ defined on X is the $\delta t \rightarrow 0$ limit of the IGO-PBIL update (31):

$$\frac{d\theta_i^t}{dt} = \int W_{\theta^t}^f(x)(x_i - \theta_i^t)P_{\theta^t}(dx) =: g_i(\theta^t) . \quad (45)$$

Although finding the analytical solution of the differential equation (45) for any initial condition seems a bit intricate, we show that the equation admits

one critical stable point, $(1, \dots, 1)$, and one critical unstable point $(0, \dots, 0)$. In addition we prove that the solution of (45) converges to $(1, \dots, 1)$ starting from any initial θ except $\theta = (0, \dots, 0)$. To do so we establish the following result:

Lemma 21. *Assume that the selection scheme w is bounded. On $f(x) = c - \sum_{i=1}^d \alpha_i x_i$, the solution of (45) satisfies $\sum_{i=1}^d \alpha_i \frac{d\theta_i^t}{dt} \geq 0$; moreover $\sum \alpha_i \frac{d\theta_i^t}{dt} = 0$ if and only if $\theta = (0, \dots, 0)$ or $\theta = (1, \dots, 1)$.*

Proof. We compute $\sum_{i=1}^d \alpha_i g_i(\theta^t)$ and find that

$$\begin{aligned} \sum_{i=1}^d \alpha_i \frac{d\theta_i^t}{dt} &= \int W_{\theta^t}^f(x) \left(\sum_{i=1}^d \alpha_i x_i - \sum_{i=1}^d \alpha_i \theta_i^t \right) P_{\theta^t}(dx) \\ &= \int W_{\theta^t}^f(x) (f(\theta^t) - f(x)) P_{\theta^t}(dx) \\ &= \mathbb{E}[W_{\theta^t}^f(x)] \mathbb{E}[f(x)] - \mathbb{E}[W_{\theta^t}^f(x) f(x)] \end{aligned}$$

where the expectations are taken under P_{θ^t} . In addition, $W_{\theta^t}^f(x)$ is a non-increasing bounded function in the variable $f(x)$, and so $-W_{\theta^t}^f(x)$ and $f(x)$ are positively correlated (see [Tho00, Chapter 1] for a proof of this result), i.e.

$$\mathbb{E}[-W_{\theta^t}^f(x) f(x)] \geq \mathbb{E}[-W_{\theta^t}^f(x)] \mathbb{E}[f(x)]$$

with equality if and only if $\theta^t = (0, \dots, 0)$ or $\theta^t = (1, \dots, 1)$. Thus $\sum_{i=1}^d \alpha_i \frac{d\theta_i^t}{dt} \geq 0$. \square

The previous result implies that the positive definite function $V(\theta) = \sum_{i=1}^d \alpha_i - \sum_{i=1}^d \alpha_i \theta_i$, which is maximal at $\theta = (0, \dots, 0)$ and minimal at $\theta = (1, \dots, 1)$, satisfies $V^*(\theta) = \nabla V(\theta) \cdot g(\theta) \leq 0$, with moreover $V^*(\theta) = 0$ if and only if $\theta = (1, \dots, 1)$ or $\theta = (0, \dots, 0)$. Thus V is a so-called Lyapunov function, and these properties imply [Kha96, AO08] the following result:

Proposition 22. *Assume that the selection scheme w is bounded. On the linear functions $f(x) = c - \sum_{i=1}^d \alpha_i x_i$, the critical points $\theta = (0, \dots, 0)$ and $\theta = (1, \dots, 1)$ of the IGO-PBIL differential equation (45) are respectively unstable and stable. For any initial condition except $\theta = (0, \dots, 0)$, the continuous-time trajectory solving (45) converges to $(1, \dots, 1)$.*

We now consider on \mathbb{R}^d the family of multivariate normal distributions $P_\theta = \mathcal{N}(m, \sigma^2 I_d)$ with covariance matrix equal to $\sigma^2 I_d$. The parameter θ thus has $d + 1$ components $\theta = (m, \sigma) \in \mathbb{R}^d \times \mathbb{R}$. The natural gradient update using this family was derived in [GSS⁺10]; from this we can derive the IGO differential equation which reads:

$$\frac{dm^t}{dt} = \int_{\mathbb{R}^d} W_{\theta^t}^f(x) (x - m^t) P_{\mathcal{N}(m^t, (\sigma^t)^2 I_d)}(x) dx \quad (46)$$

$$\frac{d\tilde{\sigma}^t}{dt} = \int_{\mathbb{R}^d} \frac{1}{2d} \left\{ \sum_{i=1}^d \left(\frac{x_i - m_i^t}{\sigma^t} \right)^2 - 1 \right\} W_{\theta^t}^f(x) P_{\mathcal{N}(m^t, (\sigma^t)^2 I_d)}(x) dx \quad (47)$$

where σ^t and $\tilde{\sigma}^t$ are linked via $\sigma^t = \exp(\tilde{\sigma}^t)$ or $\tilde{\sigma}^t = \ln(\sigma^t)$. Denoting \mathcal{N} a random vector following a centered multivariate normal distribution with identity covariance matrix we can rewrite the gradient flow as

$$\frac{dm^t}{dt} = \sigma^t \mathbb{E} \left[W_{\theta^t}^f(m^t + \sigma^t \mathcal{N}) \mathcal{N} \right] \quad (48)$$

$$\frac{d\tilde{\sigma}^t}{dt} = \mathbb{E} \left[\frac{1}{2} \left(\frac{\|\mathcal{N}\|^2}{d} - 1 \right) W_{\theta^t}^f(m^t + \sigma^t \mathcal{N}) \right]. \quad (49)$$

Let us analyze the solution of the previous system on linear functions. Without loss of generality (because of invariance) we can consider the linear function $f(x) = x_1$. We have

$$W_{\theta^t}^f(x) = w(\Pr(m_1^t + \sigma^t Z_1 < x_1))$$

where Z_1 follows a standard one-dimensional normal distribution and thus

$$W_{\theta^t}^f(m^t + \sigma^t \mathcal{N}) = w(\Pr_{Z_1 \sim \mathcal{N}(0,1)}(Z_1 < \mathcal{N}_1)) \quad (50)$$

$$= w(\mathcal{F}(\mathcal{N}_1)) \quad (51)$$

with \mathcal{F} the cumulative distribution of a standard normal distribution, and \mathcal{N}_1 the first component of \mathcal{N} . The differential equation thus simplifies into

$$\frac{dm^t}{dt} = \sigma^t \begin{pmatrix} \mathbb{E}[w(\mathcal{F}(\mathcal{N}_1))\mathcal{N}_1] \\ 0 \\ \vdots \\ 0 \end{pmatrix} \quad (52)$$

$$\frac{d\sigma^t}{dt} = \frac{1}{2d} \mathbb{E}[(|\mathcal{N}_1|^2 - 1)w(\mathcal{F}(\mathcal{N}_1))] . \quad (53)$$

Consider, for example, the truncation selection function, i.e. $w(q) = 1_{q \leq q_0}$ where $q_0 \in (0, 1)$ —also called intermediate recombination. We find that

$$\frac{dm_1^t}{dt} = \sigma^t \mathbb{E}[\mathcal{N}_1 1_{\{\mathcal{N}_1 \leq \mathcal{F}^{-1}(q_0)\}}] =: \sigma^t \beta \quad (54)$$

$$\frac{d\sigma^t}{dt} = \frac{1}{2d} \left(\int_0^{q_0} \mathcal{F}^{-1}(u)^2 du - q_0 \right) =: \alpha . \quad (55)$$

The solution of the IGO flow for the linear function $f(x) = x_1$ is thus given by

$$m_1^t = m_1^0 + \frac{\sigma^0 \beta}{\alpha} \exp(\alpha t) \quad (56)$$

$$\sigma^t = \sigma^0 \exp(\alpha t) . \quad (57)$$

The coefficient β is negative for any $q_0 < 1$. The coefficient α is positive if and only if $q_0 < 1/2$ by a simple calculus argument⁸; this corresponds to selecting less than half of the sampled points in an ES. In this case the step size σ^t grows exponentially fast to infinity and the mean vector moves along the gradient direction towards minus ∞ at the same rate. If more than half of the points are selected, $q_0 \geq 1/2$, the step size will decrease to zero exponentially fast and the mean vector will get stuck (compare also [Han06a]).

For an analysis of the solutions of the system of differential equations (48) and (49) on more complex functions, namely convex-quadratic functions and twice continuously differentiable functions, we refer to [AAH12].

⁸Indeed $\alpha = \frac{1}{2d\sqrt{2\pi}} \int_{-\infty}^{\mathcal{F}^{-1}(q_0)} (x^2 - 1) \exp(-x^2/2) dx = \frac{1}{2d\sqrt{2\pi}} g(\mathcal{F}^{-1}(q_0))$ where $g(y) = \int_{-\infty}^y (x^2 - 1) \exp(-x^2/2) dx$. Using $g(0) = 0$ and $\lim_{y \rightarrow \pm\infty} g(y) = 0$, and studying the sign of $g'(y)$, we find that g is positive for $y < 0$ and negative for $y > 0$. Since $\mathcal{F}^{-1}(q_0) < 0$ if and only if $q_0 < 1/2$, we find that $\alpha = \frac{1}{2d\sqrt{2\pi}} g(\mathcal{F}^{-1}(q_0))$ is positive if and only if $q_0 < 1/2$.

5 Multimodal optimization using restricted Boltzmann machines

We now illustrate the behavior of IGO versus the vanilla gradient on an example: the probability distributions obtained from restricted Boltzmann machines for optimization on $\{0, 1\}^d$. A purported advantage of such distributions for optimization [Ber02] is to represent dependencies between the bits: contrary to, e.g., the Bernoulli measures, restricted Boltzmann machines can in principle handle a situation where good values of the objective function are obtained, for instance, if the first and second bit are both set to 0 or both set to 1 simultaneously. The goal of this section is threefold:

- To illustrate step by step how the IGO framework can be implemented in practice on new families of probability distributions, yielding new optimization algorithms. We discuss in particular the delicate problem of estimating the Fisher matrix.
- To illustrate the (sometimes striking) difference between the optimization trajectories obtained from the natural gradient or the vanilla gradient even in a simple situation.
- To illustrate the idea that the natural gradient tries to keep the diversity of the population unchanged, thanks to its relation with Kullback–Leibler divergence (Section 1.1). Since restricted Boltzmann machines are able to represent multimodal distributions on the search space, keeping a high diversity suggests that on a multimodal objective function, natural gradient algorithms will spontaneously tend to find several optima in a single run.

Let us stress that this is *not* a systematic study of the optimization performance of IGO and restricted Boltzmann machines: the function to be optimized in this experiment is extremely simple. We choose a simple setting to get a better understanding of the consequences of using the natural gradient rather than the vanilla gradient, and to illustrate the resulting difference in behavior.

5.1 IGO for restricted Boltzmann machines

The IGO method allows to build a natural search algorithm from an arbitrary family of probability distributions on an arbitrary search space. In particular, by choosing probability distributions that are richer than Gaussian or Bernoulli, one may hope to be able to optimize functions with complex shapes. Here we study how this might help optimize multimodal functions.

Both Gaussian distributions on \mathbb{R}^d and Bernoulli distributions on $\{0, 1\}^d$ are unimodal. So at any given time, a search algorithm using such distributions concentrates around a single point in the search space, looking around that point (with some variance). The problem of designing optimization algorithms able to handle multiple hypotheses (modes) simultaneously has generated interest for a long time (see, e.g., the reviews [SK98, DMQS11]). In IGO, contrary to traditional approaches in which an ad hoc additional mechanism is incorporated into an optimization algorithm to favor multimodality, the entropy-related properties of the natural gradient (Section 1.1) suggest that diversity preservation might be a built-in feature, presumably favoring multimodality—provided the distributions in the family (P_θ) are themselves multimodal.

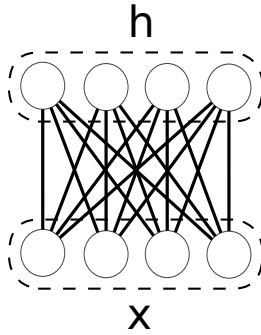


Figure 2: The RBM architecture with the observed (\mathbf{x}) and latent (\mathbf{h}) variables. In our experiments, a single hidden unit was used.

Here we apply the IGO framework to an example of multimodal distributions on $\{0, 1\}^d$: restricted Boltzmann machines (RBMs) [Smo86, AHS85]. The precise definition is given below. In RBMs, values for various blocks of bits can be switched on or off depending on the activation state of *latent variables*, hence the possibility to represent multimodal distributions. Hopefully, the optimization algorithm derived from these distributions will explore several distant zones of the search space at any given time. Boltzmann machines, a superset of restricted Boltzmann machines, were used for optimization, e.g., in [Ber02] (using the vanilla gradient) and found to perform better than PBIL on some functions.

We consider here the very simple situation of a fitness function with two distant optima and test whether IGO-based or vanilla gradient-based algorithms are able to reach both optima simultaneously or only find one of them. This provides an empirical test of Proposition 1 stating that the natural gradient minimizes loss of diversity. Our study of a bimodal RBM distribution for the optimization of a bimodal function confirms that the natural gradient does indeed behave in a more natural way than the vanilla gradient: when initialized properly, the natural gradient is able to maintain diversity by fully using the RBM distribution to learn a distribution concentrating around the two modes, while the vanilla gradient always finds only one of the two modes.

Although these experiments support using a natural gradient approach, they also establish that complications can arise for estimating the inverse Fisher matrix in the case of complex distributions such as RBMs: estimation errors may lead to a singular or unreliable estimation of the Fisher matrix, especially when the distribution becomes singular or when the learning rate is large. Further research may be needed to work around this issue.

The experiments reported here, and the fitness function used, are extremely simple from an optimization viewpoint: both algorithms using the natural and vanilla gradient find an optimum in only a few steps. The emphasis here is on the specific influence of replacing the vanilla gradient with the natural gradient, and the resulting influence on diversity and multimodality, in a simple situation.

Restricted Boltzmann machines. A restricted Boltzmann machine (RBM) [Smo86, AHS85] is a probability distribution belonging to the family of undirected graphical models (also known as Markov random fields). A set of observed variables $\mathbf{x} \in \{0, 1\}^{n_x}$ are given a probability using their joint distribution with unobserved latent variables $\mathbf{h} \in \{0, 1\}^{n_h}$ [Gha04]. The latent variables are then marginalized over. See Figure 2 for the graph structure

of a RBM.

The probability associated with an observation $\mathbf{x} = (x_i) \in \{0, 1\}^{n_x}$ and latent variable $\mathbf{h} = (h_j) \in \{0, 1\}^{n_h}$ is given by

$$P_\theta(\mathbf{x}, \mathbf{h}) = \frac{e^{-E(\mathbf{x}, \mathbf{h})}}{\sum_{\mathbf{x}', \mathbf{h}'} e^{-E(\mathbf{x}', \mathbf{h}')}}, \quad P_\theta(\mathbf{x}) = \sum_{\mathbf{h}} P_\theta(\mathbf{x}, \mathbf{h}), \quad (58)$$

where

$$E(\mathbf{x}, \mathbf{h}) = - \sum_i a_i x_i - \sum_j b_j h_j - \sum_{i,j} w_{ij} x_i h_j \quad (59)$$

is the *energy function* (compare Section 2.3). The distribution is fully parametrized by the parameter $\theta = (\mathbf{a}, \mathbf{b}, \mathbf{W})$ comprising the *bias on the observed variables* $\mathbf{a} = (a_i) \in \mathbb{R}^{n_x}$, the *bias on the latent variables* $\mathbf{b} = (b_j) \in \mathbb{R}^{n_h}$ and the *weights* $\mathbf{W} = (w_{ij}) \in \mathbb{R}^{n_x n_h}$ which account for pairwise interactions between observed and latent variables. Note that the biases can be viewed as weights, by introducing variables x_0 and h_0 always equal to one; thus in the sequel we will only write formulas involving w_{ij} , with the understanding that analogous formulas for \mathbf{a} and \mathbf{b} are readily obtained through this analogy.

RBM distributions are a special case of exponential family distributions with latent variables (see Section 2.3), where the statistics $T(\mathbf{x}, \mathbf{h})$ are all the x_i , the h_j , and the $x_i h_j$. Thus the IGO equations for the RBM stem from those for general exponential families (19, 24). In particular, for these distributions the gradient of the log-likelihood is well-known [Hin02]. This gradient has then to be multiplied with the inverse Fisher matrix.

Both the gradient and Fisher matrix in the IGO update involve expectations over (\mathbf{x}, \mathbf{h}) . For instance from (17) the gradient of the log-likelihood is

$$\frac{\partial \ln P_\theta(\mathbf{x}, \mathbf{h})}{\partial w_{ij}} = x_i h_j - \mathbb{E}_{P_\theta}[x_i h_j] \quad (60)$$

with analogous formulas for the derivatives w.r.t. a_i and to b_j . Although this quantity is often considered intractable in the context of machine learning where many variables are involved, it can be estimated accurately in the case of smaller RBMs: the expectations under P_θ can be estimated by the standard technique of Gibbs sampling (see for instance [Hin02]). We now discuss estimation of the Fisher matrix by this technique.

Estimating the Fisher matrix, and optimizing over (\mathbf{x}, \mathbf{h}) or over \mathbf{x} .

A restricted Boltzmann machine defines a distribution P_θ on both visible and hidden units (\mathbf{x}, \mathbf{h}) , whereas the function to optimize depends only on the visible units \mathbf{x} . Thus we are faced with a choice. A first possibility is to see the objective function $f(\mathbf{x})$ as a function of (\mathbf{x}, \mathbf{h}) where \mathbf{h} is a dummy variable; then we can use the IGO algorithm to optimize over (\mathbf{x}, \mathbf{h}) using the distributions $P_\theta(\mathbf{x}, \mathbf{h})$. A second possibility is to marginalize $P_\theta(\mathbf{x}, \mathbf{h})$ over the hidden units \mathbf{h} as in (58), to define the distribution $P_\theta(\mathbf{x})$; then we can use the IGO algorithm to optimize f over \mathbf{x} using $P_\theta(\mathbf{x})$.

These two approaches yield slightly different algorithms. The Fisher matrix for the distributions $P_\theta(\mathbf{x}, \mathbf{h})$ is given by (18) (exponential families) whereas the one for the distributions $P_\theta(\mathbf{x})$ is given by (23) (exponential families with latent variables). For instance, with $I_{w_{ij}w_{i'j'}}$ denoting the entry of the Fisher matrix corresponding to the components w_{ij} and $w_{i'j'}$ of the parameter θ , from (18) we get

$$I_{w_{ij}w_{i'j'}}(\theta) = \mathbb{E}_{P_\theta}[x_i h_j x_{i'} h_{j'}] - \mathbb{E}_{P_\theta}[x_i h_j] \mathbb{E}_{P_\theta}[x_{i'} h_{j'}] \quad (61)$$

whereas from (23) we get the same expression in which each h_j is replaced with its expectation \bar{h}_j knowing \mathbf{x} namely $\bar{h}_j = \mathbb{E}_{P_\theta}[h_j|\mathbf{x}] = \left(1 + e^{-b_j - \sum_i x_i w_{ij}}\right)^{-1}$ and likewise for $h_{j'}$. (Actually, since h_j and $h_{j'}$ are independent knowing \mathbf{x} when $j \neq j'$, the only difference in the Fisher matrix is when $j = j'$.)

Both versions were tested on a small instance of the problem and found to be viable. However the version using (\mathbf{x}, \mathbf{h}) is numerically more stable and requires fewer Gibbs samples to estimate the Fisher matrix, whereas the second one produces non-invertible Fisher matrix estimates more frequently. Indeed, if $I_1(\theta)$ is the Fisher matrix at θ in the first approach and $I_2(\theta)$ in the second approach, we always have $I_1(\theta) \geq I_2(\theta)$ (in the sense of positive-definite matrices). This is because probability distributions on the pair (\mathbf{x}, \mathbf{h}) carry more information than their projections on \mathbf{x} only, and so the Kullback–Leibler distances will always be larger. In particular, there exist values of θ for which the Fisher matrix I_2 is not invertible whereas I_1 is.

For this reason we selected the first approach: we optimize f as a function of (\mathbf{x}, \mathbf{h}) using IGO for the probability distributions $P_\theta(\mathbf{x}, \mathbf{h})$.

Description of a step of the algorithm. The final implementation of the IGO algorithm for RBMs with step size δt and sample size N is as follows.

At each step, N samples $(\mathbf{x}_1, \mathbf{h}_1), \dots, (\mathbf{x}_N, \mathbf{h}_N)$ are drawn from the current distribution $P_\theta(\mathbf{x}, \mathbf{h})$ using Gibbs sampling. Each Gibbs sampling starts with an element \mathbf{x} uniformly distributed in $\{0, 1\}^{n_x}$ and performs 50 Gibbs iterations for each sample.

Then the IGO update for a dataset with N sample points $(\mathbf{x}_1, \mathbf{h}_1), \dots, (\mathbf{x}_N, \mathbf{h}_N)$ is taken from (15):

$$\theta^{t+\delta t} = \theta^t + \delta t I^{-1}(\theta^t) \sum_{k=1}^N \hat{w}_k \frac{\partial \ln P_\theta(\mathbf{x}_k, \mathbf{h}_k)}{\partial \theta} \Big|_{\theta=\theta^t} \quad (62)$$

where the \hat{w}_k are the selection weights of IGO (not to be confused with the weights of the RBM).

The gradient $\partial \ln P_\theta(\mathbf{x}_k, \mathbf{h}_k)/\partial \theta$ is estimated using (60) where the expectation is estimated by taking the average over the N samples $(\mathbf{x}_1, \mathbf{h}_1), \dots, (\mathbf{x}_N, \mathbf{h}_N)$.

The Fisher matrix $I(\theta^t)$ is estimated using (61). The P_θ -expectation involved in this equation is estimated using a number N_s of Gibbs samples (\mathbf{x}, \mathbf{h}) . These samples need not coincide with the IGO samples $(\mathbf{x}_1, \mathbf{h}_1), \dots, (\mathbf{x}_N, \mathbf{h}_N)$ and in practice we take $N_s \gg N$ as described below. Note that no f -call is needed on these samples, so in a typical optimization situation where computational cost comes from the objective function f , a large N_s may not cost too much.

Fisher matrix imprecision and invertibility. The Fisher matrix (see Eq. 61) was inverted using the QR algorithm, when invertible. However, the imprecision incurred by the limited sampling size sometimes leads to an unreliable or even singular estimation of the Fisher matrix (see p. 12 for a lower bound on the number of samples needed).

Having a singular Fisher estimation happens rarely at startup; however, it occurs very frequently when the probability distribution P_θ becomes too concentrated over a few points \mathbf{x} . Unfortunately this situation arises naturally when the algorithm is allowed to continue optimization after the optimum has been reached; the experiments below confirm this. For this reason,

in our experiments, each run using the natural gradient was “frozen” as soon as estimation of the Fisher matrix was deemed to be unreliable according to the criterion below. By “freezing” a run we mean that the value of the parameter θ is not updated anymore, but the run still contributes to the statistics reported for later times, using the frozen value of θ .

The unreliability criterion is as follows: either the estimated Fisher matrix is not invertible; or it is numerically invertible but fails the following statistical cross-validation test to check reliability of the estimate. Namely: we make two estimates \hat{F}_1 and \hat{F}_2 of the Fisher matrix on two distinct sets of $N_s/2$ Gibbs samples generated from P_θ . (The final estimate of the Fisher matrix using all N_s samples can then be obtained at little computational cost by combining \hat{F}_1 and \hat{F}_2 ; this has the advantage that the cross-validation procedure does not affect computational performance significantly.) In the ideal case \hat{F}_1 and \hat{F}_2 are close.

At all steps we tested whether the rescaled squared Frobenius norms $\frac{1}{\dim(\theta)} \|\hat{F}_2^{-1/2} \hat{F}_1 \hat{F}_2^{-1/2} - \text{Id}\|_{\text{Frobenius}}^2$ and $\frac{1}{\dim(\theta)} \|\hat{F}_1^{-1/2} \hat{F}_2 \hat{F}_1^{-1/2} - \text{Id}\|_{\text{Frobenius}}^2$, which ideally are equal to 0, are both smaller than 1: this is a crude test to check eigenvalue explosion. Note that \hat{F}_1 and \hat{F}_2 represent quadratic forms on parameter space, and $\hat{F}_2^{-1/2} \hat{F}_1 \hat{F}_2^{-1/2}$ represents one of them in an orthonormal basis for the other. This test is independent of θ -parametrization. The squared Frobenius norm of $\hat{F}_2^{-1/2} \hat{F}_1 \hat{F}_2^{-1/2} - \text{Id}$ is computed as the trace of $(\hat{F}_1 \hat{F}_2^{-1} - \text{Id})^2$.

If at some point during the optimization the Fisher estimation becomes singular or unreliable according to this criterion, the corresponding run is frozen.

The number of runs that were frozen before reaching an optimum in our experiments below is reported in Table 1. Choosing a small enough learning rate appears to limit the problem.

#runs	N	N_s	δt	#iters	O	S	CV	other
300	10,000	10,000	0.5	100	98.3	0.0	1.7	0.0
			1.	100	98.0	0.0	2.0	0.0
			2.	100	95.7	0.0	4.3	0.0
20	10	10,000	0.002	25,000	100.0	0.0	0.0	0.0
			0.004	25,000	95.0	0.0	5.0	0.0
			0.008	25,000	90.0	0.0	10.0	0.0
			0.1	500	5.0	25.0	70.0	0.0
			0.2	500	0.0	30.0	70.0	0.0
			0.4	500	0.0	20.0	80.0	0.0
			0.8	500	0.0	40.0	60.0	0.0

Table 1: Percentage of runs according to their state after #iter iterations: found at least one optimum (O), frozen before hitting an optimum because of a singular matrix (S) or cross-validation test failure (CV). The confidence margin (1σ) over the reported percentages is less than ± 2.9 percent points for 300 runs and ± 11.2 percent points for 20 runs.

Computational cost. Contrary to usual optimization situations, in the experiments below the function f has negligible cost. The complexity of the algorithm is then largely determined two factors: Gibbs sampling in the RBM and Fisher matrix computation given the samples. To ensure stability of the Fisher matrix estimate (see above), the number of samples N_s used in the estimation has to scale at least like $\dim(\theta)$. With this assumption, Gibbs

sampling which essentially scales like $N_s \dim(\theta)$ then scales like $\dim(\theta)^2$, with a leading constant proportional to the number of Gibbs steps used. The computation of the Fisher matrix itself scales like $N_s \dim(\theta)^2$ because for each sample, we have to compute an additive term of the Fisher matrix which has $\dim(\theta)^2$ entries. This means that the Fisher matrix computation scales like $\dim(\theta)^3$ and can therefore be expected to be the dominating factor in the running time of experiments involving larger models. The cost of Fisher matrix inversion is expected to scale like $\dim(\theta)^3$ as the size of the RBM increases. In practice this cost was significantly smaller than that of matrix estimation (Figure 3).

Figure 3 gives empirical running times⁹ (in log-log scale) for one natural gradient step update in the experimental setting described below, together with the corresponding Gibbs sampling, Fisher matrix computation, QR inversion and cross-validation times. It shows that indeed Fisher matrix estimation and the associated Gibbs sampling are responsible for most of the computational cost.

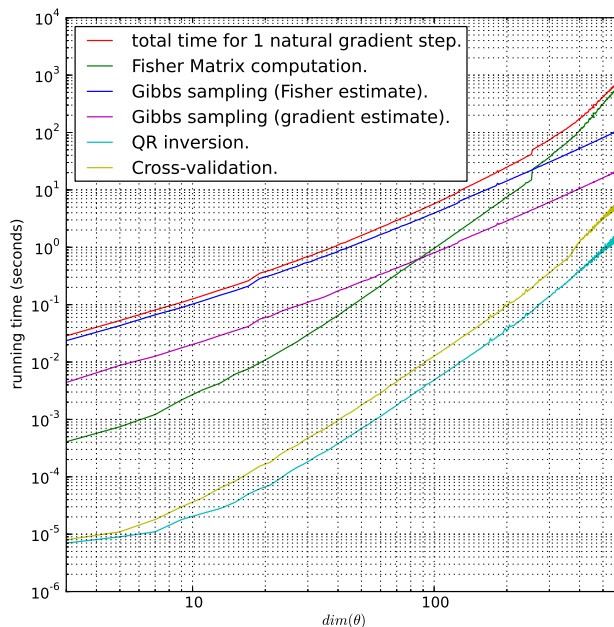


Figure 3: Log-log plot of the empirical running time (seconds) of 1 step of the natural gradient algorithm, and corresponding times for Gibbs sampling, Fisher matrix computation, QR inversion and cross-validation, for a RBM using $\dim(\theta)$ parameters. The number of samples for estimating the Fisher matrix is assumed to scale like $100 \times \dim(\theta)$ to ensure stability of the estimate. We use 5 times fewer samples to compute the gradient estimate and those samples are distinct from those used to compute the Fisher matrix estimate.

Gibbs sampling is not the fastest known method for sampling in a large RBM: a method such as parallel tempering [DCB⁺10] has the same asymptotic complexity $N_s \dim(\theta)$ for N_s samples, but usually converges faster and would therefore be more suitable for large RBMs.

A possible way to reduce the computational burden of Fisher matrix evaluation would be to use a larger learning rate together with a larger number of gradient samples at each step (e.g., using the same RBM samples for the gradient and the Fisher matrix estimation). Although this would increase

⁹on an Intel Xeon CPU E5420 at 2.50 GHz with 16 Gbytes of memory

the number of f -calls at each iteration, the experiments below suggest that it may be possible to achieve convergence in a smaller number of steps.

With this in mind, a naïve application of the natural gradient can be expected to be considerably costly for larger RBMs. Strategies already exist to deal with these issues (e.g., [LRMB07]): for instance, the Fisher matrix is not usually recomputed from scratch at each step, but a discount factor is applied to its previous value and a few new samples are incorporated; Fisher matrix inversion can then be done iteratively using the Woodbury formula; lower-rank approximations of the Fisher matrix can be used.

5.2 Experimental setup

Problem setting. In our experiments, we look at the optimization of the two-min function defined below, using a bimodal RBM: an RBM with only one latent variable ($n_h = 1$). Such an RBM is bimodal because it has two possible configurations of the latent variable: $\mathbf{h} = 0$ or $\mathbf{h} = 1$, and given \mathbf{h} , the observed variables are independent and distributed according to two Bernoulli distributions. We used $n_x = 40$, and therefore $\dim(\theta) = 81$.

Set a parameter $\mathbf{y} \in \{0, 1\}^d$. The *two-min function based at \mathbf{y}* is defined as:

$$f_{\mathbf{y}}(\mathbf{x}) = \min \left(\sum_i |x_i - y_i|, \sum_i |(1 - x_i) - y_i| \right) \quad (63)$$

This function of \mathbf{x} has two optima: one at \mathbf{y} , the other at its binary complement $\bar{\mathbf{y}}$.

We ran both the IGO algorithm as described above, and the version using the vanilla gradient instead of the natural gradient (that is, omitting the Fisher matrix in (62)).

Parameter setting. We used two different values $N = 10,000$ and $N = 10$ for the population size of the IGO algorithm. The rather comfortable setting $N = 10,000$ allows for a good illustration of the behavior of the theoretical IGO flow which corresponds to $N \rightarrow \infty$ and $\delta t \rightarrow 0$, whereas $N = 10$ is a much more realistic value for an optimization problem. The values of δt were chosen in a range as reported below.

The number of sample points used for estimating the Fisher matrix is set to $N_s = 10,000$: large enough to ensure the stability of the Fisher matrix estimates.

For the quantile rewriting of f (Section 1.2), we followed a selection scheme often applied in evolution strategies [Rec94] and set w to be $w(q) = 1_{q \leq 1/5}$ so that the best 20% of points in a sample are given weight 1 for the update, while other points are given weight 0. Ties were dealt with according to (13).

Initialization. For initialization of the RBMs, we choose random values of the parameters that guarantee that each variable (observed or latent) has a probability of activation close to 1/2 at startup, i.e., the initial distribution is almost uniform. This is in line with the discussion in Section 1.1 about starting with large initial diversity. Namely, the weights \mathbf{w} are sampled from a normal distribution centered around zero and of standard deviation $1/\sqrt{n_x \times n_h}$, where n_x is the number of observed variables (dimension d of the problem) and n_h is the number of latent variables ($n_h = 1$ in our case), so that initially the energies E are not too large. Then the bias parameters

are initialized as $b_j \leftarrow -\sum_i \frac{w_{ij}}{2}$ and $a_i \leftarrow -\sum_j \frac{w_{ij}}{2} + \mathcal{N}(\frac{0.01}{n_x^2})$: this setting guarantees initial probabilities of activation close to 1/2 for all variables.

For each run, the parameter \mathbf{y} of the two-max function was sampled randomly in $\{0,1\}^{n_x}$ in order to ensure that the presented results are not dependent on a particular location of the optima.

Step size. The value of δt is indicated for each plot. Note that the values of the parameter δt for the two gradients used are not directly comparable from a theoretical viewpoint (they correspond to parametrizations of different trajectories in Θ -space, and identifying vanilla δt with natural δt is meaningless). For a given δt the natural gradient tends to move faster than the vanilla gradient. For this reason, we selected larger values of δt for the vanilla gradient: a factor 4 seems to yield roughly comparable moving speeds in practice. (This is consistent with the remark that at time 0, the largest terms of the Fisher matrix are equal to 1/4 and most non-diagonal terms vanish, as can be seen from (61) given that the parameters are initialized close to the uniform distribution.)

Reading the plots. The plots reported below are of two types: trajectories of single runs (such as Fig. 4), and aggregate over K runs (such as Fig. 5). For the aggregate plots, we present the median together with error bars indicating the 16th percentile and the 84th percentile over the K runs, namely, 16% of runs are below the lower error bar and likewise for the upper error bar (for a Gaussian variable this is the same as the mean and $\text{mean} \pm \text{stddev}$, but applies to non-Gaussian variables and is better behaved under f -reparametrization).

Source code. The code used for these experiments can be found on the Internet at <http://www.ludovicarnold.com/projects:igocode>.

5.3 Experimental results

Approaching the optima. We now report how the vanilla and natural gradient approach the two optima of the objective function (remember the objective function is bimodal). We start with the large population case $N = 10,000$.

Figure 4 shows ten trajectories of the natural gradient (left column) and vanilla gradient (right column), using a large population size ($N = 10,000$). At each step, we report the smallest distance of the N sample points in the population to the closest optimum of the objective function (top row), as well as the smallest distance of the N sample points in the population to the *other* optimum of the objective function (bottom row). Figure 5 reports the same quantities aggregated over 300 independent runs (median over all runs, error bars as described above) for various settings of δt .

The small population case $N = 10$ is illustrated in Figure 6 (single runs) and Figure 7 (aggregate over 20 runs). For small population sizes, the dynamics is noisier, and smaller step sizes δt have been used to average out the noise (resulting in roughly the same total number of f -calls, see the discussion of finite sample size in Section 6). The results are broadly similar to those with $N = 10,000$, as revealed by the aggregate plots (Figure 7), but individual runs can exhibit less regular behavior (see the “spike” on the bottom-left graph of Figure 6, presumably due to an unreliable estimate of

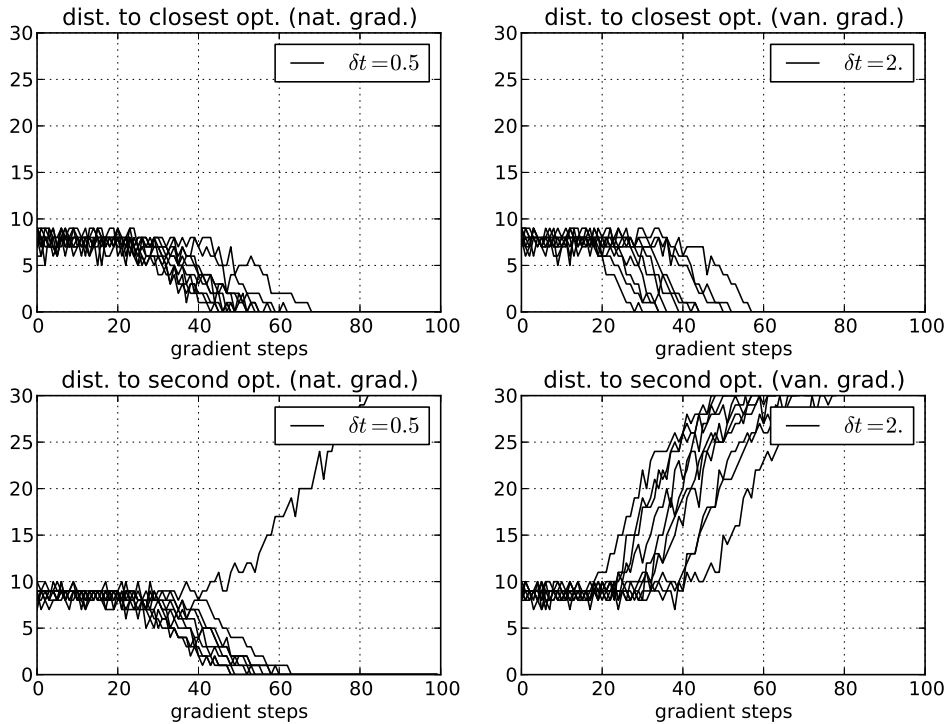


Figure 4: Distance to the two optima using a large population of 10,000 samples, during 10 IGO optimization runs and 10 vanilla gradient runs

the Fisher matrix, though the next iteration apparently cancels the effect). Smaller learning rates seem to behave better.

Larger step sizes δt have also been tested for the small population case (Figures 8 and 9). It appears that the natural gradient is more sensitive to large step sizes than the vanilla gradient: with the natural gradient for small population at large learning rates, many runs get frozen before they reach an optimum due to the problem of estimating the Fisher matrix (Table 1).

Diversity and h -statistics. Predictably, both algorithms are able to find at least one optimum of the very simple two-min function in a few steps. However, the methods fare very differently when we look at the distance from the sample points to *both* optima (Figures 4, 5, 6 and 7).

Most runs using the natural gradient get close to both optima simultaneously, reflecting the fact that the distribution P_θ becomes bimodal, as allowed by the RBM. The two optima are generally reached within a few steps of each other.

This is consistent with the intuition of Section 1.1 about maintaining diversity in natural gradient optimization. This property of IGO depends, of course, on having initialized the RBM with enough diversity. When initialized properly so that each variable (observed and latent) has a probability 1/2 of being equal to 1, the initial RBM distribution has maximal diversity over the search space and is at equal distance from the two optima of the function. From this starting position, IGO is then able to increase the likelihood of the two optima at the same time.

By stark contrast, the vanilla gradient *never* went towards both optima at the same time. In fact, the vanilla gradient only approaches one optimum at the expense of the other: for all values of δt , the distance to the second optimum increases gradually and approaches the maximum possible distance. So in these experiments the vanilla gradient never exploits the possibility

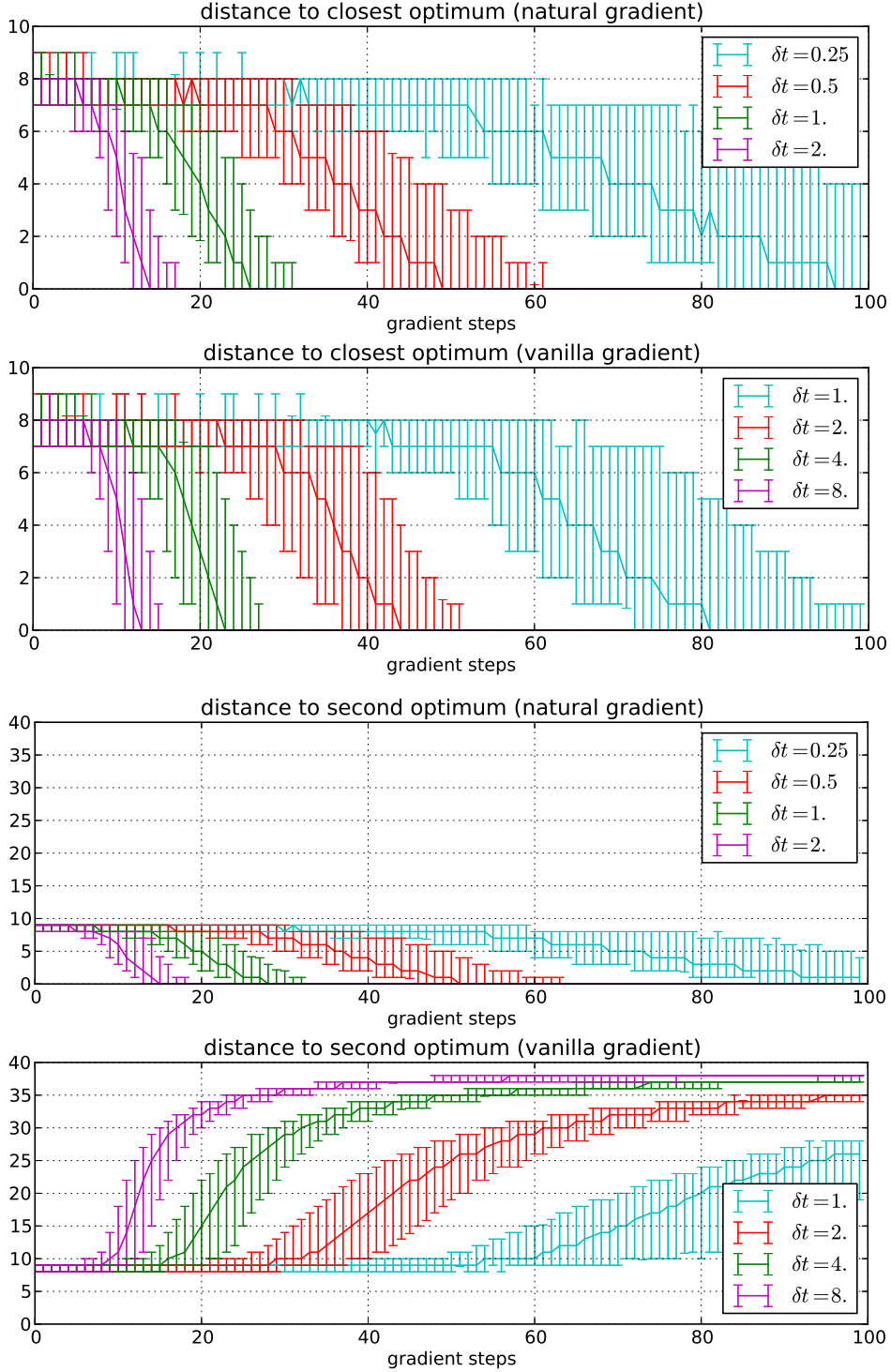


Figure 5: Median distance to an optimum with a large population of 10,000 samples over 300 optimization runs, respectively using IGO or the vanilla gradient. Top two figures: distance to the closest optimum; bottom two figures: distance to other optimum. Error bars indicate the 16th and 84th quantile over the runs.

offered by the RBM to create a bimodal probability distribution P_θ .

As mentioned earlier, each value 0 or 1 of the latent variable \mathbf{h} corresponds to a mode of the distribution. To illustrate the evolution of uni- or bi-modality of P_θ , we plot in Figure 10 the average value of \mathbf{h} in the popu-

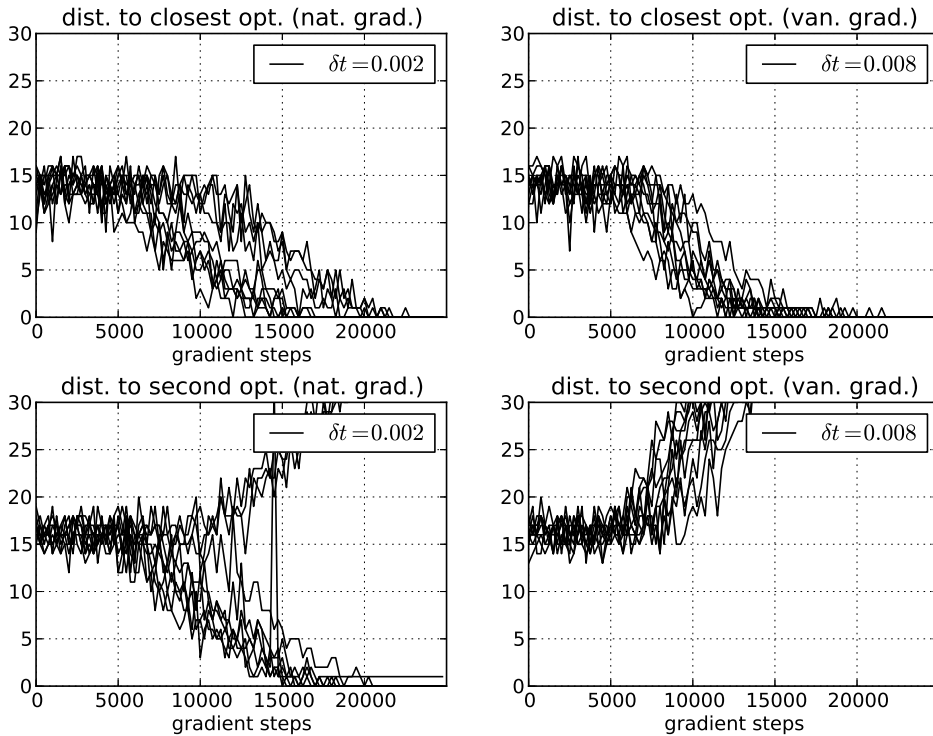


Figure 6: Distance to closest optimum using a small population of 10 samples, during 10 IGO optimization runs and 10 vanilla gradient runs. The “spike” on the bottom-left plot is presumably due to an unreliable estimate of the Fisher matrix at one step.

lation over time (aggregated over 300 runs). An average value close to $1/2$ means that the distribution samples from both modes $\mathbf{h} = 0$ or $\mathbf{h} = 1$ with a comparable probability. Conversely, average values close to 0 or 1 indicate that the distribution gives most probability to one mode at the expense of the other and is thus essentially unimodal. We can see that with IGO, the average value of \mathbf{h} stays remarkably centered during the whole optimization procedure: the distribution stays bimodal. As for the vanilla gradient, we see that the statistics for \mathbf{h} quickly tend to converge to 1: one of the two modes of the distribution has been lost during optimization.

Hidden breach of symmetry by the vanilla gradient. The experiments reveal a curious phenomenon (Figure 10): the vanilla gradient loses multimodality by always setting the hidden variable h to 1, not to 0. (We detected no obvious asymmetry on the visible units x .) So the vanilla gradient for RBMs seems to favor $h = 1$.

Of course, exchanging the values 0 and 1 for the hidden variables in a restricted Boltzmann machine still gives a distribution of another Boltzmann machine. More precisely, changing h_j into $1 - h_j$ is equivalent to resetting $a_i \leftarrow a_i + w_{ij}$, $b_j \leftarrow -b_j$, and $w_{ij} \leftarrow -w_{ij}$. IGO and the natural gradient are impervious to such a change by Proposition 10.

The vanilla gradient implicitly relies on the Euclidean norm on parameter space, as explained in Section 1.1. For this norm, the distance between the RBM distributions (a_i, b_j, w_{ij}) and (a'_i, b'_j, w'_{ij}) is simply $\sum_i |a_i - a'_i|^2 + \sum_j |b_j - b'_j|^2 + \sum_{ij} |w_{ij} - w'_{ij}|^2$. However, the change of variables $a_i \leftarrow a_i + w_{ij}$, $b_j \leftarrow -b_j$, $w_{ij} \leftarrow -w_{ij}$ does *not* preserve this Euclidean metric. Thus, exchanging 0 and 1 for the hidden variables will result in two different

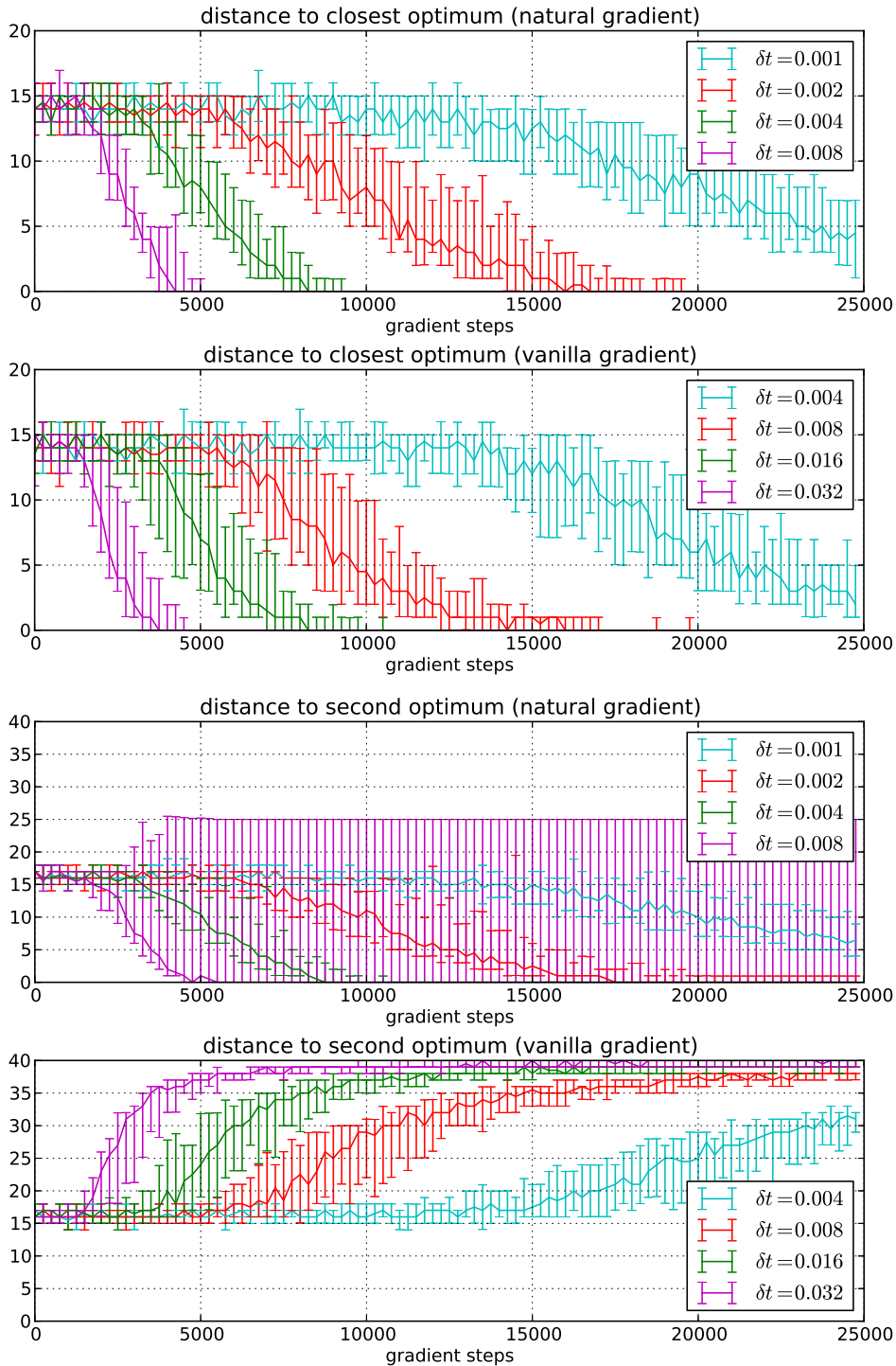


Figure 7: Median distance to an optimum using a small population of 10 samples in either 20 IGO optimization runs or 20 vanilla gradient runs, respectively. Top two figures: distance to the closest optimum; bottom two figures: distance to the other optimum. Error bars indicate the 16th and 84th quantile.

vanilla gradient ascents. The observed asymmetry on h is a consequence of this implicit asymmetry.

The same asymmetry actually exists for the visible variables x_i ; but this does not prevent convergence to an optimum in our situation, since any gradient descent eventually reaches some local optimum.

Of course it is possible to use parametrizations for which the vanilla

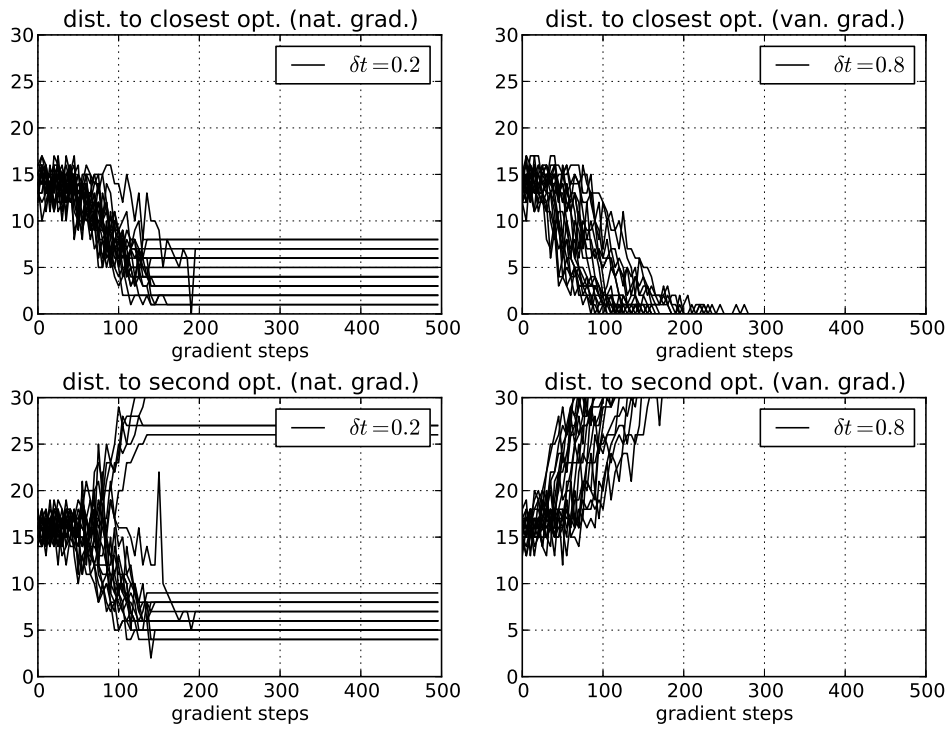


Figure 8: Distance to closest (above) and the other (below) optimum using a small population of 10 samples and learning rates too large to ensure convergence of IGO. 20 IGO optimization runs and 20 vanilla gradient runs.

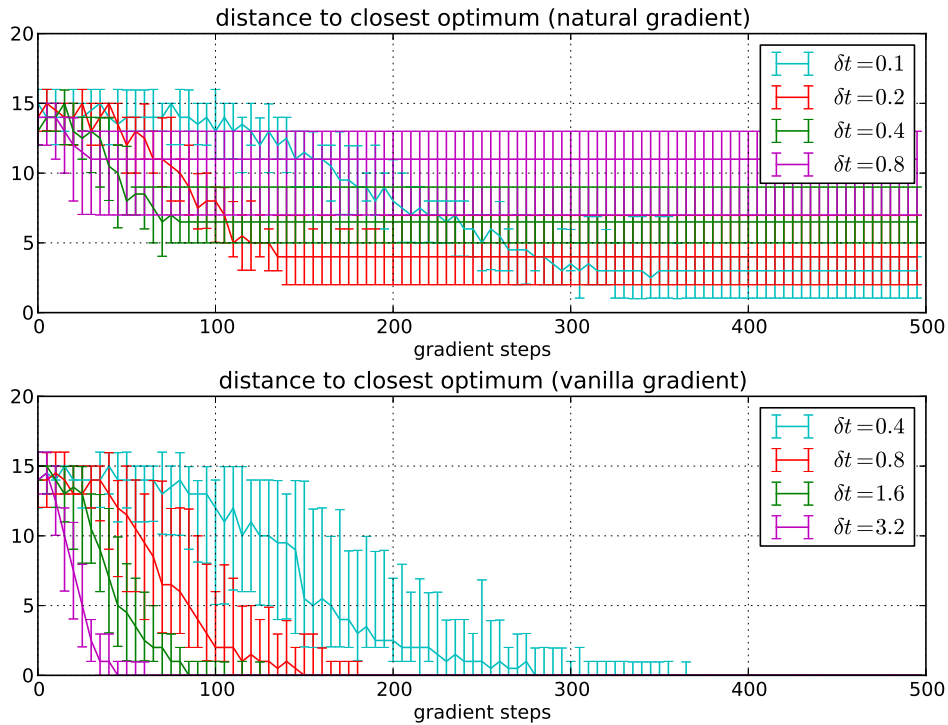


Figure 9: Median distance (over 20 runs) to closest optimum using a small population of 10 samples and learning rates too large to ensure convergence of IGO. Above: natural gradient, below: vanilla gradient. Error bars indicate the 16th and 84th quantile over the 20 runs.

gradient will be more symmetric: for instance, using $-1/1$ instead of $0/1$ for

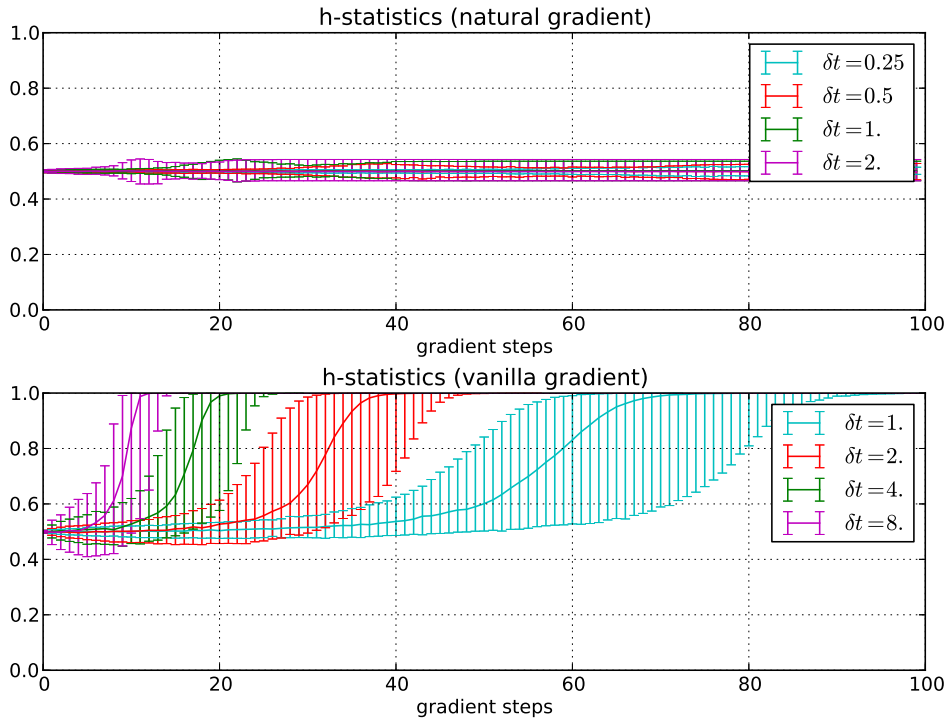


Figure 10: Median of average h -statistics in 300 IGO optimization runs and 300 vanilla gradient runs using a large population of 10,000 samples. 2,000 samples are used for selection at each step. Error bars indicate the 16th and 84th quantile over the runs.

the variables, or defining the energy by

$$E(\mathbf{x}, \mathbf{h}) = -\sum_i A_i(x_i - \frac{1}{2}) - \sum_j B_j(h_j - \frac{1}{2}) - \sum_{i,j} W_{ij}(x_i - \frac{1}{2})(h_j - \frac{1}{2}) \quad (64)$$

with “bias-free” parameters A_i, B_j, W_{ij} related to the usual parametrization by $w_{ij} = W_{ij}$, $a_i = A_i - \frac{1}{2} \sum_j w_{ij}$, and $b_j = B_j - \frac{1}{2} \sum_i w_{ij}$. The vanilla gradient might perform better in this parametrization.

However, we adopted the approach of using a family of probability distributions found in the literature, with the parametrization commonly found in the literature. We then used the vanilla gradient and the natural gradient on these distributions—and indeed the vanilla gradient or an approximation thereof is routinely applied to RBMs in the literature to optimize the log-likelihood of data [Hin02, HOT06, BLPL07]. It was not obvious a priori (at least for us) that the vanilla gradient ascent favors $h = 1$.

This directly illustrates the specific influence of the chosen gradient (the two implementations only differ by the inclusion of the Fisher matrix): the natural gradient offers a systematic way to recover symmetry from a non-symmetric gradient update.

Note that symmetry alone does not explain the fact that IGO reaches the two optima simultaneously: indeed, a symmetry-preserving stochastic algorithm could very well end up on either single optimum with 50% probability in each run. The diversity-preserving property of IGO offers a reasonable interpretation of why this does not happen.

5.4 Convergence to the continuous-time limit

In the previous figures, it looks like changing the parameter δt only results, to some extent, in a time speedup of the plots.

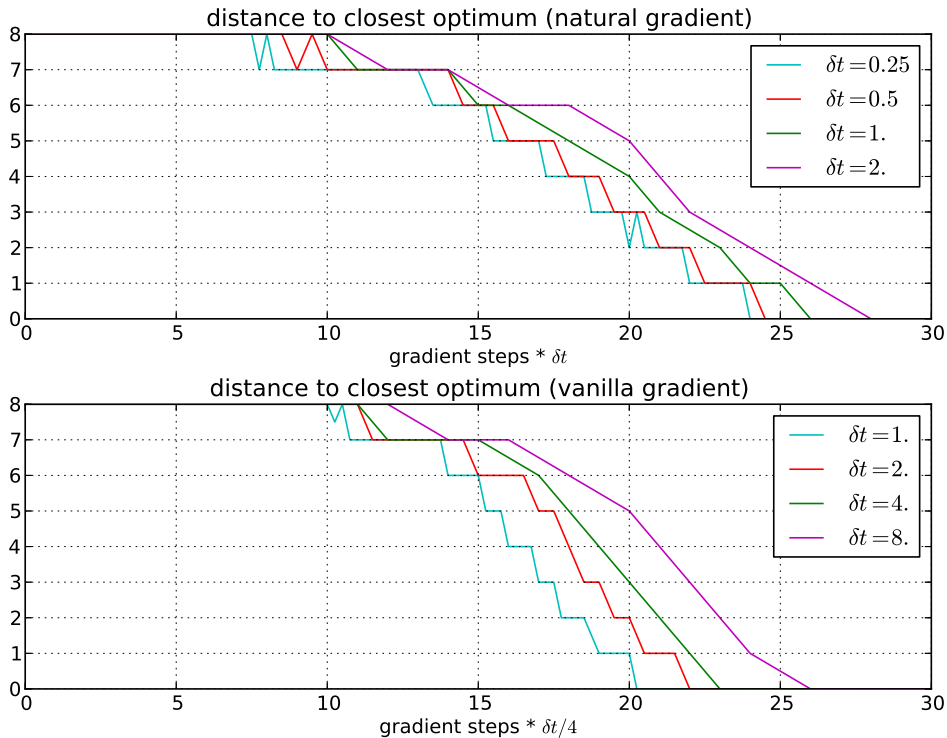


Figure 11: Median distance to closest optimum during 300 IGO optimization runs and 300 vanilla gradient runs using a large population of 10,000 samples plotted in intrinsic time. 2,000 samples are used for selection at each step.

This can be checked on Figure 11, where we plot the distance to the closest optimum as a function of $t = (\delta t \times \text{number of steps})$ instead of the number of steps. An asymptotic trajectory seems to emerge when δt decreases.

This is because update rules of the type $\theta \leftarrow \theta + \delta t \nabla_{\theta} g$ (for either gradient) are Euler approximations of the continuous-time ordinary differential equation $\frac{d\theta}{dt} = \nabla_{\theta} g$, with each iteration corresponding to an increment δt of the time t . Consequently, for small enough δt , the algorithm after k steps approximates the IGO flow or vanilla gradient flow at time $t = k \cdot \delta t$. Thus for the natural gradient, the asymptotic trajectory can be interpreted as the fitness of samples of the continuous-time IGO flow.

So on one hand, for this kind of optimization algorithms it would make theoretical sense to plot the results according to the “intrinsic time” $t = k \cdot \delta t$ of the underlying continuous-time object, to illustrate properties that do not depend on the setting of the parameter δt . Still, the raw number of steps is more directly related to algorithmic cost.

6 Further discussion and perspectives

A single framework for optimization on arbitrary spaces. A strength of the IGO viewpoint is to automatically provide a unique, distinct, and arguably optimal optimization algorithm from any family of probability distributions on any given space, discrete or continuous. This has been illustrated with restricted Boltzmann machines. IGO algorithms feature good invariance properties and make a least number of arbitrary choices.

In particular, IGO describes several well-known optimization algorithms within a single framework. For instance, to the best of our knowledge, PBIL

has never been described as a natural gradient ascent in the literature¹⁰.

For Gaussian distributions, algorithms of the same form (15) had been developed previously [HO01, WSPS08] and their close relationship with a natural gradient ascent had been recognized [ANOK10, GSS⁺10].

The wide applicability of natural gradient approaches seems not to be widely known in the optimization community (though see [MMS08]).

About quantiles. The IGO flow in (6) has, to the best of our knowledge, never been defined before. The introduction of the quantile-rewriting (3) of the objective function provides the first rigorous derivation of quantile- or rank- or comparison-based optimization from a gradient ascent in θ -space.

NES and CMA-ES have been claimed to maximize $-\mathbb{E}_{P_\theta} f$ via natural gradient ascent [WSPS08, ANOK10]. However, we have proved that when the number of samples is large and the step size is small, the NES and CMA-ES updates converge to the IGO flow, not to the similar flow with the gradient of $\mathbb{E}_{P_\theta} f$ (Theorem 5). So we find that in reality these algorithms maximize $\mathbb{E}_{P_\theta} W_{\theta^t}^f$, where $W_{\theta^t}^f$ is a decreasing transformation of the f -quantiles under the current sample distribution.

Moreover, in practice, maximizing $-\mathbb{E}_{P_\theta} f$ is a rather unstable procedure and has been discouraged, see for example [Whi89, SWSS09].

About choice of P_θ : learning a model of good points. The choice of the family of probability distributions P_θ plays a double role.

First, it is analogous to choosing the variation operators (namely *mutation* or *recombination*) as seen in evolutionary algorithms: indeed, P_θ encodes possible moves according to which new sample points are explored.

Second, optimization algorithms using distributions can be interpreted as learning a probabilistic model of where the points with good values lie in the search space. With this point of view, P_θ describes *richness of this model*: for instance, restricted Boltzmann machines with h hidden units can describe distributions with up to 2^h modes, whereas the Bernoulli distribution used in PBIL is unimodal. This influences, for instance, the ability to explore several valleys and optimize multimodal functions in a single run.

More generally, the IGO framework makes it tempting to use more complex models of where good points lie, inspired, e.g., from machine learning, and adapt them for optimization. The restricted Boltzmann machines of Section 5 are a first step in this direction. The initial idea behind these machines is that each hidden unit controls a block of coordinates of the search space (a block of features), so that the optimization algorithm hopefully builds a good model of which features must be activated or de-activated together to obtain good values of f . This is somewhat reminiscent of a crossover operator: if observation of good points shows that a block of features go together, this information is stored in the RBM structure and this block may be later activated as a whole, thus effectively transferring blocks of features from one good solution to another. Inspired by models of deep learning [BCV12], one might be tempted to stack such models on top of each other, so that optimization would operate on a more and more abstract representation of the problem. IGO and the natural gradient might help in exploiting the added expressivity that comes with richer models (in our simple experiment, the vanilla gradient ignores the additional expressivity of RBMs with respect to Bernoulli distributions).

¹⁰Thanks to Jonathan Shapiro for an early argument confirming this property (personal communication).

Natural gradient and parametrization invariance. Central to IGO is the use of the natural gradient, which follows from θ -invariance and makes sense on any search space, discrete or continuous.

While the IGO flow is exactly θ -invariant, for any practical implementation of an IGO algorithm, a parametrization choice has to be made. Still, since all IGO algorithms approximate the IGO flow, two parametrizations in combination with IGO will differ less than the same two parametrizations in combination with another algorithm (such as the vanilla gradient or the smoothed CEM method)—at least if the learning rate δt is not too large. The chosen parametrization becomes more relevant as the step size δt increases.

On the other hand, natural evolution strategies have never strived for θ -invariance, but instead, the chosen parametrization (Cholesky, exponential) has been deemed a relevant feature. We believe the term “natural evolution strategy” should rather be used independently of the chosen parameterization, thereby referring to the usage of the natural gradient as the main principle for the update of distribution parameters.

IGO, maximum likelihood and cross-entropy. The cross-entropy method (CEM) [dBKMR05] can be used to produce optimization algorithms given a family of probability distributions on an arbitrary space, by performing a jump to a maximum likelihood estimate of the parameters.

We have seen (Corollary 17) that the standard CEM is an IGO algorithm *in a particular parametrization*, with a learning rate δt equal to 1. However, it is well-known, both theoretically and experimentally [BLS07, Han06b, WAS04], that standard CEM loses diversity too fast in many situations. The usual solution [dBKMR05] is to reduce the learning rate (smoothed CEM, (28)), but this breaks the reparametrization invariance of non-smoothed CEM.

On the other hand, the IGO flow can be seen as a *maximum likelihood update with infinitesimal learning rate* (Theorem 14). This interpretation allows to define a particular IGO algorithm, the IGO-ML (Definition 15): it performs a maximum likelihood update with an arbitrary learning rate, and keeps the reparametrization invariance. It coincides with CEM when the learning rate is set to 1, but it differs from smoothed CEM by the exchange of the order of argmax and averaging (compare (26) and (28)). We argue that this new algorithm may be a better way to reduce the learning rate and achieve smoothing in CEM.

Standard CEM can lose diversity, yet is a particular case of an IGO algorithm: this illustrates the fact that reasonable values of the learning rate δt depend on the parametrization. We have studied this phenomenon in detail for various Gaussian IGO algorithms (Section 4.2).

Why would a smaller learning rate perform better than a large one in an optimization setting? It might seem more efficient to jump directly to the maximum likelihood estimate of currently known good points, instead of performing a slow gradient ascent towards this maximum. However, optimization faces a “moving target”, contrary to a learning setting in which the example distribution is often stationary. Currently known good points heavily depend on the current distribution and are likely not to indicate the *position* at which the optimum lies, but, rather, the *direction* in which the optimum is to be found. After an update, the next elite sample points are going to be located somewhere new. So the goal is certainly not to settle down around these currently known points, as a maximum likelihood update does:

by design, CEM only tries to reflect status-quo (even for $N = \infty$), whereas IGO tries to move somewhere. When the target moves over time, a progressive gradient ascent is more reasonable than an immediate jump to a temporary optimum, and realizes a kind of time smoothing.

This phenomenon is most clear when the number of sample points is small. Then, a full maximum likelihood update risks losing a lot of diversity; it may even produce a degenerate distribution if the number of sample points is smaller than the number of parameters of the distribution. On the other hand, for smaller δt , the IGO algorithms do, by design, try to maintain diversity by moving as little as possible from the current distribution P_θ in Kullback–Leibler divergence. A full ML update disregards the current distribution and tries to move as close as possible to the elite sample in Kullback–Leibler divergence [dBKMR05], thus realizing maximal diversity loss. This makes sense in a non-iterated scenario such as batch learning but is unsuited for optimization.

Diversity and multiple optima. The IGO framework emphasizes the relation of natural gradient and diversity: we argued that IGO provides minimal diversity change for a given objective function increment. In particular, provided the initial diversity is large, diversity is kept at a maximum at startup. This theoretical relationship has been confirmed experimentally for restricted Boltzmann machines.

On the other hand, using the vanilla gradient does not lead to a balanced distribution between the two optima in our experiments. Using the vanilla gradient introduces hidden arbitrary choices between those points (more exactly between moves in Θ -space). This results in unnecessary and unwelcome loss of diversity, and might also be detrimental at later stages in the optimization. This may reflect the fact that the Euclidean metric on the space of parameters, implicitly used in the vanilla gradient, becomes less and less meaningful for gradient descent on complex distributions.

IGO and the natural gradient are certainly relevant to the well-known problem of exploration-exploitation balance: as we have seen, arguably the natural gradient realizes the largest improvement in the objective with the least possible change of diversity in the distribution.

More generally, like other distribution-based optimization algorithms, IGO tries to learn a model of where the good points are. This is typical of machine learning, one of the contexts for which the natural gradient was studied. The conceptual relationship of IGO and IGO-like optimization algorithms with machine learning is still to be explored and exploited.

We now present some ideas which we believe would be worth exploring.

Adaptive learning rate. Comparing consecutive updates to evaluate a learning rate or step size is an effective measure. For example, in back-propagation, the update sign has been used to adapt the learning rate of each single weight in an artificial neural network [SA90]. In CMA-ES, a step size is adapted depending on whether recent steps tended to move in a consistent direction or to backtrack. This is measured by considering the changes of the mean m of the Gaussian distribution.

For a probability distribution P_θ on an arbitrary search space, in general no notion of mean may be defined. However, it is still possible to define “backtracking” in the evolution of θ as follows.

Consider two successive updates $\delta\theta^t = \theta^t - \theta^{t-\delta t}$ and $\delta\theta^{t+\delta t} = \theta^{t+\delta t} - \theta^t$. Their scalar product in the Fisher metric $I(\theta^t)$ is

$$\langle \delta\theta^t, \delta\theta^{t+\delta t} \rangle = \sum_{ij} I_{ij}(\theta^t) \delta\theta_i^t \delta\theta_j^{t+\delta t}.$$

Dividing by the associated norms will yield the cosine $\cos \alpha$ of the angle between $\delta\theta^t$ and $\delta\theta^{t+\delta t}$.

If this cosine is positive, the learning rate δt may be increased. If the cosine is negative, the learning rate probably needs to be decreased. Various schemes for the change of δt can be devised; for instance, inspired by step size updates commonly used in evolution strategies, one can multiply δt by $\exp(\beta(\cos \alpha))$ or $\exp(\beta \text{sign}(\cos \alpha))$, where $\beta \approx \min(N/\dim \Theta, 1/2)$.

As before, this scheme is constructed to be robust w.r.t. reparametrization of θ , thanks to the use of the Fisher metric. However, for large learning rates δt , in practice the parametrization might well become relevant.

A consistent direction of the updates does not necessarily mean that the algorithm is performing well: for instance, when CEM/EMNA exhibits premature convergence (see above), the parameters consistently move towards a zero covariance matrix and the cosines above are positive. This indicates too small steps, as the desired target value for the cosine is zero.

Geodesic parametrization. While the IGO flow is fully invariant under θ -reparametrization, an IGO algorithm does depend on the choice of parametrization for θ , even if for small δt the difference between two IGO algorithms is $O(\delta t^2)$, one order of magnitude smaller than between IGO and vanilla gradient in general.

Still one can wonder how to discretize time in the IGO flow in a fully intrinsic way, not depending at all on a parametrization for θ . A first possibility is given by the IGO-ML algorithm (Definition 15)—this means, for exponential families, that we can decide to single out the parametrization by expectation parameters.

Another, more geometric solution is to use *geodesics* on the statistical manifold. This means we approximate the trajectories of the IGO flow by successive geodesic segments of length δt in the Fisher metric, where the initial direction of each segment is given by the direction of the IGO flow.

More precisely, if

$$Y = \sum_{i=1}^N \widehat{w}_i \widetilde{\nabla}_{\theta} \ln P_{\theta}(x_i) \Big|_{\theta=\theta^t} = I^{-1}(\theta^t) \sum_{i=1}^N \widehat{w}_i \frac{\partial \ln P_{\theta}(x_i)}{\partial \theta} \Big|_{\theta=\theta^t}$$

is the direction of the IGO update (14) at θ^t , one can define

$$\theta^{t+\delta t} = \exp_{\theta^t}(\delta t \cdot Y)$$

where \exp is the exponential map of the Riemannian manifold Θ equipped with the Fisher information metric.

This defines an approximation to the IGO flow that depends on the step size δt and sample size N , but *not* on any choice of parametrization.

Practical implementation will depend on being able to compute the geodesics of the Fisher metric. The equation of geodesics may be computed explicitly in some particular cases [Bur86], [ABNK+87, Chapter 5], such as Bernoulli distributions or Gaussian distributions with a fixed mean or with a fixed covariance matrix. Interestingly, for Gaussian distributions with a fixed mean, the geodesic update resembles the one in xNES.

When no closed formula for geodesics is available, $\theta^{t+\delta t}$ can always be found by numerically integrating the geodesic equation starting at θ^t with initial speed Y . This is, of course, an added computational cost, but it does not require any calls to the objective function f .

Finite sample size and noisy IGO flow. The IGO flow is an ideal model of the IGO algorithms. But the IGO flow is deterministic while IGO algorithms are stochastic, depending on a finite number N of random samples. This might result in important differences in their behavior and one can wonder if there is a way to reflect stochasticity directly into the definition of the IGO flow.

The IGO update (14) is a stochastic update

$$\theta^{t+\delta t} = \theta^t + \delta t \sum_{i=1}^N \hat{w}_i \tilde{\nabla}_{\theta} \ln P_{\theta}(x_i) \Big|_{\theta=\theta^t}$$

because the term $\sum_{i=1}^N \hat{w}_i \tilde{\nabla}_{\theta} \ln P_{\theta}(x_i) \Big|_{\theta=\theta^t}$ involves a random sample. As such, this term has an expectation and a variance. So for a fixed N and δt , this random update is a weak approximation with step size δt [KP92, Chapter 9.7] of a stochastic differential equation on θ , whose drift is the expectation of the IGO update (which tends to the IGO flow when $N \rightarrow \infty$), and whose noise term is $\sqrt{\delta t}$ times the square root of the covariance matrix of the update applied to a normal random vector.

Such a stochastic differential equation, defining a *noisy IGO flow*, might be a better theoretical object with which to compare the actual behavior of IGO algorithms, than the ideal noiseless IGO flow.

For instance, this strongly suggests that if we have $\delta t \rightarrow 0$ while N is kept fixed in an IGO algorithm, noise will disappear (compare Remark 2 in [AAH12]).

Second, for large N , one expects the variance of the IGO update to scale like $1/N$, so that the noise term will scale like $\sqrt{\delta t/N}$. This formally suggests that, within reasonable bounds, multiplying or dividing both N and δt by the same factor should result in similar behavior of the algorithm, so that for instance it should be reasonable to reset N to 10 and δt to $10\delta t/N$. (Note that the cost in terms of f -calls of these two algorithms is similar.)

This dependency is reflected in evolution strategies in several ways, with typical values for N ranging between ten and a few hundred. First, theoretical results on the function $f(x) = \|x\|$ indicate that the optimal step size δt for the mean vector is proportional to N , provided the weighting function w reflects truncation selection with a fixed truncation ratio [Bey01] or optimal weights [Arn06]. Second, the learning rate δt of the covariance matrix in CMA-ES is chosen proportional to $(\sum_{i=1}^N \hat{w}_i)^2 / \sum_{i=1}^N \hat{w}_i^2$ which is again proportional to N [HK04]. For small enough N , the progress per f -call is then in both cases rather independent of the choice of N .

Influence of the Fisher geometry of the statistical manifold. The global Riemannian geometry of the statistical manifold P_{θ} might have a bearing on the behavior of stochastic algorithms exploring this manifold. For instance, the Fisher metric identifies the set of 1-dimensional normal distributions $\mathcal{N}(m, \sigma^2)$ with the two-dimensional hyperbolic plane. The latter has negative curvature. The sign of curvature has a strong influence on the behavior of random walks in a Riemannian manifold: in particular, in negative curvature, successive random errors tend to not compensate as

much as in the Euclidean case (because geodesics diverge more quickly); this might be relevant to the settings of a stochastic optimization algorithm, suggesting to use larger sample size (or smaller steps) when curvature is negative. This is speculative and remains to be explored.

Summary and conclusion

We sum up:

- The information-geometric optimization (IGO) framework derives from invariance principles and allows to build optimization algorithms from any family of distributions on any search space. In some instances (Gaussian distributions on \mathbb{R}^d or Bernoulli distributions on $\{0, 1\}^d$) it recovers versions of known algorithms (CMA-ES or PBIL); in other instances (restricted Boltzmann machine distributions) it produces new, hopefully efficient optimization algorithms.
- The use of a quantile-based, time-dependent transform of the objective function (Equation (3)) provides a rigorous derivation of rank-based update rules currently used in optimization algorithms. Theorem 5 uniquely identifies the infinite-population limit of these update rules.
- The IGO flow is singled out by its equivalent description as an infinitesimal weighted maximum log-likelihood update (Theorem 14). In a particular parametrization and with a step size of 1, IGO recovers the cross-entropy method (Corollary 17). This allows to define a new, fully parametrization-invariant smoothed maximum likelihood update, the IGO-ML.
- Theoretical arguments suggest that the IGO flow minimizes the change of diversity in the course of optimization. In particular, starting with high diversity and using multimodal distributions may allow simultaneous exploration of multiple optima of the objective function. Preliminary experiments with restricted Boltzmann machines confirm this effect in a simple situation.

Thus, the IGO framework is an attempt to provide sound theoretical foundations to optimization algorithms based on probability distributions. In particular, this viewpoint helps to bridge the gap between continuous and discrete optimization.

The invariance properties, which reduce the number of arbitrary choices, together with the relationship between natural gradient and diversity, may contribute to a theoretical explanation of the good practical performance of those currently used algorithms, such as CMA-ES, which can be interpreted as instantiations of IGO.

We hope that invariance properties will acquire in computer science the importance they have in mathematics, where intrinsic thinking is the first step for abstract linear algebra or differential geometry, and in modern physics, where the notions of invariance w.r.t. the coordinate system and so-called gauge invariance play a central role.

Acknowledgements

The authors would like to thank Michèle Sebag for the acronym and for helpful comments. We also thank Youhei Akimoto for helpful feedback.

Y. O. would like to thank Cédric Villani and Bruno Sévenec for helpful discussions on the Fisher metric. A. A. and N. H. would like to acknowledge the Dagstuhl Seminar No 10361 on the Theory of Evolutionary Computation (<http://www.dagstuhl.de/10361>) for inspiring their work on natural gradients and beyond. This work was partially supported by the ANR-2010-COSI-002 grant (SIMINOLE) of the French National Research Agency.

Appendix: Proofs

Proof of Theorem 5 (Convergence of empirical means and quantiles)

Let us give a more precise statement including the necessary regularity conditions.

Proposition 23. *Let $\theta \in \Theta$. Assume that the derivative $\frac{\partial \ln P_\theta(x)}{\partial \theta}$ exists for P_θ -almost all $x \in X$ and that $\mathbb{E}_{P_\theta} \left| \frac{\partial \ln P_\theta(x)}{\partial \theta} \right|^2 < +\infty$. Assume that the function w is non-decreasing and bounded.*

Let $(x_i)_{i \in \mathbb{N}}$ be a sequence of independent samples of P_θ . Then with probability 1, as $N \rightarrow \infty$ we have

$$\frac{1}{N} \sum_{i=1}^N \widehat{W}^f(x_i) \frac{\partial \ln P_\theta(x_i)}{\partial \theta} \rightarrow \int W_\theta^f(x) \frac{\partial \ln P_\theta(x)}{\partial \theta} P_\theta(dx)$$

where

$$\widehat{W}^f(x_i) = w \left(\frac{\text{rk}_N(x_i) + 1/2}{N} \right)$$

with $\text{rk}_N(x_i) = \#\{1 \leq j \leq N, f(x_j) < f(x_i)\}$. (When there are f -ties in the sample, $W^f(x_i)$ is defined as the average of $w((r+1/2)/N)$ over the possible rankings r of x_i .)

Proof. Let $g : X \rightarrow \mathbb{R}$ be any function with $\mathbb{E}_{P_\theta} g^2 < \infty$. We will show that $\frac{1}{N} \sum \widehat{W}^f(x_i) g(x_i) \rightarrow \int W_\theta^f(x) g(x) P_\theta(dx)$. Applying this with g equal to the components of $\frac{\partial \ln P_\theta(x)}{\partial \theta}$ will yield the result.

Let us decompose

$$\frac{1}{N} \sum \widehat{W}^f(x_i) g(x_i) = \frac{1}{N} \sum W_\theta^f(x_i) g(x_i) + \frac{1}{N} \sum (\widehat{W}^f(x_i) - W_\theta^f(x_i)) g(x_i).$$

Each summand in the first term involves only one sample x_i (contrary to $\widehat{W}^f(x_i)$ which depends on the whole sample). So by the strong law of large numbers, almost surely $\frac{1}{N} \sum W_\theta^f(x_i) g(x_i)$ converges to $\int W_\theta^f(x) g(x) P_\theta(dx)$. So we have to show that the second term converges to 0 almost surely.

By the Cauchy–Schwarz inequality, we have

$$\left| \frac{1}{N} \sum (\widehat{W}^f(x_i) - W_\theta^f(x_i)) g(x_i) \right|^2 \leq \left(\frac{1}{N} \sum (\widehat{W}^f(x_i) - W_\theta^f(x_i))^2 \right) \left(\frac{1}{N} \sum g(x_i)^2 \right)$$

By the strong law of large numbers, the second term $\frac{1}{N} \sum g(x_i)^2$ converges to $\mathbb{E}_{P_\theta} g^2$ almost surely. So we have to prove that the first term $\frac{1}{N} \sum (\widehat{W}^f(x_i) - W_\theta^f(x_i))^2$ converges to 0 almost surely.

Since w is bounded by assumption, we can write

$$\begin{aligned} (\widehat{W}^f(x_i) - W_\theta^f(x_i))^2 &\leq 2B \left| \widehat{W}^f(x_i) - W_\theta^f(x_i) \right| \\ &= 2B \left| \widehat{W}^f(x_i) - W_\theta^f(x_i) \right|_+ + 2B \left| \widehat{W}^f(x_i) - W_\theta^f(x_i) \right|_- \end{aligned}$$

where B is the bound on $|w|$. We will bound each of these terms.

Let us abbreviate $q_i^< = \Pr_{x' \sim P_\theta}(f(x') < f(x_i))$, $q_i^{\leq} = \Pr_{x' \sim P_\theta}(f(x') \leq f(x_i))$, $r_i^< = \#\{j \leq N, f(x_j) < f(x_i)\}$, $r_i^{\leq} = \#\{j \leq N, f(x_j) \leq f(x_i)\}$.

By definition of \widehat{W}^f we have

$$\widehat{W}^f(x_i) = \frac{1}{r_i^{\leq} - r_i^<} \sum_{k=r_i^<}^{r_i^{\leq}-1} w((k+1/2)/N)$$

and moreover $W_\theta^f(x_i) = w(q_i^<)$ if $q_i^< = q_i^{\leq}$ or $W_\theta^f(x_i) = \frac{1}{q_i^{\leq} - q_i^<} \int_{q_i^<}^{q_i^{\leq}} w$ otherwise.

The Glivenko–Cantelli theorem [Bil95, Theorem 20.6] implies that $\sup_i |q_i^{\leq} - r_i^{\leq}/N|$ tends to 0 almost surely, and likewise for $\sup_i |q_i^< - r_i^</N|$. So let N be large enough so that these errors are bounded by ε .

Since w is non-increasing, we have $w(q_i^<) \leq w(r_i^</N - \varepsilon)$. In the case $q_i^< \neq q_i^{\leq}$, we decompose the interval $[q_i^<; q_i^{\leq}]$ into $(r_i^{\leq} - r_i^<)$ subintervals. The average of w over each such subinterval is compared to a term in the sum defining $w^N(x_i)$: since w is non-increasing, the average of w over the k^{th} subinterval is at most $w((r_i^< + k)/N - \varepsilon)$. So we get

$$W_\theta^f(x_i) \leq \frac{1}{r_i^{\leq} - r_i^<} \sum_{k=r_i^<}^{r_i^{\leq}-1} w(k/N - \varepsilon)$$

so that

$$W_\theta^f(x_i) - \widehat{W}^f(x_i) \leq \frac{1}{r_i^{\leq} - r_i^<} \sum_{k=r_i^<}^{r_i^{\leq}-1} (w(k/N - \varepsilon) - w((k+1/2)/N)).$$

Let us sum over i , remembering that there are $(r_i^{\leq} - r_i^<)$ values of j for which $f(x_j) = f(x_i)$. Taking the positive part, we get

$$\frac{1}{N} \sum_{i=1}^N \left| W_\theta^f(x_i) - \widehat{W}^f(x_i) \right|_+ \leq \frac{1}{N} \sum_{k=0}^{N-1} (w(k/N - \varepsilon) - w((k+1/2)/N)).$$

Since w is non-increasing we have

$$\frac{1}{N} \sum_{k=0}^{N-1} w(k/N - \varepsilon) \leq \int_{-\varepsilon-1/N}^{1-\varepsilon-1/N} w$$

and

$$\frac{1}{N} \sum_{k=0}^{N-1} w((k+1/2)/N) \geq \int_{1/2N}^{1+1/2N} w$$

(we implicitly extend the range of w so that $w(q) = w(0)$ for $q < 0$). So we have

$$\frac{1}{N} \sum_{i=1}^N \left| W_\theta^f(x_i) - \widehat{W}^f(x_i) \right|_+ \leq \int_{-\varepsilon-1/N}^{1/2N} w - \int_{1-\varepsilon-1/N}^{1+1/2N} w \leq (2\varepsilon + 3/N)B$$

where B is the bound on $|w|$.

Reasoning symmetrically with $w(k/N + \varepsilon)$ and the inequalities reversed, we get a similar bound for $\frac{1}{N} \sum \left| W_\theta^f(x_i) - \widehat{W}^f(x_i) \right|_-$. This ends the proof. \square

Proof of Proposition 6 (Quantile improvement)

Let us use the weight $w(u) = 1_{u \leq q}$. Let m be the value of the q -quantile of f under P_{θ^t} . We want to show that the value of the q -quantile of f under $P_{\theta^{t+\delta t}}$ is less than m , unless the gradient vanishes and the IGO flow is stationary.

Let $p_- = \Pr_{x \sim P_{\theta^t}}(f(x) < m)$, $p_m = \Pr_{x \sim P_{\theta^t}}(f(x) = m)$ and $p_+ = \Pr_{x \sim P_{\theta^t}}(f(x) > m)$. By definition of the quantile value we have $p_- + p_m \geq q$ and $p_+ + p_m \geq 1 - q$. Let us assume that we are in the more complicated case $p_m \neq 0$ (for the case $p_m = 0$, simply remove the corresponding terms).

We have $W_{\theta^t}^f(x) = 1$ if $f(x) < m$, $W_{\theta^t}^f(x) = 0$ if $f(x) > m$ and $W_{\theta^t}^f(x) = \frac{1}{p_m} \int_{p_-}^{p_-+p_m} w(u) du = \frac{q-p_-}{p_m}$ if $f(x) = m$.

Using the same notation as above, let $g_t(\theta) = \int W_{\theta^t}^f(x) P_{\theta}(dx)$. Decomposing this integral on the three sets $f(x) < m$, $f(x) = m$ and $f(x) > m$, we get that $g_t(\theta) = \Pr_{x \sim P_{\theta}}(f(x) < m) + \Pr_{x \sim P_{\theta}}(f(x) = m) \frac{q-p_-}{p_m}$. In particular, $g_t(\theta^t) = q$.

Since we follow a gradient ascent of g_t , for δt small enough we have $g_t(\theta^{t+\delta t}) > g_t(\theta^t)$ unless the gradient vanishes. If the gradient vanishes we have $\theta^{t+\delta t} = \theta^t$ and the quantiles are the same. Otherwise we get $g_t(\theta^{t+\delta t}) > g_t(\theta^t) = q$.

Since $\frac{q-p_-}{p_m} \leq \frac{(p_-+p_m)-p_-}{p_m} = 1$, we have $g_t(\theta) \leq \Pr_{x \sim P_{\theta}}(f(x) < m) + \Pr_{x \sim P_{\theta}}(f(x) = m) = \Pr_{x \sim P_{\theta}}(f(x) \leq m)$.

So $\Pr_{x \sim P_{\theta^{t+\delta t}}}(f(x) \leq m) \geq g_t(\theta^{t+\delta t}) > q$. This implies, by definition, that the q -quantile value of $P_{\theta^{t+\delta t}}$ is at most m . Moreover, if the objective function has no plateau then $\Pr_{x \sim P_{\theta^{t+\delta t}}}(f(x) = m) = 0$ and so $\Pr_{x \sim P_{\theta^{t+\delta t}}}(f(x) < m) > q$ which implies that the q -quantile of $P_{\theta^{t+\delta t}}$ is strictly less than m .

Proof of Proposition 11 (Speed of the IGO flow)

Lemma 24. *Let X be a centered L^2 random variable with values in \mathbb{R}^d and let A be a real-valued L^2 random variable. Then*

$$\|\mathbb{E}(AX)\| \leq \sqrt{\lambda \text{Var } A}$$

where λ is the largest eigenvalue of the covariance matrix of X expressed in an orthonormal basis.

Proof of the lemma. Let v be any vector in \mathbb{R}^d ; its norm satisfies

$$\|v\| = \sup_{w, \|w\| \leq 1} (v \cdot w)$$

and in particular

$$\begin{aligned} \|\mathbb{E}(AX)\| &= \sup_{w, \|w\| \leq 1} (w \cdot \mathbb{E}(AX)) \\ &= \sup_{w, \|w\| \leq 1} \mathbb{E}(A(w \cdot X)) \\ &= \sup_{w, \|w\| \leq 1} \mathbb{E}((A - \mathbb{E}A)(w \cdot X)) \quad \text{since } (w \cdot X) \text{ is centered} \\ &\leq \sup_{w, \|w\| \leq 1} \sqrt{\text{Var } A} \sqrt{\mathbb{E}((w \cdot X)^2)} \end{aligned}$$

by the Cauchy–Schwarz inequality.

Now, in an orthonormal basis we have

$$(w \cdot X) = \sum_i w_i X_i$$

so that

$$\begin{aligned} \mathbb{E}((w \cdot X)^2) &= \mathbb{E}\left(\left(\sum_i w_i X_i\right)\left(\sum_j w_j X_j\right)\right) \\ &= \sum_i \sum_j \mathbb{E}(w_i X_i w_j X_j) \\ &= \sum_i \sum_j w_i w_j \mathbb{E}(X_i X_j) \\ &= \sum_i \sum_j w_i w_j C_{ij} \end{aligned}$$

with C_{ij} the covariance matrix of X . The latter expression is the scalar product $(w \cdot Cw)$. Since C is a symmetric positive-semidefinite matrix, $(w \cdot Cw)$ is at most $\lambda \|w\|^2$ with λ the largest eigenvalue of C . \square

For the IGO flow we have $\frac{d\theta^t}{dt} = \mathbb{E}_{x \sim P_\theta} W_\theta^f(x) \tilde{\nabla}_\theta \ln P_\theta(x)$.

So applying the lemma, we get that the norm of $\frac{d\theta}{dt}$ is at most $\sqrt{\lambda \text{Var}_{x \sim P_\theta} W_\theta^f(x)}$ where λ is the largest eigenvalue of the covariance matrix of $\tilde{\nabla}_\theta \ln P_\theta(x)$ (expressed in a coordinate system where the Fisher matrix at the current point θ is the identity).

By construction of the quantiles, we have $\text{Var}_{x \sim P_\theta} W_\theta^f(x) \leq \text{Var}_{[0,1]} w$ (with equality unless there are ties). Indeed, for a given x , let \mathcal{U} be a uniform random variable in $[0, 1]$ independent from x and define the random variable $Q = q^<(x) + (q^\leq(x) - q^<(x))\mathcal{U}$. Then Q is uniformly distributed between the upper and lower quantiles $q^\leq(x)$ and $q^<(x)$ and thus we can rewrite $W_\theta^f(x)$ as $\mathbb{E}(w(Q)|x)$. By the Jensen inequality we have $\text{Var} W_\theta^f(x) = \text{Var} \mathbb{E}(w(Q)|x) \leq \text{Var} w(Q)$. In addition when x is taken under P_θ , Q is uniformly distributed in $[0, 1]$ and thus $\text{Var} w(Q) = \text{Var}_{[0,1]} w$, i.e., $\text{Var}_{x \sim P_\theta} W_\theta^f(x) \leq \text{Var}_{[0,1]} w$.

Besides, consider the tangent space in Θ -space at point θ^t , and let us choose an orthonormal basis in this tangent space for the Fisher metric. Then, in this basis we have $\tilde{\nabla}_i \ln P_\theta(x) = \partial_i \ln P_\theta(x)$. So the covariance matrix of $\tilde{\nabla} \ln P_\theta(x)$ is $\mathbb{E}_{x \sim P_\theta}(\partial_i \ln P_\theta(x) \partial_j \ln P_\theta(x))$, which is equal to the Fisher matrix by definition. So this covariance matrix is the identity, whose largest eigenvalue is 1.

Proof of Proposition 13 (Noisy IGO)

On the one hand, let P_θ be a family of distributions on X . The IGO algorithm (14) applied to a random function $f(x) = \tilde{f}(x, \omega)$ where ω is a random variable uniformly distributed in $[0, 1]$ reads

$$\theta^{t+\delta t} = \theta^t + \delta t \sum_{i=1}^N \hat{w}_i \tilde{\nabla}_\theta \ln P_\theta(x_i) \quad (65)$$

where $x_i \sim P_\theta$ and \hat{w}_i is according to (12) where ranking is applied to the values $\tilde{f}(x_i, \omega_i)$, with ω_i uniform variables in $[0, 1]$ independent from x_i and from each other.

On the other hand, for the IGO algorithm using $P_\theta \otimes U_{[0,1]}$ and applied to the deterministic function \tilde{f} , \hat{w}_i is computed using the ranking according to the \tilde{f} values of the sampled points $\tilde{x}_i = (x_i, \omega_i)$, and thus coincides with the one in (65).

Besides,

$$\tilde{\nabla}_\theta \ln P_{\theta \otimes U_{[0,1]}}(\tilde{x}_i) = \tilde{\nabla}_\theta \ln P_\theta(x_i) + \underbrace{\tilde{\nabla}_\theta \ln U_{[0,1]}(\omega_i)}_{=0}$$

and thus the IGO algorithm update on space $X \times [0, 1]$, using the family of distributions $\tilde{P}_\theta = P_\theta \otimes U_{[0,1]}$, applied to the deterministic function \tilde{f} , coincides with (65).

Proof of Theorem 14 (Natural gradient as ML with infinitesimal weights)

We begin with a calculus lemma (proof omitted).

Lemma 25. *Let f be real-valued function on a finite-dimensional vector space E equipped with a definite positive quadratic form $\|\cdot\|^2$. Assume f is smooth and has at most quadratic growth at infinity. Then, for any $x \in E$, we have*

$$\nabla f(x) = \lim_{\varepsilon \rightarrow 0} \frac{1}{\varepsilon} \arg \max_h \left\{ f(x+h) - \frac{1}{2\varepsilon} \|h\|^2 \right\}$$

where ∇ is the gradient associated with the norm $\|\cdot\|$. Equivalently,

$$\arg \max_y \left\{ f(y) - \frac{1}{2\varepsilon} \|y-x\|^2 \right\} = x + \varepsilon \nabla f(x) + O(\varepsilon^2)$$

when $\varepsilon \rightarrow 0$.

We are now ready to prove Theorem 14. Let W be a function of x , and fix some θ_0 in Θ .

We need some regularity assumptions: we assume that no two points $\theta \in \Theta$ define the same probability distribution and that the map $P_\theta \mapsto \theta$ is continuous. We also assume that the map $\theta \mapsto P_\theta$ is smooth enough, so that $\int \ln P_\theta(x) W(x) P_{\theta_0}(dx)$ is a smooth function of θ . (These are restrictions on θ -regularity: this does not mean that W has to be continuous as a function of x .)

The two statements of Theorem 14 using a sum and an integral have similar proofs, so we only include the first. For $\varepsilon > 0$, let θ be the solution of

$$\theta = \arg \max \left\{ (1-\varepsilon) \int \ln P_\theta(x) P_{\theta_0}(dx) + \varepsilon \int \ln P_\theta(x) W(x) P_{\theta_0}(dx) \right\}.$$

Then we have

$$\begin{aligned} \theta &= \arg \max \left\{ \int \ln P_\theta(x) P_{\theta_0}(dx) + \varepsilon \int \ln P_\theta(x) (W(x) - 1) P_{\theta_0}(dx) \right\} \\ &= \arg \max \left\{ \int \ln P_\theta(x) P_{\theta_0}(dx) - \int \ln P_{\theta_0}(x) P_{\theta_0}(dx) + \varepsilon \int \ln P_\theta(x) (W(x) - 1) P_{\theta_0}(dx) \right\} \end{aligned}$$

(because the added term does not depend on θ)

$$\begin{aligned} &= \arg \max \left\{ -\text{KL}(P_{\theta_0} \| P_\theta) + \varepsilon \int \ln P_\theta(x) (W(x) - 1) P_{\theta_0}(dx) \right\} \\ &= \arg \max \left\{ -\frac{1}{\varepsilon} \text{KL}(P_{\theta_0} \| P_\theta) + \int \ln P_\theta(x) (W(x) - 1) P_{\theta_0}(dx) \right\} \end{aligned}$$

When $\varepsilon \rightarrow 0$, the first term exceeds the second one if $\text{KL}(P_{\theta_0} \parallel P_\theta)$ is too large (because W is bounded), and so $\text{KL}(P_{\theta_0} \parallel P_\theta)$ tends to 0. So we can assume that θ is close to θ_0 .

When $\theta = \theta_0 + \delta\theta$ is close to θ_0 , we have

$$\text{KL}(P_{\theta_0} \parallel P_\theta) = \frac{1}{2} \sum I_{ij}(\theta_0) \delta\theta_i \delta\theta_j + O(\delta\theta^3)$$

with $I_{ij}(\theta_0)$ the Fisher matrix at θ_0 . (This actually holds both for $\text{KL}(P_{\theta_0} \parallel P_\theta)$ and $\text{KL}(P_\theta \parallel P_{\theta_0})$.)

Thus, we can apply the lemma above using the Fisher metric $\sum I_{ij}(\theta_0) \delta\theta_i \delta\theta_j$, and working on a small neighborhood of θ_0 in θ -space (which can be identified with $\mathbb{R}^{\dim \Theta}$). The lemma states that the argmax above is attained at

$$\theta = \theta_0 + \varepsilon \tilde{\nabla}_\theta \int \ln P_\theta(x) (W(x) - 1) P_{\theta_0}(dx)$$

up to $O(\varepsilon^2)$, with $\tilde{\nabla}$ the natural gradient.

Finally, the gradient cancels the constant -1 because $\int (\tilde{\nabla} \ln P_\theta) P_{\theta_0} = 0$ at $\theta = \theta_0$. This proves Theorem 14.

Proof of Theorem 16 (IGO, CEM and IGO-ML)

Let P_θ be a family of probability distributions of the form

$$P_\theta(x) = \frac{1}{Z(\theta)} \exp\left(\sum \theta_i T_i(x)\right) H(dx)$$

where T_1, \dots, T_k is a finite family of functions on X and $H(dx)$ is some reference measure on X . We assume that the family of functions $(T_i)_i$ together with the constant function $T_0(x) = 1$, are linearly independent. This prevents redundant parametrizations where two values of θ describe the same distribution; this also ensures, by elementary linear algebra, that the Fisher matrix $\text{Cov}(T_i, T_j)$ is invertible.

The IGO update (15) in the parametrization \bar{T}_i is a sum of terms of the form

$$\tilde{\nabla}_{\bar{T}_i} \ln P(x).$$

So we will compute the natural gradient $\tilde{\nabla}_{\bar{T}_i}$ in those coordinates. We first need some general results about the Fisher metric for exponential families.

The next proposition gives the expression of the Fisher scalar product between two tangent vectors δP and $\delta' P$ of a statistical manifold of exponential distributions. It is one way to express the duality between the coordinates θ_i and \bar{T}_i (compare [AN00, (3.30) and Section 3.5]).

Proposition 26. *Let $\delta\theta_i$ and $\delta'\theta_i$ be two small variations of the parameters θ_i . Let $\delta P(x)$ and $\delta' P(x)$ be the resulting variations of the probability distribution P , and $\delta\bar{T}_i$ and $\delta'\bar{T}_i$ the resulting variations of \bar{T}_i . Then the scalar product, in Fisher information metric, between the tangent vectors δP and $\delta' P$, is*

$$\langle \delta P, \delta' P \rangle = \sum_i \delta\theta_i \delta'\bar{T}_i = \sum_i \delta'\theta_i \delta\bar{T}_i.$$

Proof. By definition of the Fisher metric:

$$\begin{aligned}
\langle \delta P, \delta' P \rangle &= \sum_{i,j} I_{ij} \delta\theta_i \delta'\theta_j \\
&= \sum_{i,j} \delta\theta_i \delta'\theta_j \int_x \frac{\partial \ln P(x)}{\partial \theta_i} \frac{\partial \ln P(x)}{\partial \theta_j} P(x) \\
&= \int_x \sum_i \frac{\partial \ln P(x)}{\partial \theta_i} \delta\theta_i \sum_j \frac{\partial \ln P(x)}{\partial \theta_j} \delta'\theta_j P(x) \\
&= \int_x \sum_i \frac{\partial \ln P(x)}{\partial \theta_i} \delta\theta_i \delta'(\ln P(x)) P(x) \\
&= \int_x \sum_i \frac{\partial \ln P(x)}{\partial \theta_i} \delta\theta_i \delta' P(x) \\
&= \int_x \sum_i (T_i(x) - \bar{T}_i) \delta\theta_i \delta' P(x) \quad \text{by (17)} \\
&= \sum_i \delta\theta_i \left(\int_x T_i(x) \delta' P(x) \right) - \sum_i \delta\theta_i \bar{T}_i \int_x \delta' P(x) \\
&= \sum_i \delta\theta_i \delta' \bar{T}_i
\end{aligned}$$

because $\int_x \delta' P(x) = 0$ since the total mass of P is 1, and $\int_x T_i(x) \delta' P(x) = \delta' \bar{T}_i$ by definition of \bar{T}_i . \square

Proposition 27. *Let f be a function on the statistical manifold of an exponential family as above. Then the components of the natural gradient w.r.t. the expectation parameters are given by the vanilla gradient w.r.t. the natural parameters:*

$$\tilde{\nabla}_{\bar{T}_i} f = \frac{\partial f}{\partial \theta_i}$$

and conversely

$$\tilde{\nabla}_{\theta_i} f = \frac{\partial f}{\partial \bar{T}_i}.$$

(Beware this does *not* mean that the gradient ascent in any of those parametrizations is the vanilla gradient ascent.)

We could not find a reference for this result, though we think it is known (as a consequence of [AN00, (3.32)]).

Proof. By definition, the natural gradient $\tilde{\nabla} f$ of a function f is the unique tangent vector δP such that that, for any other tangent vector $\delta' P$, we have

$$\delta' f = \langle \delta P, \delta' P \rangle$$

with $\langle \cdot, \cdot \rangle$ the scalar product associated with the Fisher metric. We want to compute this natural gradient in coordinates \bar{T}_i , so we are interested in the variations $\delta \bar{T}_i$ associated with δP .

By Proposition 26, the scalar product above is

$$\langle \delta P, \delta' P \rangle = \sum \delta \bar{T}_i \delta' \theta_i$$

where $\delta \bar{T}_i$ is the variation of \bar{T}_i associated with δP , and $\delta' \theta_i$ the variation of θ_i associated with $\delta' P$.

On the other hand we have $\delta' f = \sum_i \frac{\partial f}{\partial \theta_i} \delta' \theta_i$. So we must have

$$\sum_i \delta \bar{T}_i \delta' \theta_i = \sum_i \frac{\partial f}{\partial \theta_i} \delta' \theta_i$$

for any $\delta'P$, which leads to

$$\delta\bar{T}_i = \frac{\partial f}{\partial \theta_i}$$

as needed. The converse relation is proved *mutatis mutandis*. \square

Back to the proof of Theorem 16. We can now compute the desired terms:

$$\tilde{\nabla}_{\bar{T}_i} \ln P(x) = \frac{\partial \ln P(x)}{\partial \theta_i} = T_i(x) - \bar{T}_i$$

by (17). This proves the first statement (30) in Theorem 16 about the form of the IGO update in these parameters.

The other statements follow easily from this together with the additional fact (29) that, for any set of (positive or negative) weights a_i with $\sum a_i = 1$, the value $T^* = \sum_i a(i)T(x_i)$ is the maximum likelihood estimate of $\sum_i a(i) \ln P(x_i)$.

References

- [AAH12] Youhei Akimoto, Anne Auger, and Nikolaus Hansen. Convergence of the continuous time trajectories of isotropic evolution strategies on monotonic \mathcal{C}^2 -composite functions. In Carlos A. Coello Coello, Vincenzo Cutello, Kalyanmoy Deb, Stephanie Forrest, Giuseppe Nicosia, and Mario Pavone, editors, *PPSN (1)*, volume 7491 of *Lecture Notes in Computer Science*, pages 42–51. Springer, 2012.
- [ABNK⁺87] S.-I. Amari, O. E. Barndorff-Nielsen, R. E. Kass, S. L. Lauritzen, and C. R. Rao. *Differential geometry in statistical inference*. Institute of Mathematical Statistics Lecture Notes—Monograph Series, 10. Institute of Mathematical Statistics, Hayward, CA, 1987.
- [AHS85] D.H. Ackley, G.E. Hinton, and T.J. Sejnowski. A learning algorithm for Boltzmann machines. *Cognitive Science*, 9(1):147–169, 1985.
- [Ama98] Shun-Ichi Amari. Natural gradient works efficiently in learning. *Neural Comput.*, 10:251–276, February 1998.
- [AN00] Shun-ichi Amari and Hiroshi Nagaoka. *Methods of information geometry*, volume 191 of *Translations of Mathematical Monographs*. American Mathematical Society, Providence, RI, 2000. Translated from the 1993 Japanese original by Daishi Harada.
- [ANOK10] Youhei Akimoto, Yuichi Nagata, Isao Ono, and Shigenobu Kobayashi. Bidirectional relation between CMA evolution strategies and natural evolution strategies. In *Proceedings of Parallel Problem Solving from Nature - PPSN XI*, volume 6238 of *Lecture Notes in Computer Science*, pages 154–163. Springer, 2010.
- [AO08] Ravi P. Agarwal and Donal O’Regan. *An Introduction to Ordinary Differential Equations*. Springer, 2008.
- [Arn06] D.V. Arnold. Weighted multirecombination evolution strategies. *Theoretical computer science*, 361(1):18–37, 2006.

- [Bal94] Shumeet Baluja. Population based incremental learning: A method for integrating genetic search based function optimization and competitive learning. Technical Report CMU-CS-94-163, Carnegie Mellon Report, 1994.
- [BC95] Shumeet Baluja and Rich Caruana. Removing the genetics from the standard genetic algorithm. In *Proceedings of ICML '95*, pages 38–46, 1995.
- [BCV12] Yoshua Bengio, Aaron C. Courville, and Pascal Vincent. Unsupervised feature learning and deep learning: A review and new perspectives. *CoRR*, abs/1206.5538, 2012.
- [Ber00a] A. Berny. An adaptive scheme for real function optimization acting as a selection operator. In *Combinations of Evolutionary Computation and Neural Networks, 2000 IEEE Symposium on*, pages 140–149, 2000.
- [Ber00b] A. Berny. Selection and reinforcement learning for combinatorial optimization. In Marc Schoenauer, Kalyanmoy Deb, Günther Rudolph, Xin Yao, Evelyne Lutton, Juan Merelo, and Hans-Paul Schwefel, editors, *Parallel Problem Solving from Nature PPSN VI*, volume 1917 of *Lecture Notes in Computer Science*, pages 601–610. Springer Berlin Heidelberg, 2000.
- [Ber02] Arnaud Berny. Boltzmann machine for population-based incremental learning. In *ECAI*, pages 198–202, 2002.
- [Bey01] H.-G. Beyer. *The Theory of Evolution Strategies*. Natural Computing Series. Springer-Verlag, 2001.
- [Bil95] Patrick Billingsley. *Probability and measure*. Wiley Series in Probability and Mathematical Statistics. John Wiley & Sons Inc., New York, third edition, 1995. A Wiley-Interscience Publication.
- [BLPL07] Y. Bengio, P. Lamblin, V. Popovici, and H. Larochelle. Greedy layer-wise training of deep networks. In B. Schölkopf, J. Platt, and T. Hoffman, editors, *Advances in Neural Information Processing Systems 19*, pages 153–160. MIT Press, Cambridge, MA, 2007.
- [BLS07] J. Branke, C. Lode, and J.L. Shapiro. Addressing sampling errors and diversity loss in UMDA. In *Proceedings of the 9th annual conference on Genetic and evolutionary computation*, pages 508–515. ACM, 2007.
- [BS02] H.G. Beyer and H.P. Schwefel. Evolution strategies—a comprehensive introduction. *Natural computing*, 1(1):3–52, 2002.
- [Bur86] Jacob Burbea. Informative geometry of probability spaces. *Exposition. Math.*, 4(4):347–378, 1986.
- [CT06] Thomas M. Cover and Joy A. Thomas. *Elements of information theory*. Wiley-Interscience [John Wiley & Sons], Hoboken, NJ, second edition, 2006.

- [dBKMR05] Pieter-Tjerk de Boer, Dirk P. Kroese, Shie Mannor, and Reuven Y. Rubinstein. A tutorial on the cross-entropy method. *Annals OR*, 134(1):19–67, 2005.
- [DCB⁺10] G. Desjardins, A. Courville, Y. Bengio, P. Vincent, and O. Delalleau. Parallel tempering for training of restricted Boltzmann machines. In *Proceedings of the Thirteenth International Conference on Artificial Intelligence and Statistics (AISTATS)*, 2010.
- [DM02] Elizabeth D. Dolan and Jorge J. Moré. Benchmarking optimization software with performance profiles. *Mathematical programming*, 91(2):201–213, 2002.
- [DMQS11] Swagatam Das, Sayan Maity, Bo-Yang Qu, and Ponnuthurai Nagarathnam Suganthan. Real-parameter evolutionary multimodal optimization - a survey of the state-of-the-art. *Swarm and Evolutionary Computation*, 1(2):71–88, 2011.
- [GF05] Marcus Gallagher and Marcus Frean. Population-based continuous optimization, probabilistic modelling and mean shift. *Evol. Comput.*, 13(1):29–42, January 2005.
- [Gha04] Zoubin Ghahramani. Unsupervised learning. In Olivier Bousquet, Ulrike von Luxburg, and Gunnar Rätsch, editors, *Advanced Lectures on Machine Learning*, volume 3176 of *Lecture Notes in Computer Science*, pages 72–112. Springer Berlin / Heidelberg, 2004.
- [GSS⁺10] Tobias Glasmachers, Tom Schaul, Yi Sun, Daan Wierstra, and Jürgen Schmidhuber. Exponential natural evolution strategies. In *Proceedings of the 12th annual conference on Genetic and evolutionary computation GECCO'10*, pages 393–400. ACM, 2010.
- [Han06a] N. Hansen. An analysis of mutative σ -self-adaptation on linear fitness functions. *Evolutionary Computation*, 14(3):255–275, 2006.
- [Han06b] N. Hansen. The CMA evolution strategy: a comparing review. In J.A. Lozano, P. Larranaga, I. Inza, and E. Bengoetxea, editors, *Towards a new evolutionary computation. Advances on estimation of distribution algorithms*, pages 75–102. Springer, 2006.
- [Han09] N. Hansen. Benchmarking a BI-population CMA-ES on the BBOB-2009 function testbed. In *Proceedings of the 11th Annual Conference Companion on Genetic and Evolutionary Computation Conference: Late Breaking Papers, GECCO '09*, pages 2389–2396, New York, NY, USA, 2009. ACM.
- [Hin02] G.E. Hinton. Training products of experts by minimizing contrastive divergence. *Neural Computation*, 14:1771–1800, 2002.
- [HJ61] R. Hooke and T.A. Jeeves. “Direct search” solution of numerical and statistical problems. *Journal of the ACM*, 8:212–229, 1961.

- [HK04] N. Hansen and S. Kern. Evaluating the CMA evolution strategy on multimodal test functions. In X. Yao et al., editors, *Parallel Problem Solving from Nature PPSN VIII*, volume 3242 of *LNCS*, pages 282–291. Springer, 2004.
- [HMK03] N. Hansen, S.D. Müller, and P. Koumoutsakos. Reducing the time complexity of the derandomized evolution strategy with covariance matrix adaptation (CMA-ES). *Evolutionary Computation*, 11(1):1–18, 2003.
- [HO96] N. Hansen and A. Ostermeier. Adapting arbitrary normal mutation distributions in evolution strategies: The covariance matrix adaptation. In *ICEC96*, pages 312–317. IEEE Press, 1996.
- [HO01] Nikolaus Hansen and Andreas Ostermeier. Completely derandomized self-adaptation in evolution strategies. *Evolutionary Computation*, 9(2):159–195, 2001.
- [HOT06] G.E. Hinton, S. Osindero, and Yee-Whye Teh. A fast learning algorithm for deep belief nets. *Neural Computation*, 18:1527–1554, 2006.
- [JA06] G.A. Jastrebski and D.V. Arnold. Improving evolution strategies through active covariance matrix adaptation. In *Evolutionary Computation, 2006. CEC 2006. IEEE Congress on*, pages 2814–2821. IEEE, 2006.
- [JA10] Mohamed Jebalia and Anne Auger. Log-linear convergence of the scale-invariant $(\mu/\mu_w, \lambda)$ -ES and optimal μ for intermediate recombination for large population sizes. In R. Schaefer et al., editor, *Parallel Problem Solving from Nature (PPSN XI)*, volume 6239, pages 52–61. Springer, 2010.
- [Jef46] Harold Jeffreys. An invariant form for the prior probability in estimation problems. *Proc. Roy. Soc. London. Ser. A.*, 186:453–461, 1946.
- [Kha96] Hassan K. Khalil. *Nonlinear Systems*. Nonlinear Systems. Prentice-Hall, Inc., second edition, 1996.
- [KP92] Peter E. Kloeden and Eckhard Platen. *Numerical solution of stochastic differential equations*, volume 23 of *Applications of Mathematics (New York)*. Springer-Verlag, Berlin, 1992.
- [Kul97] Solomon Kullback. *Information theory and statistics*. Dover Publications Inc., Mineola, NY, 1997. Reprint of the second (1968) edition.
- [LL02] P. Larranaga and J.A. Lozano. *Estimation of distribution algorithms: A new tool for evolutionary computation*. Springer Netherlands, 2002.
- [LRMB07] Nicolas Le Roux, Pierre-Antoine Manzagol, and Yoshua Bengio. Topmoumoute online natural gradient algorithm. In *NIPS*, 2007.
- [MGH81] Jorge J. Moré, Burton S. Garbow, and Kenneth E. Hillstom. Testing unconstrained optimization software. *ACM Transactions on Mathematical Software (TOMS)*, 7(1):17–41, 1981.

- [MMP11] Luigi Malagò, Matteo Matteucci, and Giovanni Pistone. Towards the geometry of estimation of distribution algorithms based on the exponential family. In Hans-Georg Beyer and William B. Langdon, editors, *FOGA, Proceedings*, pages 230–242. ACM, 2011.
- [MMS08] Luigi Malagò, Matteo Matteucci, and Bernardo Dal Seno. An information geometry perspective on estimation of distribution algorithms: boundary analysis. In *GECCO (Companion)*, pages 2081–2088, 2008.
- [NM65] John Ashworth Nelder and R Mead. A simplex method for function minimization. *The Computer Journal*, pages 308–313, 1965.
- [PGL02] M. Pelikan, D.E. Goldberg, and F.G. Lobo. A survey of optimization by building and using probabilistic models. *Computational optimization and applications*, 21(1):5–20, 2002.
- [Rao45] Calyampudi Radhakrishna Rao. Information and the accuracy attainable in the estimation of statistical parameters. *Bull. Calcutta Math. Soc.*, 37:81–91, 1945.
- [Rec73] I. Rechenberg. *Evolutionstrategie: Optimierung technischer Systeme nach Prinzipien der biologischen Evolution*. Frommann-Holzboog Verlag, Stuttgart, 1973.
- [Rec94] I. Rechenberg. *Evolutionstrategie '94*. Frommann-Holzboog Verlag, 1994.
- [RH08] R. Ros and N. Hansen. A simple modification in CMA-ES achieving linear time and space complexity. In Günter Rudolph, Thomas Jansen, Simon Lucas, Carlo Polini, and Nicola Beume, editors, *Proceedings of Parallel Problem Solving from Nature (PPSN X)*, volume 5199 of *Lecture Notes in Computer Science*, pages 296–305. Springer, 2008.
- [RK04] R.Y. Rubinstein and D.P. Kroese. *The cross-entropy method: a unified approach to combinatorial optimization, Monte-Carlo simulation, and machine learning*. Springer-Verlag New York Inc, 2004.
- [Rub99] Reuven Rubinstein. The cross-entropy method for combinatorial and continuous optimization. *Methodology and Computing in Applied Probability*, 1:127–190, 1999. 10.1023/A:1010091220143.
- [SA90] F. Silva and L. Almeida. Acceleration techniques for the back-propagation algorithm. *Neural Networks*, pages 110–119, 1990.
- [Sal09] Ruslan Salakhutdinov. Learning in Markov random fields using tempered transitions. In Y. Bengio, D. Schuurmans, J. Lafferty, C. K. I. Williams, and A. Culotta, editors, *Advances in Neural Information Processing Systems 22*, pages 1598–1606. MIT Press, 2009.

- [Sch92] Laurent Schwartz. *Analyse. II*, volume 43 of *Collection Enseignement des Sciences [Collection: The Teaching of Science]*. Hermann, Paris, 1992. Calcul différentiel et équations différentielles, With the collaboration of K. Zizi.
- [Sch95] H.-P. Schwefel. *Evolution and Optimum Seeking*. Sixth-generation computer technology series. John Wiley & Sons, Inc. New York, NY, USA, 1995.
- [SGS11] Tom Schaul, Tobias Glasmachers, and Jürgen Schmidhuber. High dimensions and heavy tails for natural evolution strategies. In *Proceedings of the 13th annual conference on Genetic and evolutionary computation, GECCO '11*, pages 845–852, New York, NY, USA, 2011. ACM.
- [SHI09] Thorsten Suttorp, Nikolaus Hansen, and Christian Igel. Efficient covariance matrix update for variable metric evolution strategies. *Machine Learning*, 75(2):167–197, 2009.
- [SK98] Bruno Sareni and Laurent Krähenbühl. Fitness sharing and niching methods revisited. *IEEE Trans. Evolutionary Computation*, 2(3):97–106, 1998.
- [SM08] Ruslan Salakhutdinov and Iain Murray. On the quantitative analysis of deep belief networks. In *Proceedings of the 25th international conference on Machine learning, ICML '08*, pages 872–879, New York, NY, USA, 2008. ACM.
- [Smo86] P. Smolensky. Information processing in dynamical systems: foundations of harmony theory. In D. Rumelhart and J. McClelland, editors, *Parallel Distributed Processing*, volume 1, chapter 6, pages 194–281. MIT Press, Cambridge, MA, USA, 1986.
- [SWSS09] Yi Sun, Daan Wierstra, Tom Schaul, and Juergen Schmidhuber. Efficient natural evolution strategies. In *Proceedings of the 11th Annual conference on Genetic and evolutionary computation, GECCO '09*, pages 539–546, New York, NY, USA, 2009. ACM.
- [Tho00] H. Thorisson. *Coupling, Stationarity, and Regeneration*. Springer, 2000.
- [Tor97] Virginia Torczon. On the convergence of pattern search algorithms. *SIAM Journal on optimization*, 7(1):1–25, 1997.
- [Tou04] M. Toussaint. Notes on information geometry and evolutionary processes. eprint arXiv:nlin/0408040, 2004.
- [WAS04] Michael Wagner, Anne Auger, and Marc Schoenauer. EEDA : A new robust estimation of distribution algorithms. Research Report RR-5190, INRIA, 2004.
- [Whi89] D. Whitley. The genitor algorithm and selection pressure: Why rank-based allocation of reproductive trials is best. In *Proceedings of the third international conference on Genetic algorithms*, pages 116–121, 1989.
- [WSPS08] Daan Wierstra, Tom Schaul, Jan Peters, and Jürgen Schmidhuber. Natural evolution strategies. In *IEEE Congress on Evolutionary Computation*, pages 3381–3387, 2008.